



Science & Technology Indonesia

<https://sciencetechindonesia.com>



Vol 9 No 3
July

2024

SERTIFIKAT

Direktorat Jenderal Pendidikan Tinggi, Riset dan Teknologi
Kementerian Pendidikan, Kebudayaan, Riset dan Teknologi Republik Indonesia



Kutipan dari Keputusan Direktorat Jenderal Pendidikan Tinggi, Riset dan Teknologi
Kementerian Pendidikan, Kebudayaan, Riset, dan Teknologi Republik Indonesia

Nomor 164/E/KPT/2021

Peringkat Akreditasi Jurnal Ilmiah Periode 2 Tahun 2021

Nama Jurnal Ilmiah

Science and Technology Indonesia

E-ISSN: 25804391

Penerbit: ART Publishing, Universitas Sriwijaya

Ditetapkan Sebagai Jurnal Ilmiah

TERAKREDITASI PERINGKAT 1

Akreditasi Berlaku selama 5 (lima) Tahun, yaitu
Volume 6 Nomor 1 Tahun 2021 Sampai Volume 10 Nomor 4 Tahun 2025

Jakarta, 27 Desember 2021

Plt. Direktur Jenderal Pendidikan Tinggi,
Riset, dan Teknologi



Prof. Ir. Nizam, M.Sc., DIC, Ph.D., IPU, ASEAN Eng
NIP. 196107061987101001



Relai
Sertifikasi
Elektronik

Catatan:

1. UU ITE No 11 Tahun 2008 Pasal 5 Ayat 1 "Informasi Elektronik dan/atau hasil cetakan merupakan alat bukti yang sah"
2. Dokumen ini telah ditandatangani secara elektronik menggunakan sertifikat elektronik yang diterbitkan oleh BSE

Twitter share

FB share

Scimago Journal Rank



Scopus CiteScore Rank 2022

Metrics

1.5
CiteScore 2022

0.227
SJR 2022

0.300
SNIP 2022

CiteScore Rank

ASJC Category	Quartile	Percentile	Rank
Pharmacology, Toxicology and Pharmaceutics (miscellaneous)	Q2	60th	13 / 32
General Mathematics	Q2	58th	162 / 387
Physics and Astronomy (miscellaneous)	Q5	35th	44 / 67
General Chemistry	Q5	30th	282 / 407

Scopus CiteScore Rank 2023

Home / Editorial Team

Editorial Team

Editor-in-Chief



Prof. Aldes Lesbani, Ph.D.
Universitas Sriwijaya, INDONESIA



Vice Editor-in-Chief



Prof. Dr. rer. nat. Risfidian Mohadi
Universitas Sriwijaya INDONESIA



Hendrik Oktendy Lintang, Dr.
Indonesian Chemical Society, INDONESIA



Section Editors



Dodi Devianto, Dr.
Universitas Andalas, INDONESIA



Tarmizi Taher, Dr.
Institut Teknologi Sumatera, INDONESIA



Metrics

1.8 CiteScore 2021
0.201 SJR 2021
0.531 h-index 2021

CiteScore Rank

ASJC Category	Quartile	Percentile	Rank
General Mathematics	Q2	66th	134 / 399
Pharmacology, Toxicology and Pharmacotics (miscellaneous)	Q2	66th	15 / 43
Physics and Astronomy (miscellaneous)	Q3	41st	48 / 81
General Chemistry	Q3	33rd	278 / 408

Scopus CiteScore Rank 2024

Metrics

2.3 CiteScore 2024
0.240 SJR 2024
0.606 h-index 2024

CiteScore Rank

ASJC Category	Quartile	Percentile	Rank
General Mathematics	Q1	76th	97 / 414
Pharmacology, Toxicology and Pharmacotics (miscellaneous)	Q2	58th	15 / 46
Physics and Astronomy (miscellaneous)	Q3	47th	46 / 87
General Chemistry	Q3	37th	252 / 404



Fitri Maya Puspita, Dr.
Universitas Sriwijaya, INDONESIA



Mohammad Basyuni, Prof. Dr.
Universitas Sumatera Utara, INDONESIA



Neza Rahayu Palapa, Dr.
Universitas Sriwijaya, INDONESIA



Editorial Boards



Ambara Rachmat Pradipta, Dr.
Tokyo Institute of Technology, JAPAN



Bidyut Saha, Prof. Dr.
The University of Burdwan, INDIA



Fabien Silly, Dr.
CEA Saclay, FRANCE



Supa Hannongbua, Prof. Dr.
Kasetsart University, THAILAND





Iskhag Iskandar, Prof. Dr.
Universitas Sriwijaya, INDONESIA



Faheem K. Butt, Dr.
University of Education, PAKISTAN



Ivandini T. Anggraningrum, Prof. Dr.
Universitas Indonesia, INDONESIA



Roland Tomašiūnas, Prof. Dr.
Vilnius University, LITHUANIA



Khairul Basar, Dr.
Institut Teknologi Bandung, INDONESIA



Ammar Z. Alshemary, Dr.
Karabuk Üniversitesi, TURKEY



Lusi Safriani, Dr.
Universitas Padjadjaran, INDONESIA



Reviewer Acknowledgement

The editorial team Science and Technology Indonesia would like to thank all the reviewers, who have contributed to Science and Technology Indonesia manuscript article review.

We deeply appreciate your academic support for improving the Science and Technology Indonesia in the future.

Hilda Zulkifli, Universitas Sriwijaya, Indonesia ([Scopus ID = 55234932600](#))

Hermansyah, Universitas Sriwijaya, Indonesia ([Scopus ID = 35102189300](#))

Siew Ling Lee, Universiti Teknologi Malaysia, Malaysia ([Scopus ID = 57193482292](#))

M. Lutfi Firdaus, Universitas Bengkulu, Indonesia ([Scopus ID = 57220603047](#))

Muhammad Said, Universitas Sriwijaya, Indonesia ([Scopus ID = 57189487421](#))

Hendrik Oktendi Lintang, Indonesian Chemical Society, Indonesia ([Scopus ID = 36496933500](#))

Senthil Kumar Subburaj, New Prince Shri Bhavani College of Engineering and Technology, India ([Scopus ID = 57219443244](#))

Zati Aqmar Zaharudin, Universiti Teknologi MARA, Malaysia ([Scopus ID = 55140797700](#))

Dedi Rohendi, Universitas Sriwijaya, Indonesia ([Scopus ID = 57190369223](#))

Lyra Yulianti, Universitas Andalas, Indonesia ([Scopus ID = 36053960400](#))

Nuni Gofar, Universitas Sriwijaya, Indonesia ([Scopus ID = 57205609513](#))

Huda Zuhrah Ab Halim, Universiti Teknologi MARA, Malaysia ([Scopus ID = 26026567300](#))

Laila Hanum, Universitas Sriwijaya, Indonesia ([Scopus ID = 57194601647](#))

Maria Azees, GMR Institute of Technology, India ([Scopus ID = 55823331700](#))

Dodi Devianto, Universitas Andalas, Indonesia ([Scopus ID = 56747957200](#))

Alfan Wijaya, Universitas Sriwijaya, Indonesia ([Scopus ID = 57222756982](#))

Rino R. Mukti, Institut Teknologi Bandung, Indonesia ([Scopus ID = 12244105600](#))

Muhafzan, Universitas Andalas, Indonesia ([Scopus ID = 36782699400](#))

Yulita Molliq Rangkuti, Universitas Negeri Medan, Indonesia ([Scopus ID = 56230086300](#))

Fitri Maya Puspita, Universitas Sriwijaya, Indonesia ([Scopus ID = 55761767800](#))

Wamiliana, Universitas Lampung, Indonesia ([Scopus ID = 36053853700](#))

Iskhaq Iskandar, Universitas Sriwijaya, Indonesia ([Scopus ID = 8637688700](#))

Risfidian Mohadi, Universitas Sriwijaya, Indonesia ([Scopus ID = 55991505100](#))

Elfiti, Universitas Sriwijaya, Indonesia ([Scopus ID = 55532411800](#))

Pranom Chantaranothai, Khon Kaen University, Thailand ([Scopus ID = 6602249290](#))

Mardiyanto, Universitas Sriwijaya, Indonesia ([Scopus ID = 55872786400](#))

Tarmizi Taher, Institut Teknologi Sumatera, Indonesia ([Scopus ID = 56104271500](#))

M. Yusup Nur Khakim, Universitas Sriwijaya, Indonesia ([Scopus ID = 55466639800](#))

Is Fatimah, Universitas Islam Indonesia, Indonesia ([Scopus ID = 35104706400](#))

Amri, Universitas Sriwijaya, Indonesia ([Scopus ID = 57537889500](#))

Siti Suzlin Binti Supadi, Universiti Malaya, Malaysia ([Scopus ID = 24450952300](#))

Addy Rachmat, Universitas Sriwijaya, Indonesia ([Scopus ID = 57204633876](#))

Ahmad Fatoni, Sekolah Tinggi Ilmu Farmasi Bakti Pertiwi, Indonesia ([Scopus ID = 56736774600](#))

Nurul Hidayat Arpilita, Universitas Gadjah Mada, Indonesia ([Scopus ID 10039580700](#))

Ferra Yanuar, Universitas Andalas, Indonesia ([Scopus ID = 35772766900](#))

Fitrya, Universitas Sriwijaya, Indonesia ([Scopus ID = 55993294400](#))

Tri Atmojo Kusmayadi, Universitas Sebelas Maret, Indonesia ([Scopus ID = 57217189365](#))

Nurlisa Hidayati, Universitas Sriwijaya, Indonesia ([Scopus ID = 56737023800](#))

ARTIKEL
YANG SUDAH
TERBIT

Nickel Salt Dependency as Catalyst in the Plating Bath on the Film Properties of Cu/Cu-Ni

Cahaya Rosyidan^{1*}, Budhy Kurniawan², Bambang Soegijono³, Mustamina Maulani¹, Lisa Samura¹, Frederik Gresia Nababan¹, Valentinus Galih Vidia Putra⁴ Ferry Budhi Susetyo⁵

¹Department of Petroleum Engineering, Universitas Trisakti, Jakarta, 11440, Indonesia

²Department of Physics, Universitas Indonesia, Depok, 16424, Indonesia

³Department of Geoscience, Universitas Indonesia, Depok, 16424, Indonesia

⁴Plasma and Nanomaterial Research Group, Politeknik STTT Bandung, Bandung, 40272, Indonesia

⁵Department of Mechanical Engineering, Universitas Negeri Jakarta, Jakarta, 13220, Indonesia

*Corresponding author: cahayarosyidan@trisakti.ac.id

Abstract

Metal plating frequently employs nickel (Ni) and copper (Cu) as anodes. Cu/ Cu-Ni film formed has many advantages, such as better corrosion resistance and high hardness characteristics. This study aims to assess the properties of Cu/Cu-Ni film, such as phase, surface morphology, crystallographic orientation, hardness, corrosion analysis, and contact angle, which were fabricated using electrodeposition with various Ni salt additions (0.3, 0.5 and 0.7 M). In addition, the cathode current efficiency (CCE) and deposition rate of the Cu/Cu-Ni electrodeposition were also investigated. An increase in Ni salt in the plating bath could enhance the pH, promoting higher CCE and depleting hydrogen evolution at the cathode, leading to the presenting Ni phase in the alloy. The higher concentration of Ni salt in the solution could also enhance the deposition rate due to a shift to a pH value, which affects the roughening of the surface morphology, promoting a higher contact angle. All crystal structures generated by Cu/Cu-Ni electrodeposition were FCC, with the preferred orientation of the (111) plane. Crystallite size and lattice strain depend on the deposition rate. Less crystallite size and lattice strain affect the film's hardness and corrosion resistance. Moreover, the third bath had the resulting Cu-Ni layer with the best hardness and corrosion rate of around 136 HV and 0.081 mmpy.

Keywords

Cathode Current Efficiency, Deposition Rate, Electrodeposition, Corrosion, Hardness

Received: , Accepted:

<https://doi.org/10.26554/sti.2024.9.3.->

1. INTRODUCTION

The electrodeposition procedure is one of the numerous metal coating methods. Metal coating using electrodeposition technology has created many industries that work on coating vehicle engine parts such as pistons, drums, shafts, and other engine parts (Jariwala et al., 2018; Lajevardi et al., 2013). Electrodeposition is done to take advantage of the better properties of the coating element than a substrate. These benefits include heat resistance, a low coefficient of friction, and the prevention of corrosion and erosion properties (Soegijono and Susetyo, 2022; Ghosh et al., 2000; Matsuda et al., 2022). Many factors influence these properties, including solution concentration, temperature, current density, immersion time, pH, and electrical voltage (Kalubowila et al., 2019; Ollivier et al., 2009). Those factors could significantly influence the deposition rate during the electrodeposition process. Moreover, by adjusting

the deposition rate, structure, grain size, crystallite size, and surface morphology could be controlled (Augustin et al., 2016; Gomez et al., 2005; Rosyidan et al., 2024).

Metals such as copper (Cu) and nickel (Ni) are commonly employed in metal electrodeposition (Hakim and Pangestu, 2022; Setiamukti et al., 2020). Ni is corrosion resistant and has sufficient strength and hardness properties; meanwhile, Cu is a soft and ductile metal that is not too oxidized by air. Cu's reduction potential (+0.34 V) and Ni's reduction potential (-0.25 V) indicate that copper is nobler than Ni. As a result, Cu ions dissolve in solution via diffusion, and Ni ions dissolve via charge transfer (Ghosh et al., 2006; Goranova et al., 2016). Therefore, the concentration of Ni and Cu needs special attention (Ganesan et al., 2022). In addition, a complexing agent is needed to reduce the potential gap between Ni and Cu. Several studies reported the use of pyrophosphate, citrate, acetate, sulfamate, and glycine as complexing agents (Silaimani et al., 2015).

Ghosh et al. (2000) conducted Ni-Cu plating with PC and DC apparatus using bath composition 0.475 M $\text{NiSO}_4 \cdot 7\text{H}_2\text{O}$, 0.125 M $\text{CuSO}_4 \cdot 5\text{H}_2\text{O}$, and 0.2 M sodium citrate (pH was maintained using ammonia solution) and resulting corrosion current between 0.17- 5.77 A cm^{-2} in 3% NaCl, hardness between 384-482 KHN₅₀. Dai et al. (2016) fabricated Ni-Cu film with an electrodeposition technique using 300 g L^{-1} Ni sulfamic acid, 2.5 to 15 g L^{-1} Cu sulfates, 20 g L^{-1} Ni chloride, and 20 g L^{-1} boric acid, resulting in a reduction grain size by increasing Cu content in the alloy. Nady and Negem (2016) studied the electrodeposition of Ni-Cu alloys using various pH and concentration of NiSO_4 and CuSO_4 , with fixed sodium gluconate boric acid and cysteine at 0.025 A cm^{-2} of current density resulting in mostly FCC (111) and FCC (200) crystal planes of the alloys. Goranova et al. (2016) fabricated Ni-Cu using electrodeposition in 0.2 $\text{C}_6\text{H}_5\text{Na}_3\text{O}_7 \cdot 2\text{H}_2\text{O}$ with different concentrations of Ni salts (0.2, 0.25, 0.5, and 0.6 M $\text{NiSO}_4 \cdot 7\text{H}_2\text{O}$) and 0.1M $\text{CuSO}_4 \cdot 5\text{H}_2\text{O}$. The pH (~ 9) was maintained using a 25% NH_4OH solution. The study found that increasing Ni salt (0.6 M NiSO_4) has a levelling effect.

Unfortunately, presenting a complexing agent could enhance the cost of production of Cu-Ni alloy. Therefore, presenting a Ni salt as a catalyst (without a complexing agent) in the plating bath needs further investigation. This study aims to create a Cu/Cu-Ni alloy on Cu alloy through electrodeposition and investigate the relationship between physical and hardness-corrosion properties. The layers were made using various solutions at 25°C, and then the CCE and deposition rate were investigated. The Cu/Cu-Ni coating underwent characterization for scanning electron microscope-energy dispersive spectroscopy (SEM-EDS), x-ray diffraction (XRD), hardness, corrosion, and water droplets.

2. EXPERIMENTAL SECTION

2.1 Materials and Preparation

Electrodeposition solutions were made using $\text{CuSO}_4 \cdot 5\text{H}_2\text{O}$ and $\text{NiSO}_4 \cdot 6\text{H}_2\text{O}$. All chemicals used in the present research are analytical grade from Merck manufacturer. Pure Cu and Ni were used as an anode, while Cu alloy was used as a cathode with chemical compositions of P 0.22 wt.%, Cd 0.684 wt.%, Si 0.137 wt.%, and Cu balance. Before electrodeposition, the cathode was cleaned using ultrasonic cleaner (DELTA D68H) for 5 min. Electrodeposition was performed with a current density of 30 mA/cm^2 for 1 hour at 25°C using a power supply (SANFIX 305 E). The specimens were electrodeposited using various plating baths, as seen in Table 1.

2.2 Characterization

The CCE and deposition rate of the Cu/Cu-Ni electrodeposition were investigated by weighing samples before (initial weight) and after (final weight) electrodeposition and then calculated using equations in the previously reported (Soegijono and Susetyo, 2022; Rosyidan et al., 2024). Afterward, XRD (PANalytical Aeris with Cu K radiation, $\lambda=0.15418$ nm, step size=0.02°) was used to determine the crystal structure of the

Table 1. Plating Baths Composition for Cu/Cu-Ni Electrodeposition

Plating Bath	Composition (M)		Measured pH
	$\text{CuSO}_4 \cdot 5\text{H}_2\text{O}$	$\text{NiSO}_4 \cdot 7\text{H}_2\text{O}$	
Bath 1	0.1	0.3	2.35
Bath 2	0.1	0.5	2.51
Bath 3	0.1	0.7	2.53

Cu-Ni coating. MAUD software was used to refine and find the crystal parameter using XRD data. Moreover, the Debye-Scherrer formula (Equation 1) was used to calculate the crystal size of various samples (Seakr, 2017).

$$D = \frac{0.9\lambda}{\beta \cos \theta} \quad (1)$$

Where D is the average crystallite size, k is a Scherrer constant of (0.9), λ is radiation wavelength (nm), β is the width of the FWHM diffraction peak (radians), and θ is peak position (° or radians).

FE-SEM equipped with EDS (Thermofisher Quanta 650 EDAX EDS Analyzer) was used to analyze the film surface morphology and phase. Afterward, roughness analysis was performed according to SEM picture using Image J software. Moreover, the hardness of the Cu-Ni film was measured using a MicroMet®5100 Series micro indentation Vickers hardness tester using 100 g of load for 10 s. Measurement was conducted for five spot indentation.

Corrosion investigation was performed using potentiodynamic polarization methods (Digi-Ivy DY2311) in a 3.5% NaCl solution with a volume of 100 ml, the reference electrode being Ag/AgCl and the counter electrode being platinum (Pt) wire. Potentiodynamic polarization was carried out at a speed of 0.002 Vs^{-1} from -1.35 to -0.05 V. Information on corrosion current (i_{corr}) and corrosion voltage (E_{corr}) was acquired from the measurement data using the Tafel extrapolation method. The corrosion rate was calculated using Equation 2 utilizing the corrosion current information (Ahmad, 2006).

$$\text{Cr} = C \frac{M i_{\text{corr}}}{n_r} \quad (2)$$

Where Cr is the corrosion rate (mmpy), C is a constant for the corrosion rate calculation and is 3.27 mmpy, M is the atomic weight (g mol^{-1}), i_{corr} is corrosion current density (A cm^{-2}), n is the number of electrons involved, and p is the density of Cu and Ni (g cm^{-3}). Last step of the samples characterization is measured water contact angle. The contact angle was observed with a water droplet test on the film surface coated. Some criteria of the angle θ were determined by the value as $\theta < 90^\circ$, $90^\circ \leq \theta < 150^\circ$, and $150^\circ \leq \theta < 180^\circ$ for being hydrophilic, hydrophobic, and super hydrophobic, respectively (Lee et al., 2014).

3. RESULTS AND DISCUSSION

3.1 CCE and Deposition Rate

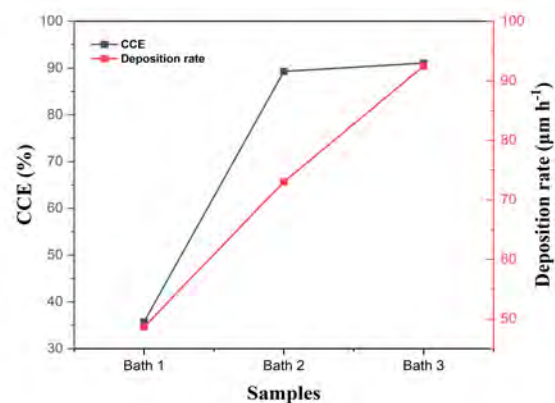


Figure 1. CCE and Deposition Rate for Cu/Cu-Ni Electrodeposited from Bath 1, 2, and 3

Table 2. Average Grain Size Calculation Results of Various Samples

Sample	Grain Size (μm)
Bath 1	105.05
Bath 2	88.22
Bath 3	79.32

Table 3. Average Roughness Value of Various Samples

Sample	Roughness Average (Ra) μm
Bath 1	30.63
Bath 2	37.49
Bath 3	37.82

Table 4. Crystal Parameters of Various Samples

Parameter	Bath 1	Sample Bath 2	Bath 3
Crystal structure		FCC	
Space Group		Fm-3m	
Lattice constant (Å) a = b = c	3.631	3.618	3.612
Cell volume (Å³)	47.89	47.37	47.14
d-spacing (Å)	1.7530	1.7549	1.7578
Crystallite Size (nm)	43.39	27.54	25.70
Lattice strain	0.27	0.41	0.25

The composition of CuSO₄.5H₂O and NiSO₄.6H₂O was determined at the start of the experiment. Figure 1 shows

Table 5. Corrosion Measurements of Various Samples

Sample	i _{corr} (A cm ⁻²)	E _{corr} (V)	Cr (mmpy)	Criteria
Bath 1	4.40×10 ⁻⁶	-0.261	0.196	Good
Bath 2	5.01×10 ⁻⁶	-0.244	0.223	Good
Bath 3	1.82×10 ⁻⁶	-0.248	0.081	Excellent

the CCE and deposition rate results of various experiments. CCE and deposition rate have similar tendencies; an increase in Ni salt would increase both CCE and deposition rate. CCE refers to the fraction of total current used for metal plating (Rosyidan et al., 2024). At the same time, the deposition rate is the amount of anode material deposited on the cathode at a particular current and time (Park et al., 2008). The first, second, and third solutions had a CCE of 35.71, 89.28, and 91.07%, respectively. The first, second, and third solutions had a deposition rate of 48.66, 72.99, and 92.46, respectively. Hacısmailoğlu and Alper (2011) have found that increased pH leads to increased transient current. Moreover, Rosyidan et al. (2024) have seen that an increase in the current leads to a rise in CCE and deposition rate. Therefore, increased Ni salt promotes increased CCE and deposition rate due to rise and pH (see Table 1).

Hydrogen evolution could happen at the cathode when electrodeposition is conducted. Hydrogen evolution could disrupt ion’s movement to the substrate’s surfaces during deposition by blocking the cathode surface. Deo et al. have stated that hydrogen evolution is a competitor at Ni and Cu electrodeposition (Deo et al., 2020). According to the CCE result, higher hydrogen evolution occurred in the samples made using the first solution, and increasing a Ni salt in the solution led to a decrease in hydrogen evolution. Güler et al. (2013) have stated that presenting a hydrogen evolution at the cathode during electrodeposition leads to a decrease in CCE.

3.2 Phase and Surface Morphology

In this study, film deposition involved diffusion and charge transfer by Cu/Cu-Ni. The various films were obtained using a current density of 30 mA cm⁻² for an hour for all solution variations. The results of the EDS investigation can be seen in Figure 2. Based on Figure 2, it can be seen that 100 wt.% Cu phases are seen when electrodeposited using baths 1 and 2. This means presenting a Ni salt 0.3 and 0.5 M doesn’t cause an exhibit of Ni in the film. Meanwhile, when Ni salt concentration rises to 0.7 M, Ni is exhibited in the film around 0.2 wt. %. The solution seems to have a salt limitation, resulting in a Cu-Ni Alloy. Decrease a Cu salt by less than 0.1 M or increasing a Ni salt by more than 0.7 M is needed. Baskaran et al. (2006) electrodeposited Ni using the composition between Ni and Ni and Cu salt, which is 20:1.. Sarac et al. (2012) electrodeposited Ni using the composition between Ni and Cu salt are 50:1. Moreover, Hacısmailoğlu and Alper (2011) have stated that hydrogen evolution was occurring at the surface of the substrate during the electrodeposition process, which could prevent the

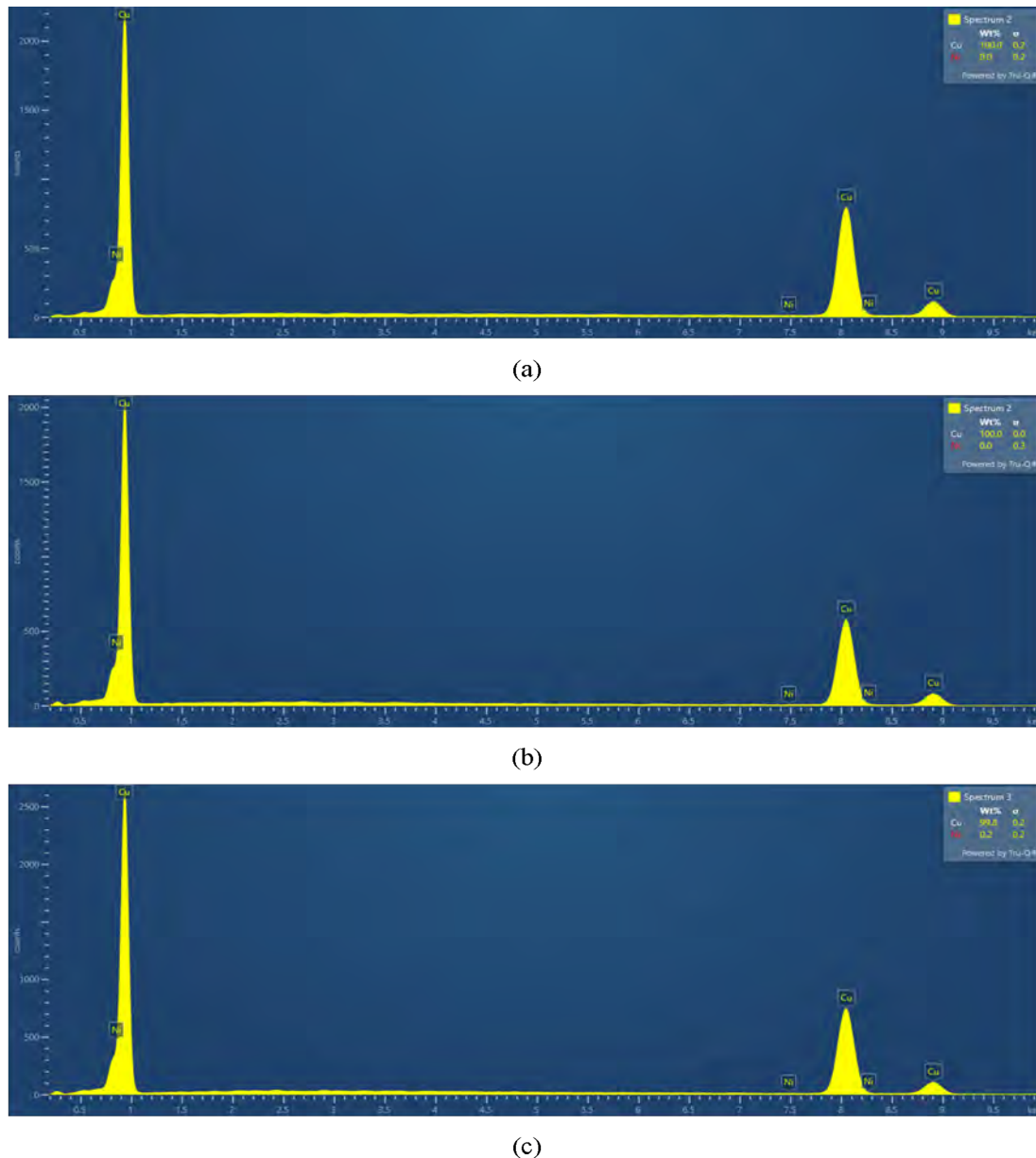


Figure 2. EDS Test Results of Various Samples

reduction of Ni in the film. This statement is corroborated by the fact that Ni formed in the sample was made using a third solution due to electrodeposition using the first and second solutions, which still caused hydrogen evolution on the substrate surface.

Figures 3 (a)-(c) show the morphology of the deposited non-uniform and compact films, which is affected by the hydrogen evolution. Güler et al. (2013) have stated the disruption is due to hydrogen evolution at the cathode, which could be resulting a non-uniform film. Moreover, pure Cu (Figures 3 (a) and (b)) show morphology with nodules form. In contrast, presenting a Ni in the alloy, which changes nodules to a cauliflower-like form (Figure 3 (c)). As mentioned above, exhibiting a Ni salt

in the solution could increase the pH of the solution (Table 1). Kalubowila et al. (2019) have found that increasing the pH bath could transform surface morphology. Furthermore, raising a pH solution leads to an increased deposition rate and change in surface morphology. Therefore, there is transformation from nodules to a cauliflower-like form. Statistical analysis using Image J combined Origin with the corresponding Gauss fitting function was used to identify the grain size distribution. The result is presented in Figure 3.

Image J software was used to calculate the average grain size diameter. Table 2 shows the results of calculating the average grain size. The calculation results show that the grain size average has decreased by increasing the Ni salt in the solution.

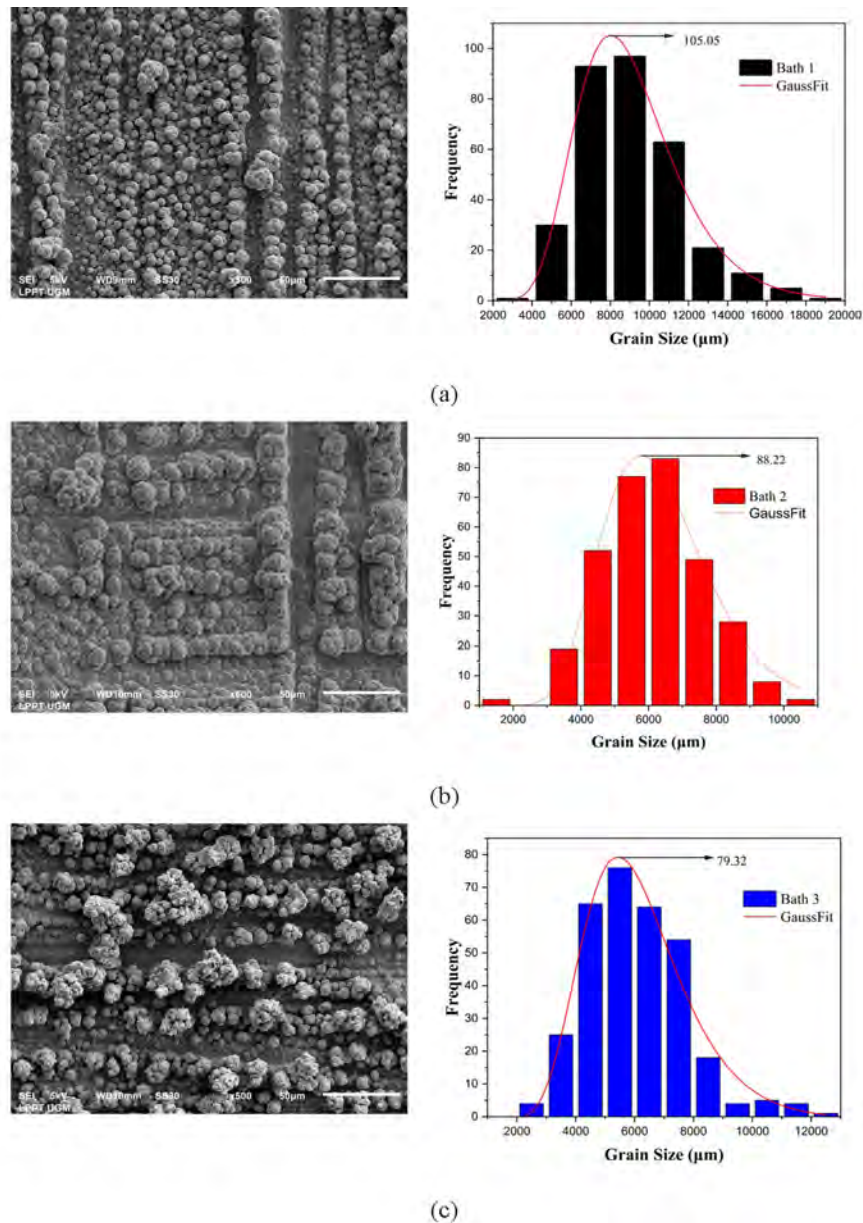


Figure 3. SEM Micrographs and Grain Distribution for Different Samples (a) Bath 1, (b) Bath 2, and (c) Bath 3

Baskaran et al. (2006) stated that grain size decreased due to increased electrodeposition current density. Previous research shows that increasing current density increases deposition rate (Rosyidan et al., 2024). Compared to Figure 1, it is seen that rising Ni salt leads to an increased deposition rate. An increase in the deposition rate leads to an increased speed of the ion species deposited on the cathode surface. Therefore, grain size is decreasing in the present research.

Image processing was done using Image J software to obtain detailed information about the resulting image pattern. Image patterns were investigated from SEM pictures to interpret the results of surface roughness parameters and 3-D images from surface scanning. The result of the Image J software investiga-

tion can be seen in Figure 4, which presents the relationship between distance (μm) and gray value varies with increasing distance.

Table 3 shows the average surface roughness of Cu-Ni/Cu coating morphology fabricated from various baths according to Image J software investigation. According to Table 3, increasing Ni salt in the solution increases the films' roughness average. Deo et al. (2020) reported that increasing a current density led to an increase in surface roughness. As mentioned above, increasing current density increases deposition rate (Rosyidan et al., 2024). Compared to the deposition rate measurement (Figure 1), it can be seen that rising Ni salt leads to an increased deposition rate due to pH increments. An increase in the

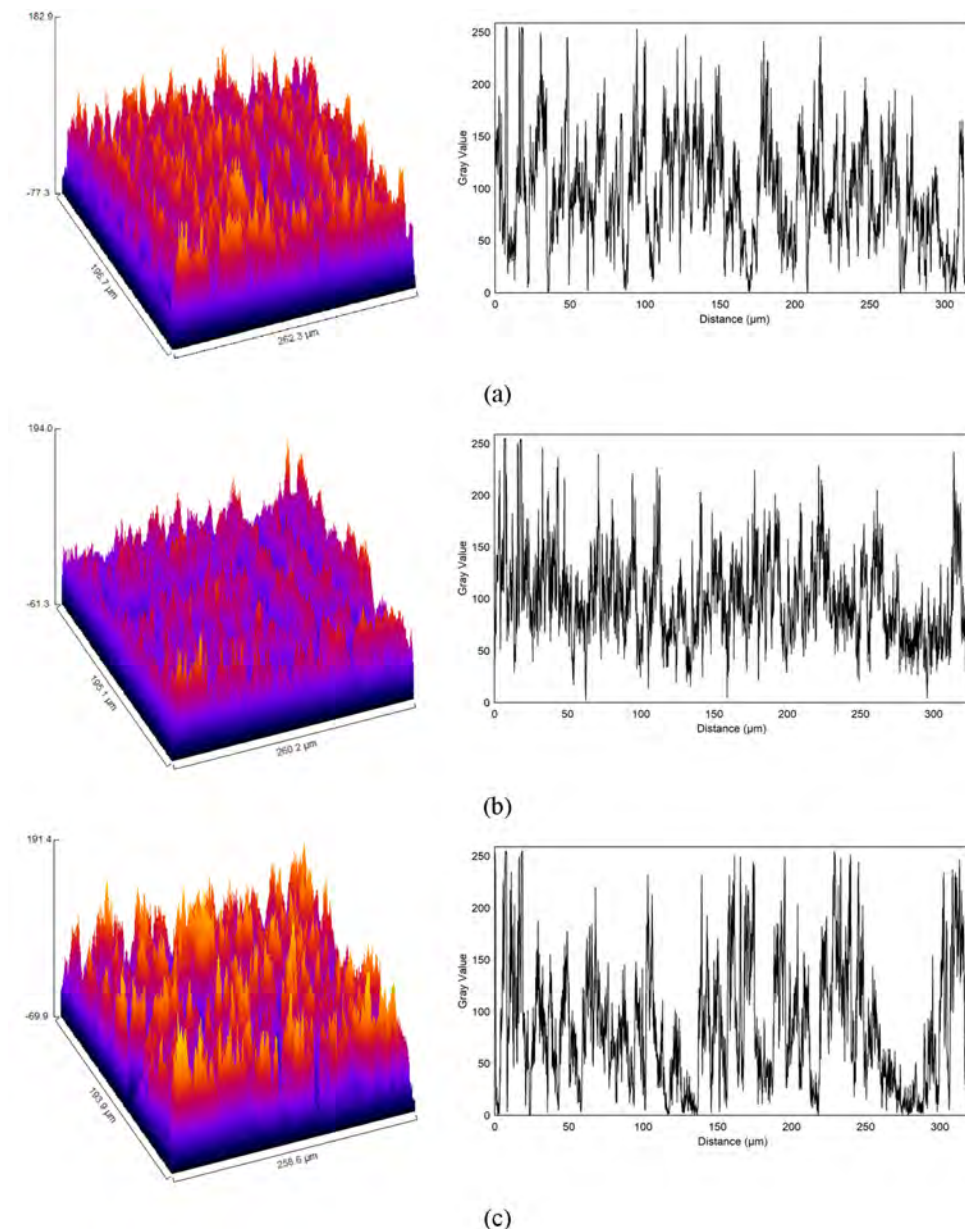


Figure 4. Analysis of Sample Surfaces Roughness in 3D SEM Image and Graph of Grey Value Against Distance (Left-Right) (a) Bath 1, (b) Bath 2, and (c) Bath 3

deposition rate leads to an increased speed of the ion species deposited on the cathode surface. Therefore, the roughness average is increased in the present research.

3.3 Crystallographic Orientation

According to the XRD data in Figure 5, three planes formed namely the (111), (002), and (022) planes. The (111) plane dominated when the films were made using baths 1, 2, and 3. The dominance of the (111) plane orientation had benefits such as anticorrosion, increased electrical conductivity, and improved mechanical properties (Seakr, 2017). Moreover, all of the collected XRD data were then analyzed using MAUD

software, and the crystal parameters are shown in Table 4. All led to the same crystal structure and space group, FCC and Fm-3m, which can be concluded that atoms of the Cu and Ni form a substitutional solid solution (Dai et al., 2016).

Table 4 shows that the lattice constant and cell volume decrease due to the increase in the Ni phase in the alloy, which perfectly agrees with other reports (Baskaran et al., 2006). Moreover, increased Ni salt in the plating bath decreases crystallite size. Augustin et al. (2016) have reported an increase in current density promoting reduced crystallite size. Increasing the electrodeposition process's current density influences the deposition rate's increase; the amount of ion species deposited

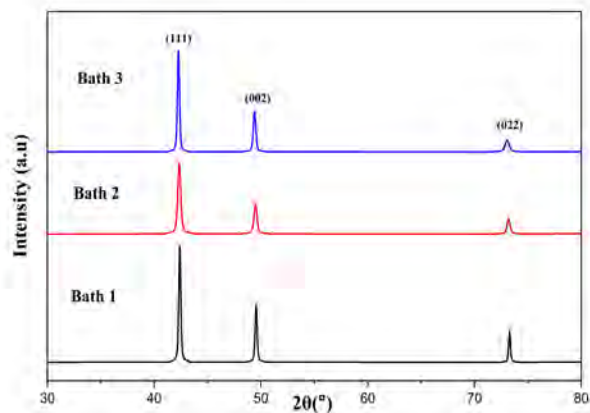


Figure 5. XRD Pattern of Various Samples

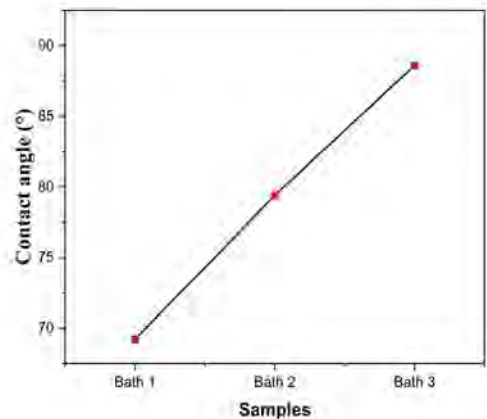


Figure 8. Water contact angle of various samples

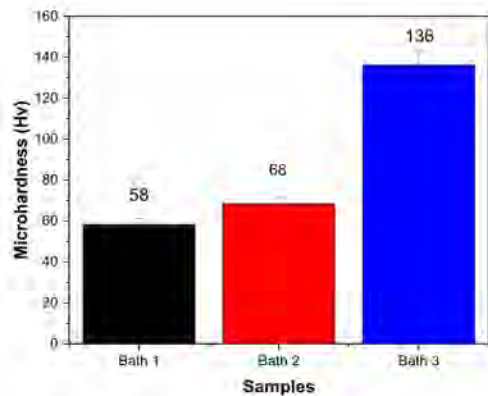


Figure 6. Hardness Test Results of Various Samples

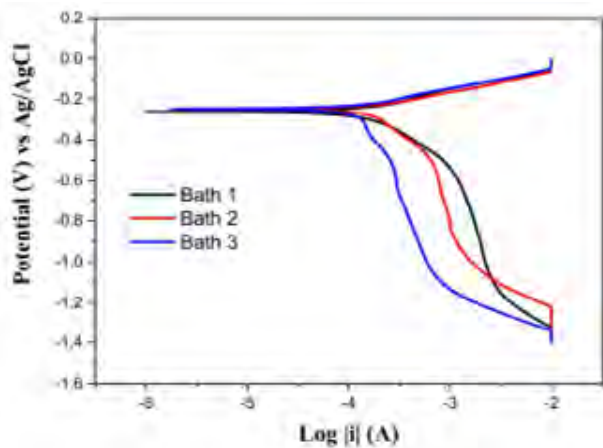


Figure 7. Corrosion Curve for Various Samples

on the cathode rose; therefore, crystallite size decreased. Small crystal size indicates that the distance between grains is close, contributing to material qualities with more roughness proper-

ties (Dai et al., 2016). This result is in perfect agreement with the average roughness in Table 3. Moreover, a smaller lattice strain is seen in the sample made using bath 3.

3.4 Hardness

Hardness is a material’s resistance to plastic deformation. A coating procedure is considered successful if it can enhance the qualities of the coated objects. One of the purposes of electrodeposition in the present research is to improve material deposited hardness. The results of the hardness of the coating were obtained using a Vickers micro-hardness tester. The Vickers microhardness method obtained 58 HV in the first solution, 68 HV in the second solution, and 136 HV in the third solution. It seems an increase in Ni salt would increase the hardness. In their study, Augustin et al. found that a decrease in crystallite size promotes an increase in hardness, which is in perfect agreement with the present research (Augustin et al., 2016). Besides crystallite size, the exhibit of Ni in the alloy also influences the hardness of the sample (Rosyidan et al., 2024). As seen in Figure 6, a sample was made using bath 3, resulting in higher hardness, which is affected by the exhibit of Ni in the alloy. According to the EDS result, only one sample was made using bath 3, resulting in Ni in the alloy. Compared to the Monel 400, hardness is between 150 to 200 HV, and present research has lower hardness (Kukliński et al., 2020).

3.5 Corrosion

Figure 7 shows the corrosion curves of the electrodeposition of Cu/Cu-Ni on the Cu alloy substrate. The i_{corr} and E_{corr} were found using the Tafel extrapolation method. Meanwhile, CR was calculated using Equation (2). The summary of the calculations for the CR of various samples is shown in Table 5. The crystal plane could determine the corrosion rate behavior of materials with the FCC crystal system. The (111) crystal plane is more corrosion-resistant in materials with the FCC system than the (002) and (022) crystal planes (Al Kharafi et al., 2012). Therefore, all of the samples met good and excellent

criteria. Moreover, based on Table 5, it can be seen that the third solution has the best corrosion rate. This behavior is influenced by the lattice strain that was formed. Lattice strain is sample defect concentration measured due to a void core in the lattice (Basori et al., 2023). Therefore, the smallest lattice strain leads to the highest corrosion resistance. According to Wang et al. and Ghosh et al. studies, Monel-400 i_{corr} is 2.24×10^{-6} and 2.2×10^{-6} (A cm^{-2}) (Ghosh et al., 2000; Wang et al., 2014). Compared with Table 5, it can be seen that the sample made using a third solution has lower i_{corr} than Monel-400.

3.6 Contact Angle

The water droplet test can be used to determine the hydrophilic, hydrophobic, and superhydrophobic properties of a film. Figure 8 shows a snapshot of the drip test findings for various samples. All samples possess hydrophilic properties since they have contact angles between 0° and 90° (Thurber et al., 2016). The contact angles achieved in the first, second, and third solution 1 are 69.2° , 79.4° and 88.6° , respectively. Increment of the water contact angle is probably due to an increased film surface roughness. In their research, Huang et al. found that increasing roughness would increase the water contact angle (Huang and Gates, 2020). Moreover, Yu et al. found that increasing electrolyte pH from 2 to 4 increases the film's water contact angle (Yu et al., 2013), probably due to an increase in the surface roughness of the samples.

4. CONCLUSION

Cu/Cu-Ni film was electrodeposited onto Cu alloy using various bath compositions, and according to the multiple findings, increased Ni salt content led to increased deposition rate and CCE due to an increased pH and depleting hydrogen evolution, which impacted grain size, more roughness, less crystallite size and presenting small amount of a Ni in the film. The formed crystal structure was a single-phase FCC with the dominant (111) plane. The hardness increment is due to a decrease in crystallite size. Lesser lattice strain contributed to a higher corrosion resistance. The films have more roughness and impact on the higher water contact angle. The 99.8Cu0.3Ni alloy has the best corrosion resistance and is recommended as an alternative to change Monel-400.

5. ACKNOWLEDGMENT

This project was financially supported by Universitas Trisakti based on the assignment letter number 800/C-4/FTKE/USA KTI/X/2023.

REFERENCES

- Ahmad, Z. (2006). *Principles of Corrosion Engineering and Corrosion Control*. 1th edition. Elsevier
- Al Kharafi, F., I. Ghayad, and R. Abdullah (2012). Corrosion Inhibition of Copper in Non-Polluted and Polluted Sea Water Using 5-Phenyl-1-H-Tetrazole. *International Journal of Electrochemical Science*, 7(4); 3289–3298
- Augustin, A., P. Huilgol, K. R. Udupa, and U. Bhat (2016). Effect of Current Density during Electrodeposition on Microstructure and Hardness of Textured Cu Coating in the Application of Antimicrobial Al Touch Surface. *Journal of the mechanical behavior of Biomedical materials*, 63(October); 352–360
- Baskaran, I., T. S. Narayanan, and A. Stephen (2006). Pulsed Electrodeposition of Nanocrystalline Cu–Ni Alloy Films and Evaluation of Their Characteristic Properties. *Materials Letters*, 60(16); 1990–1995
- Basori, B., B. Soegijono, S. Yudanto, D. Nanto, and F. Susetyo (2023). Effect of Low Magnetic Field during Nickel Electroplating on Morphology, Structure, and Hardness. In *Journal of Physics: Conference Series*, volume 2596. IOP Publishing, page 012014
- Dai, P., C. Zhang, J. Wen, H. Rao, and Q. Wang (2016). Tensile Properties of Electrodeposited Nanocrystalline Ni–Cu Alloys. *Journal of Materials Engineering and Performance*, 25(January); 594–600
- Deo, Y., S. Guha, K. Sarkar, P. Mohanta, D. Pradhan, and A. Mondal (2020). Electrodeposited Ni–Cu Alloy Coatings on Mild Steel for Enhanced Corrosion Properties. *Applied Surface Science*, 515(June); 146078
- Ganesan, M., C.-C. Liu, S. Pandiyarajan, C.-T. Lee, and H.-C. Chuang (2022). Post-Supercritical CO_2 Electrodeposition Approach for Ni–Cu Alloy Fabrication: An Innovative Eco-Friendly Strategy for High-Performance Corrosion Resistance with Durability. *Applied Surface Science*, 577(1); 151955
- Ghosh, S., A. Grover, G. Dey, U. Kulkarni, R. Dusane, A. Suri, and S. Banerjee (2006). Structural Characterization of Electrodeposited Nanophase Ni–Cu Alloys. *Journal of Materials Research*, 21(1); 45–61
- Ghosh, S., A. Grover, G. Dey, and M. Totlani (2000). Nanocrystalline Ni–Cu Alloy Plating by Pulse Electrolysis. *Surface and Coatings Technology*, 126(1); 48–63
- Gomez, E., S. Pane, and E. Valles (2005). Electrodeposition of Co–Ni and Co–Ni–Cu Systems in Sulphate–Citrate Medium. *Electrochimica Acta*, 51(1); 146–153
- Goranova, D., R. Rashkov, G. Avdeev, and V. Tonchev (2016). Electrodeposition of Ni–Cu Alloys at High Current Densities: Details of the Elements Distribution. *Journal of Materials Science*, 51(June); 8663–8673
- Güler, E. S., E. Konca, and İ. Karakaya (2013). Effect of Electrodeposition Parameters on the Current Density of Hydrogen Evolution Reaction in Ni and Ni–MoS₂ Composite Coatings. *International Journal of Electrochemical Science*, 8(4); 5496–5505
- Hacıismailoğlu, M. Ş. and M. Alper (2011). Effect of Electrolyte pH and Cu Concentration on Microstructure of Electrodeposited Ni–Cu Alloy Films. *Surface and Coatings Technology*, 206(6); 1430–1438
- Hakim, M. S. and H. Pangestu (2022). Preparation and Application of Nickel Electroplating on Copper (Ni/EC) Electrode for Glucose Detection. *Science and Technology Indonesia*, 7(2);

- 208–212
- Huang, X. and I. Gates (2020). Apparent Contact Angle around the Periphery of a Liquid Drop on Roughened Surfaces. *Scientific Reports*, **10**(1); 8220
- Jariwala, F., R. Gohil, P. Trivedi, J. Parmar, B. Borda, S. Patel, B. Goyal, and V. Rao (2018). Electroplating of Nickel and Chromium on Aluminum 6082-T6 Alloy. *Proceedings of the International Conference on Recent Advances in Metallurgy for Sustainable Development*, pages 1–3
- Kalubowila, K., K. Jayathileka, L. Kumara, K. Ohara, S. Kohara, O. Sakata, M. Gunewardene, J. Jayasundara, D. Dissanayake, and J. Jayanetti (2019). Effect of Bath pH on Electronic and Morphological Properties of Electrodeposited Cu_2O Thin Films. *Journal of The Electrochemical Society*, **166**(4); D113
- Kukliński, M., A. Bartkowska, D. Przystacki, and G. Kinal (2020). Influence of Microstructure and Chemical Composition on Microhardness and Wear Properties of Laser Borided Monel 400. *Materials*, **13**(24); 5757
- Lajevardi, S., T. Shahrabi, J. Szpunar, A. S. Rouhaghdam, and S. Sanjabi (2013). Characterization of the Microstructure and Texture of Functionally Graded Nickel- Al_2O_3 Nano Composite Coating Produced by Pulse Deposition. *Surface and Coatings Technology*, **232**(October); 851–859
- Lee, J. M., K. M. Bae, K. K. Jung, J. H. Jeong, and J. S. Ko (2014). Creation of Microstructured Surfaces Using Cu–Ni Composite Electrodeposition and Their Application to Superhydrophobic Surfaces. *Applied Surface Science*, **289**(January); 14–20
- Matsuda, T., R. Saeki, M. Hayashida, and T. Ohgai (2022). Microhardness and Heat-Resistance Performance of Ferromagnetic Cobalt-Molybdenum Nanocrystals Electrodeposited from an Aqueous Solution Containing Citric Acid. *Materials Research Express*, **9**(4); 046502
- Nady, H. and M. Negem (2016). Ni-Cu Nano-Crystalline Alloys for Efficient Electrochemical Hydrogen Production in Acid Water. *RSC Advances*, **6**(56); 51111–51119
- Ollivier, A., L. Muhr, S. Delbos, P. Grand, M. Matlosz, and E. Chassaing (2009). Copper–Nickel Codeposition As a Model for Mass-Transfer Characterization in Copper–Indium–Selenium Thin-Film Production. *Journal of Applied Electrochemistry*, **39**(May); 2337–2344
- Park, B. N., Y. S. Sohn, and S. Y. Choi (2008). Effects of a Magnetic Field on the Copper Metallization Using the Electroplating Process. *Microelectronic Engineering*, **85**(2); 308–314
- Rosyidan, C., B. Kurniawan, B. Soegijono, V. Vidia Putra, D. R. Munazat, and F. B. Susetyo (2024). Effect of Current Density on Magnetic and Hardness Properties of Ni-Cu Alloy Coated on Al Via Electrodeposition. *International Journal of Engineering*, **37**(2); 213–223
- Sarac, U., R. M. Öksüzöğlü, and M. C. Baykul (2012). Deposition Potential Dependence of Composition, Microstructure, and Surface Morphology of Electrodeposited Ni–Cu Alloy Films. *Journal of Materials Science: Materials in Electronics*, **23**(April); 2110–2116
- Seakr, R. (2017). Microstructure and Crystallographic Characteristics of Nanocrystalline Copper Prepared from Acetate Solutions by Electrodeposition Technique. *Transactions of Nonferrous Metals Society of China*, **27**(6); 1423–1430
- Setiamukti, D., A. Khusnani, and M. Toifur (2020). The Effect of Electrolyte Concentration on the Sensitivity of Low-Temperature Sensor Performance of Cu/nl Film. *Science and Technology Indonesia*, **5**(2); 28–33
- Silaimani, S., G. Vivekanandan, and P. Veeramani (2015). Nano-Nickel-Copper Alloy Deposit for Improved Corrosion Resistance in Marine Environment. *International Journal of Environmental Science and Technology*, **12**(May); 2299–2306
- Soegijono, B. and F. Susetyo (2022). Magnetic Field Exposure on Electroplating Process of Ferromagnetic Nickel Ion on Copper Substrate. In *Journal of Physics: Conference Series*, volume 2377. IOP Publishing, page 012002
- Thurber, C. R., Y. H. Ahmad, S. F. Sanders, A. Al-Shenawa, N. D'Souza, A. M. Mohamed, and T. D. Golden (2016). Electrodeposition of 70-30 Cu-Ni Nanocomposite Coatings for Enhanced Mechanical and Corrosion Properties. *Current Applied Physics*, **16**(3); 387–396
- Wang, S., X. Guo, H. Yang, J. Dai, R. Zhu, J. Gong, L. Peng, and W. Ding (2014). Electrodeposition Mechanism and Characterization of Ni-Cu Alloy Coatings from a Eutectic-Based Ionic Liquid. *Applied Surface Science*, **288**(January); 530–536
- Yu, Q., Z. Zeng, W. Zhao, M. Li, X. Wu, and Q. Xue (2013). Fabrication of Adhesive Superhydrophobic Ni-Cu-P Alloy Coatings with High Mechanical Strength by One Step Electrodeposition. *Colloids and Surfaces A: Physicochemical and Engineering Aspects*, **427**(June); 1–6

Nickel Salt Dependency as Catalyst in the Plating Bath on the Film Properties of Cu/Cu-Ni

by Cahaya Rosyidan FTKE

Submission date: 12-Aug-2024 02:33PM (UTC+0700)

Submission ID: 2426507799

File name: STI_template_13.pdf (3.57M)

Word count: 5100

Character count: 26591

7
Nickel Salt Dependency as Catalyst in the Plating Bath on the Film Properties of Cu/Cu-Ni

Cahaya Rosyidan^{1*}, Budhy Kurniawan², Bambang Soegijono³, Mustamina Maulani¹, Lisa Samura¹, Frederik Gresia Nababan¹, Valentinus Galih Vidia Putra⁴, Ferry Budhi Susetyo⁵

¹Department of Petroleum Engineering, Universitas Trisakti, Jakarta, 11440, Indonesia

²Department of Physics, Universitas Indonesia, Depok, 16424, Indonesia

³Department of Geoscience, Universitas Indonesia, Depok, 16424, Indonesia

⁴Plasma and Nanomaterial Research Group, Politeknik STTT Bandung, Bandung, 40272, Indonesia

⁵Department of Mechanical Engineering, Universitas Negeri Jakarta, Jakarta, 13220, Indonesia

*Corresponding author: cahayarosyidan@trisakti.ac.id

Abstract

Metal plating frequently employs nickel (Ni) and copper (Cu) as anodes. Cu/Cu-Ni film formed has many advantages, such as better corrosion resistance and high hardness characteristics. This study aims to assess the properties of Cu/Cu-Ni film, such as phase, surface morphology, crystallographic orientation, hardness, corrosion analysis, and contact angle, which were fabricated using electrodeposition with various Ni salt additions (0.3, 0.5 and 0.7 M). In addition, the cathode current efficiency (CCE) and deposition rate of the Cu/Cu-Ni electrodeposition were also investigated. An increase in Ni salt in the plating bath could enhance the pH, promoting higher CCE and depleting hydrogen evolution at the cathode, leading to the presenting Ni phase in the alloy. The higher concentration of Ni salt in the solution could also enhance the deposition rate due to a shift to a pH value, which affects the roughening of the surface morphology, promoting a higher contact angle. All crystal structures generated by Cu/Cu-Ni electrodeposition were FCC, with the preferred orientation of the (111) plane. Crystallite size and lattice strain depend on the deposition rate. Less crystallite size and lattice strain affect the film's hardness and corrosion resistance. Moreover, the third bath had the resulting Cu-Ni layer with the best hardness and corrosion rate of around 136 HV and 0.081 mmpy.

Keywords

Cathode Current Efficiency, Deposition Rate, Electrodeposition, Corrosion, Hardness

Received: , Accepted:

<https://doi.org/10.26554/sti.2024.9.3.->

1. INTRODUCTION

The electrodeposition procedure is one of the numerous metal coating methods. Metal coating using electrodeposition technology has created many industries that work on coating vehicle engine parts such as pistons, drums, shafts, and other engine parts (Jariwala et al., 2018; Lajevardi et al., 2013). Electrodeposition is done to take advantage of the better properties of the coating element than a substrate. These benefits include heat resistance, a low coefficient of friction, and the prevention of corrosion and erosion properties (Soegijono and Susetyo, 2022; Ghosh et al., 2000; Matsuda et al., 2022). Many factors influence these properties, including solution concentration, temperature, current density, immersion time, pH, and electrical voltage (Kalubowila et al., 2019; Ollivier et al., 2009). Those factors could significantly influence the deposition rate during the electrodeposition process. Moreover, by adjusting

31
the deposition rate, structure, grain size, crystallite size, and surface morphology could be controlled (Augustin et al., 2016; Gomez et al., 2005; Rosyidan et al., 2024).

Metals such as copper (Cu) and nickel (Ni) are commonly employed in metal electrodeposition (Hakim and Pangestu, 2022; Setiamukti et al., 2020). Ni is corrosion resistant and has sufficient strength and hardness properties; meanwhile, Cu is a soft and ductile metal that is not too oxidized by air. Cu's reduction potential (+0.34 V) and Ni's reduction potential (-0.25 V) indicate that copper is nobler than Ni. As a result, Cu ions dissolve in solution via diffusion, and Ni ions dissolve via charge transfer (Ghosh et al., 2006; Goranova et al., 2016). Therefore, the concentration of Ni and Cu needs special attention (Ganesan et al., 2022). In addition, a complexing agent is needed to reduce the potential gap between Ni and Cu. Several studies reported the use of pyrophosphate, citrate, acetate, sulfamate, and glycine as complexing agents (Silaimani et al., 2015).

Ghosh et al. (2000) conducted Ni-Cu plating with PC and DC apparatus using bath composition 0.475 M $\text{NiSO}_4 \cdot 7\text{H}_2\text{O}$, 0.125 M $\text{CuSO}_4 \cdot 5\text{H}_2\text{O}$, and 0.2 M sodium citrate (pH was maintained using ammonia solution) and resulting corrosion current between $0.17 - 5.77 \text{ A cm}^{-2}$ in 3% NaCl, hardness between 384–482 KHN₅₀. Dai et al. (2016) fabricated Ni-Cu film with an electrodeposition technique using 300 g L^{-1} Ni sulfamic acid, 2.5 to 15 g L^{-1} Cu sulfates, 20 g L^{-1} Ni chloride, and 20 g L^{-1} boric acid, resulting in a reduction grain size by increasing Cu content in the alloy. Nady and Nagem (2016) studied the electrodeposition of Ni-Cu alloys using various pH and concentration of NiSO_4 and CuSO_4 , with fixed sodium gluconate boric acid and cysteine at 0.025 A cm^{-2} of current density resulting in mostly FCC (111) and FCC (200) crystal planes of the alloys. Goranova et al. (2016) fabricated Ni-Cu using electrodeposition in $0.2 \text{ C}_6\text{H}_5\text{Na}_3\text{O}_7 \cdot 2\text{H}_2\text{O}$ with different concentrations of Ni salts (0.2, 0.25, 0.5, and 0.6 M $\text{NiSO}_4 \cdot 7\text{H}_2\text{O}$) and 0.1M $\text{CuSO}_4 \cdot 5\text{H}_2\text{O}$. The pH (~9) was maintained using a 25% NH_4OH solution. The study found that increasing Ni salt (0.6 M NiSO_4) has a levelling effect.

Unfortunately, presenting a complexing agent could enhance the cost of production of Cu-Ni alloy. Therefore, presenting a Ni salt as a catalyst (without a complexing agent) in the plating bath needs further investigation. This study aims to create a Cu/Cu-Ni alloy on Cu alloy through electrodeposition and investigate the relationship between physical and hardness-corrosion properties. The layers were made using various solutions at 25°C , and then the CCE and deposition rate were investigated. The Cu/Cu-Ni coating underwent characterization for scanning electron microscope-energy dispersive spectroscopy (SEM-EDS), x-ray diffraction (XRD), hardness, corrosion, and water droplets.

2. EXPERIMENTAL SECTION

2.1 Materials and Preparation

Electrodeposition solutions were made using $\text{CuSO}_4 \cdot 5\text{H}_2\text{O}$ and $\text{NiSO}_4 \cdot 6\text{H}_2\text{O}$. All chemicals used in the present research are analytical grade from Merck manufacturer. Pure Cu and Ni were used as an anode, while Cu alloy was used as a cathode with chemical compositions of P 0.22 wt.%, Cd 0.684 wt.%, Si 0.137 wt.%, and Cu balance. Before electrodeposition, the cathode was cleaned using ultrasonic cleaner (DELTA D68H) for 5 min. Electrodeposition was performed with a current density of 30 mA/cm^2 for 1 hour at 25°C using a power supply (SANFIX 305 E). The specimens were electrodeposited using various plating baths, as seen in Table 1.

2.2 Characterization

The CCE and deposition rate of the Cu/Cu-Ni electrodeposition were investigated by weighing samples before (initial weight) and after (final weight) electrodeposition and then calculated using equations in the previously reported (Saegjiono and Susetyo, 2022; Rosyidan et al., 2024). Afterward, XRD (PANalytical Aeris with Cu K radiation, $\lambda=0.15418 \text{ nm}$, step size= 0.02°) was used to determine the crystal structure of the

Table 1. Plating Baths Composition for Cu/Cu-Ni Electrodeposition

Plating Bath	Composition (M)		Measured pH
	$\text{CuSO}_4 \cdot 5\text{H}_2\text{O}$	$\text{NiSO}_4 \cdot 7\text{H}_2\text{O}$	
Bath 1	0.1	0.3	2.35
Bath 2	0.1	0.5	2.51
Bath 3	0.1	0.7	2.53

Cu-Ni coating. MAUD software was used to refine and find the crystal parameter using XRD data. Moreover, the Debye-Scherrer formula (Equation 1) was used to calculate the crystal size of various samples (Seakr, 2017).

$$D = \frac{0.9\lambda}{\beta \cos \theta} \quad (1)$$

Where D is the average crystallite size, k is a Scherrer constant of (0.9), λ is radiation wavelength (nm), β is the width of the FWHM diffraction peak (radians), and θ is peak position ($^\circ$ or radians).

FE-SEM equipped with EDS (Thermofisher Quanta 650 EDAX EDS Analyzer) was used to analyze the film surface morphology and phase. Afterward, roughness analysis was performed according to SEM picture using Image J software. Moreover, the hardness of the Cu-Ni film was measured using a MicroMet®5100 Series micro indentation Vickers hardness tester using 100 g of load for 10 s. Measurement was conducted for five spot indentation.

Corrosion investigation was performed using potentiodynamic polarization methods (Digi-Lvy DY2311) in a 3.5% NaCl solution with a volume of 100 ml, the reference electrode being Ag/AgCl and the counter electrode being platinum (Pt) wire. Potentiodynamic polarization was carried out at a speed of 0.002 Vs^{-1} from -1.35 to -0.05 V. Information on corrosion current (i_{corr}) and corrosion voltage (E_{corr}) was acquired from the measurement data using the Tafel extrapolation method. The corrosion rate was calculated using Equation 2 utilizing the corrosion current information (Almad, 2006).

$$\text{Cr} = C \frac{M_{\text{corr}}}{n_f} \quad (2)$$

Where Cr is the corrosion rate (mmpy), C is a constant for the corrosion rate calculation and is 3.27 mmpy, M is the atomic weight (g mol^{-1}), i_{corr} is corrosion current density (A cm^{-2}), n is the number of electrons involved, and p is the density of Cu and Ni (g cm^{-3}). Last step of the samples characterization is measured water contact angle. The contact angle was observed with a water droplet test on the film surface coated. Some criteria of the angle θ were determined by the value as $\theta < 90^\circ$, $90^\circ \leq \theta < 150^\circ$, and $150^\circ \leq \theta < 180^\circ$ for being hydrophilic, hydrophobic, and super hydrophobic, respectively (Lee et al., 2014).

10 3. RESULTS AND DISCUSSION

3.1 CCE and Deposition Rate

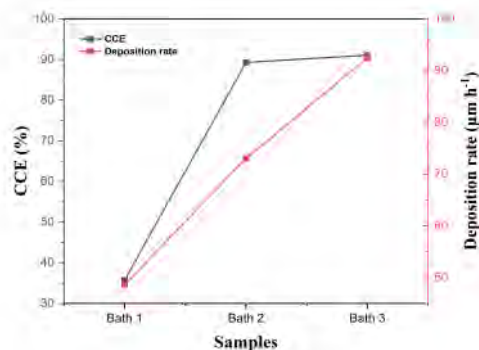


Figure 1. CCE and Deposition Rate for Cu/Cu-Ni Electrodeposited from Bath 1, 2, and 3

Table 2. Average Grain Size Calculation Results of Various Samples

Sample	Grain Size (μm)
Bath 1	105.05
Bath 2	88.22
Bath 3	79.32

Table 3. Average Roughness Value of Various Samples

Sample	Roughness Average (Ra) μm
Bath 1	30.63
Bath 2	37.49
Bath 3	37.82

Table 4. Crystal Parameters of Various Samples

Parameter	Bath 1	Bath 2	Bath 3
Crystal structure	FCC		
Space Group	Fm-3m		
Lattice constant (Å) a = b = c	3.631	3.618	3.612
Cell volume (Å³)	47.89	47.37	47.14
d-spacing (Å)	1.7530	1.7549	1.7578
Crystallite Size (nm)	43.39	27.54	25.70
Lattice strain	0.27	0.41	0.25

The composition of $\text{CuSO}_4 \cdot 5\text{H}_2\text{O}$ and $\text{NiSO}_4 \cdot 6\text{H}_2\text{O}$ was determined at the start of the experiment. Figure 1 shows

Table 5. Corrosion Measurements of Various Samples

Sample	i_{corr} (A cm ⁻²)	E_{corr} (V)	Cr (mmpy)	Criteria
Bath 1	4.40×10^{-6}	-0.261	0.196	Good
Bath 2	5.01×10^{-6}	-0.244	0.223	Good
Bath 3	1.82×10^{-6}	-0.248	0.081	Excellent

the CCE and deposition rate results of various experiments. CCE and deposition rate have similar tendencies; an increase in Ni salt would increase both CCE and deposition rate. CCE refers to the fraction of total current used for metal plating (Rosyidan et al., 2024). At the same time, the deposition rate is the amount of anode material deposited on the cathode at a particular current and time (Park et al., 2008). The first, second, and third solutions had a CCE of 35.71, 89.28, and 91.07%, respectively. The first, second, and third solutions had a deposition rate of 48.66, 72.99, and 92.46, respectively. Hacismailoglu and Alper (2011) have found that increased pH leads to increased transient current. Moreover, Rosyidan et al. (2024) have seen that an increase in the current leads to a rise in CCE and deposition rate. Therefore, increased Ni salt promotes increased CCE and deposition rate due to rise and pH (see Table 1).

Hydrogen evolution could happen at the cathode when electrodeposition is conducted. Hydrogen evolution could disruption's movement to the substrate's surfaces during deposition by blocking the cathode surface. Deo et al. have stated that hydrogen evolution is a competitor at Ni and Cu electrodeposition (Deo et al., 2020). According to the CCE result, higher hydrogen evolution occurred in the samples made using the first solution, and increasing a Ni salt in the solution led to a decrease in hydrogen evolution. Güler et al. (2013) have stated that presenting a hydrogen evolution at the cathode during electrodeposition leads to a decrease in CCE.

3.2 Phase and Surface Morphology

In this study, film deposition involved diffusion and charge transfer by Cu/Cu-Ni. The various films were obtained using a current density of 30 mA cm^{-2} for an hour for all solution variations. The results of the EDS investigation can be seen in Figure 2. Based on Figure 2, it can be seen that 100 wt.% Cu phases are seen when electrodeposited using baths 1 and 2. This means presenting a Ni salt 0.3 and 0.5 M doesn't cause an exhibit of Ni in the film. Meanwhile, when Ni salt concentration rises to 0.7 M, Ni is exhibited in the film around 0.2 wt. %. The solution seems to have a salt limitation, resulting in a Cu-Ni Alloy. Decrease a Cu salt by less than 0.1 M or increasing a Ni salt by more than 0.7 M is needed. Baskaran et al. (2006) electrodeposited Ni using the composition between Ni and Cu salt, which is 20:1. Sarac et al. (2012) electrodeposited Ni using the composition between Ni and Cu salt are 50:1. Moreover, Hacismailoglu and Alper (2011) have stated that hydrogen evolution was occurring at the surface of the substrate during the electrodeposition process, which could prevent the

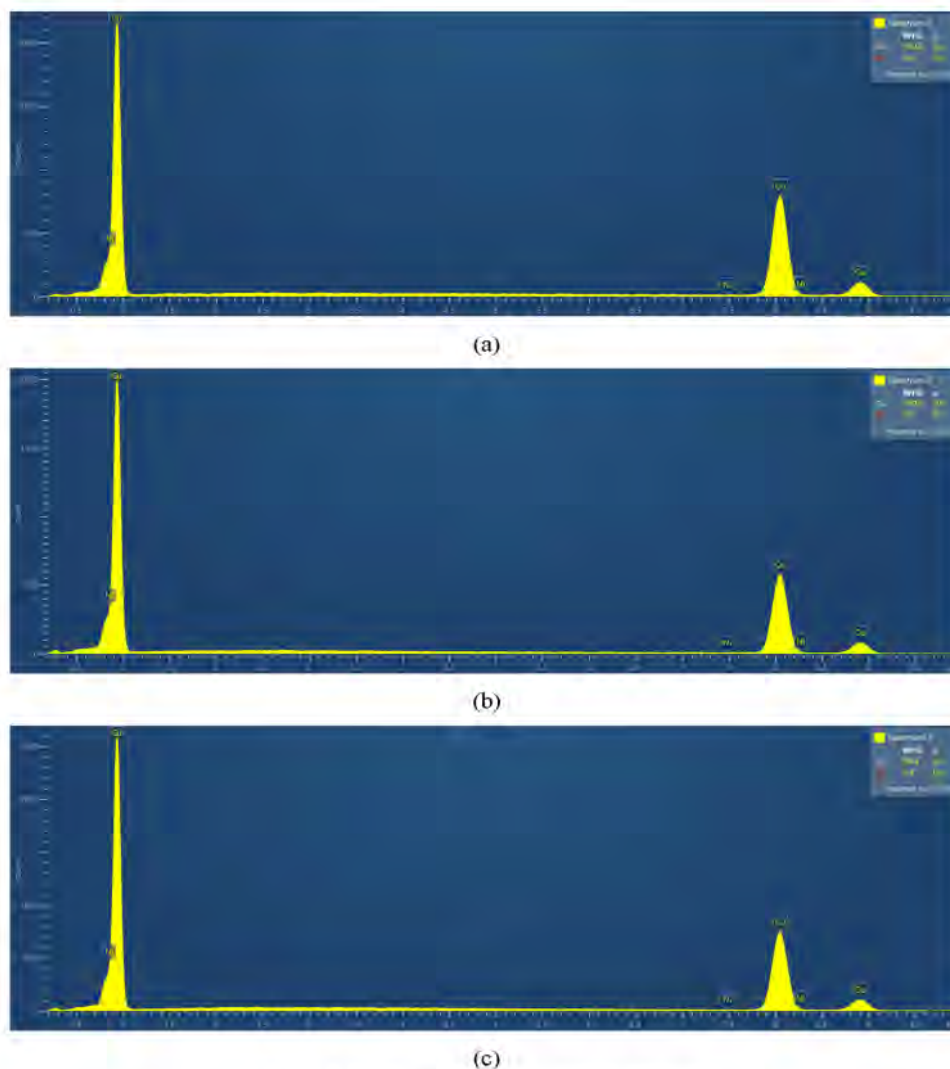


Figure 2. EDS Test Results of Various Samples

reduction of Ni in the film. This statement is corroborated by the fact that Ni formed in the sample was made using a third solution due to electrodeposition using the first and second solutions, which still caused hydrogen evolution on the substrate surface.

Figures 3 (a)-(c) show the morphology of the deposited non-uniform and compact films, which is affected by the hydrogen evolution. Güler et al. (2013) have stated the disruption is due to hydrogen evolution at the cathode, which could be resulting a non-uniform film. Moreover, pure Cu (Figures 3 (a) and (b)) show morphology with nodules form. In contrast, presenting a Ni in the alloy, which changes nodules to a cauliflower-like form (Figure 3 (c)). As mentioned above, exhibiting a Ni salt

in the solution could increase the pH of the solution (Table 1). Kalubowila et al. (2019) have found that increasing the pH bath could transform surface morphology. Furthermore, raising a pH solution leads to an increased deposition rate and change in surface morphology. Therefore, there is transformation from nodules to a cauliflower-like form. Statistical analysis using Image J combined Origin with the corresponding Gauss fitting function was used to identify the grain size distribution. The result is presented in Figure 3.

Image J software was used to calculate the average grain size diameter. Table 2 shows the results of calculating the average grain size. The calculation results show that the grain size average has decreased by increasing the Ni salt in the solution.

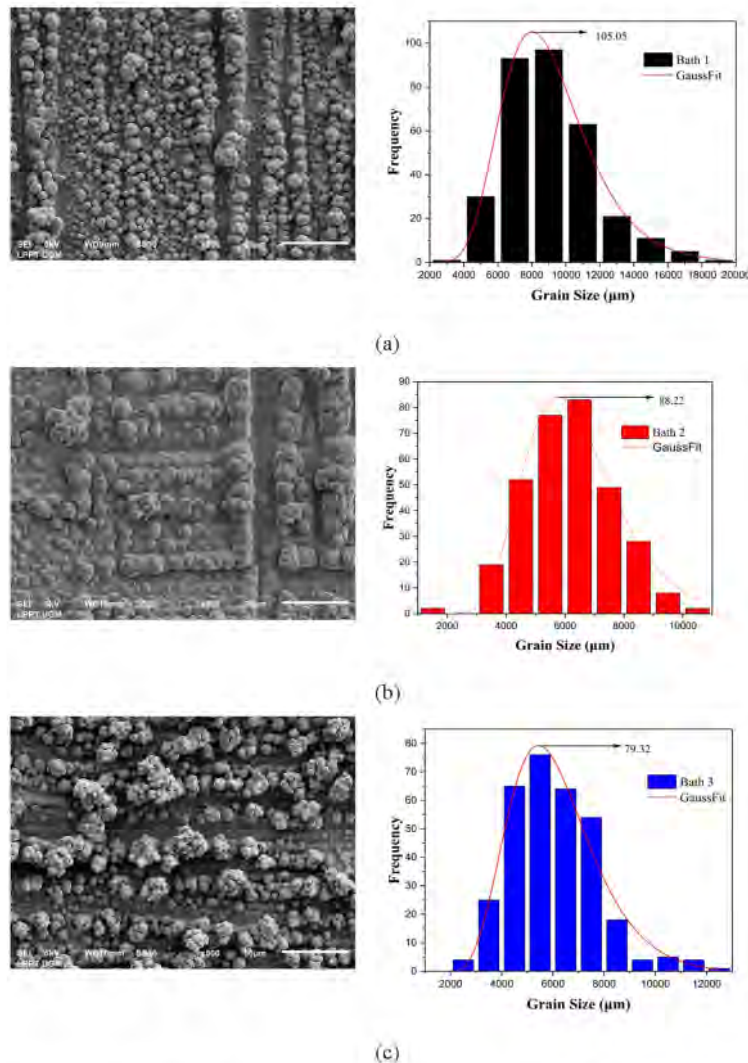


Figure 3. SEM Micrographs and Grain Distribution for Different Samples (a) Bath 1, (b) Bath 2, and (c) Bath 3

Baskaran et al. (2006) stated that grain size decreased due to increased electrodeposition current density. Previous research shows that increasing current density increases deposition rate (Rosyidan et al., 2024). Compared to Figure 1, it is seen that rising Ni salt leads to an increased deposition rate. An increase in the deposition rate leads to an increased speed of the ion species deposited on the cathode surface. Therefore, grain size is decreasing in the present research.

Image processing was done using Image J software to obtain detailed information about the resulting image pattern. Image patterns were investigated from SEM pictures to interpret the results of surface roughness parameters and 3-D images from surface scanning. The result of the Image J software investiga-

tion can be seen in Figure 4, which presents the relationship between distance (μm) and gray value varies with increasing distance.

Table 3 shows the average surface roughness of Cu-Ni/Cu coating morphology fabricated from various baths according to Image J software investigation. According to Table 3, increasing Ni salt in the solution increases the films' roughness average. Deo et al. (2020) reported that increasing a current density led to an increase in surface roughness. As mentioned above, increasing current density increases deposition rate (Rosyidan et al., 2024). Compared to the deposition rate measurement (Figure 1), it can be seen that rising Ni salt leads to an increased deposition rate due to pH increments. An increase in the

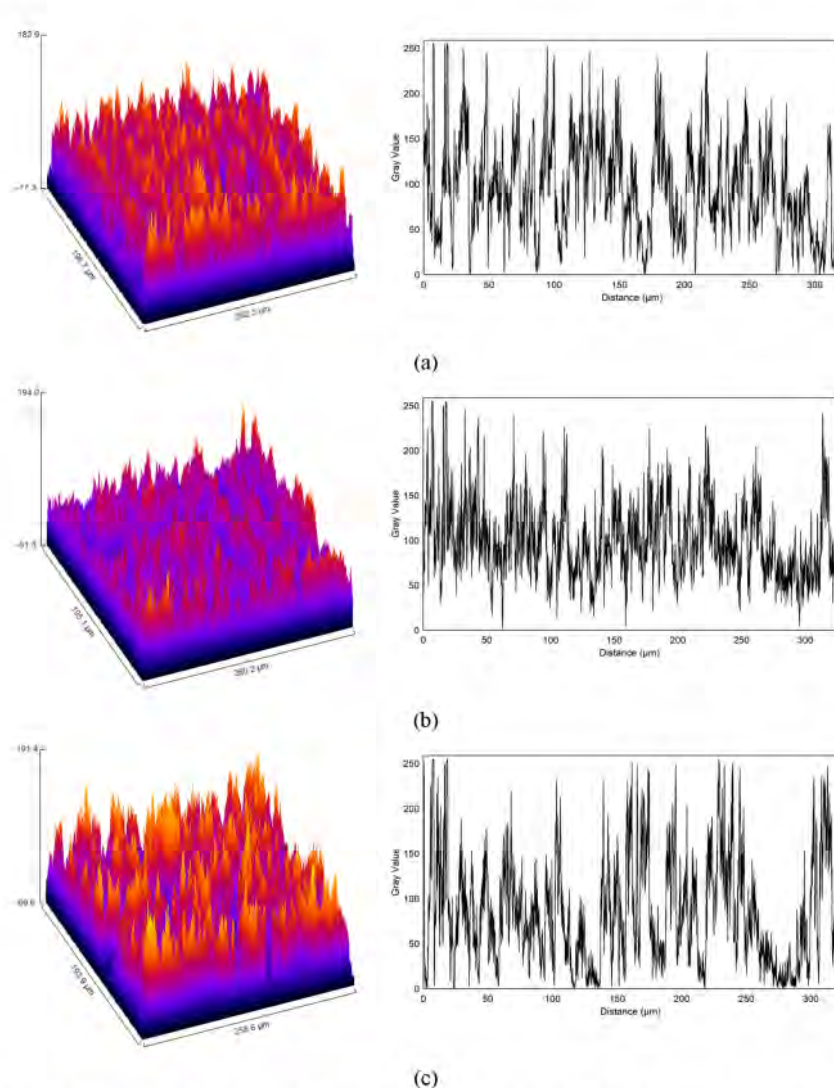


Figure 4. Analysis of Sample Surfaces Roughness in 3D SEM Image and Graph of Grey Value Against Distance (Left-Right) (a) Bath 1, (b) Bath 2, and (c) Bath 3

9
deposition rate leads to an increased speed of the ion species deposited on the cathode surface. Therefore, the roughness average is increased in the present research.

3.3 Crystallographic Orientation

According to the XRD data in Figure 5, three planes formed namely the (111), (002), and (022) planes. The (111) plane dominated when the films were made using baths 1, 2, and 3. The dominance of the (111) plane orientation had benefits such as anticorrosion, increased electrical conductivity, and improved mechanical properties (Seakr, 2017). Moreover, all of the collected XRD data were then analyzed using MAUD

software, and the crystal parameters are shown in Table 4. All led to the same crystal structure and space group, FCC and Fm-3m, which can be concluded that atoms of the Cu and Ni form a substitutional solid solution (Dai et al., 2016).

Table 4 shows that the lattice constant and cell volume decrease due to the increase in the Ni phase in the alloy, which perfectly agrees with other reports (Baskaran et al., 2006). Moreover, increased Ni salt in the plating bath decreases crystallite size. Augustin et al. (2016) have reported an increase in current density promoting reduced crystallite size. Increasing the electrodeposition process's current density influences the deposition rate's increase; the amount of ion species deposited

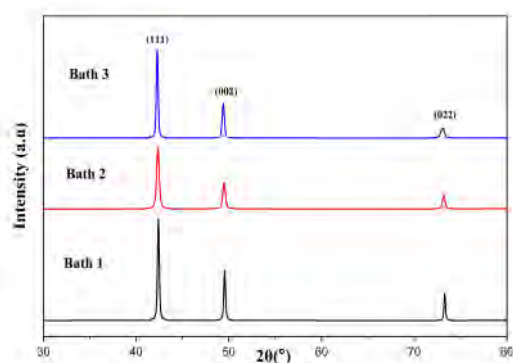


Figure 5. XRD Pattern of Various Samples

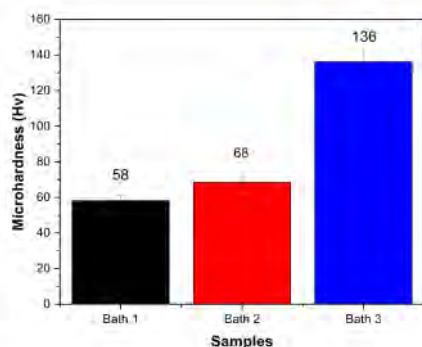


Figure 6. Hardness Test Results of Various Samples

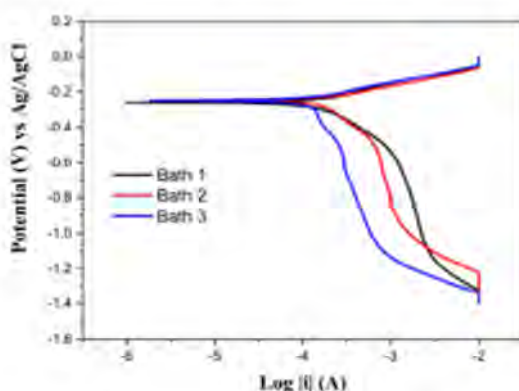


Figure 7. Corrosion Curve for Various Samples

on the cathode rose; therefore, crystallite size decreased. Small crystal size indicates that the distance between grains is close, contributing to material qualities with more roughness proper-

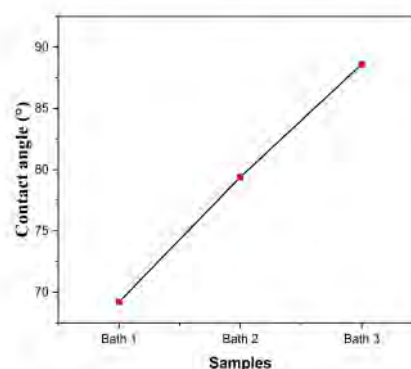


Figure 8. Water contact angle of various samples

ties (Dai et al., 2016). This result is in perfect agreement with the average roughness in Table 3. Moreover, a smaller lattice strain is seen in the sample made using bath 3.

3.4 Hardness

Hardness is a material's resistance to plastic deformation. A coating procedure is considered successful if it can enhance the qualities of the coated objects. One of the purposes of electrodeposition in the present research is to improve material deposited hardness. The results of the hardness of the coating were obtained using a Vickers micro-hardness tester. The Vickers microhardness method obtained 58 HV in the first solution, 68 HV in the second solution, and 136 HV in the third solution. It seems an increase in Ni salt would increase the hardness. In their study, Augustin et al. found that a decrease in crystallite size promotes an increase in hardness, which is in perfect agreement with the present research (Augustin et al., 2016). Besides crystallite size, the exhibit of Ni in the alloy also influences the hardness of the sample (Rosyidan et al., 2024). As seen in Figure 6, a sample was made using bath 3, resulting in higher hardness, which is affected by the exhibit of Ni in the alloy. According to the EDS result, only one sample was made using bath 3, resulting in Ni in the alloy. Compared to the Monel 400, hardness is between 150 to 200 HV, and present research has lower hardness (Kuklinski et al., 2020).

3.5 Corrosion

Figure 7 shows the corrosion curves of the electrodeposition of Cu/Cu-Ni on the Cu alloy substrate. The i_{corr} and E_{corr} were found using the Tafel extrapolation method. Meanwhile, CR was calculated using Equation (2). The summary of the calculations for the CR of various samples is shown in Table 5. The crystal plane could determine the corrosion rate behavior of materials with the FCC crystal system. The (111) crystal plane is more corrosion-resistant in materials with the FCC system than the (002) and (022) crystal planes (Al Khwarafi et al., 2012). Therefore, all of the samples met good and excellent

criteria. Moreover, based on Table 5, it can be seen that the third solution has the best corrosion rate. This behavior is influenced by the lattice strain that was formed. Lattice strain is sample defect concentration measured due to a void core in the lattice (Basori et al., 2023). Therefore, the smallest lattice strain leads to the highest corrosion resistance. According to Wang et al. and Ghosh et al. studies, Monel-400 i_{corr} is 2.24×10^{-6} and 2.2×10^{-6} ($A\ cm^{-2}$) (Ghosh et al., 2000; Wang et al., 2014). Compared with Table 5, it can be seen that the sample made using a third solution has lower i_{corr} than Monel-400.

3.6 Contact Angle

The water droplet test can be used to determine the hydrophilic, hydrophobic, and superhydrophobic properties of a film. Figure 8 shows a snapshot of the drip test findings for various samples. All samples possess hydrophilic properties since they have contact angles between 0° and 90° (Thurber et al., 2016). The contact angles achieved in the first, second, and third solution 1 are 69.2° , 79.4° and 88.6° , respectively. Increment of the water contact angle is probably due to an increased film surface roughness. In their research, Huang et al. found that increasing roughness would increase the water contact angle (Huang and Gates, 2020). Moreover, Yu et al. found that increasing electrolyte pH from 2 to 4 increases the film's water contact angle (Yu et al., 2013), probably due to an increase in the surface roughness of the samples.

4. CONCLUSION

Cu/Cu-Ni film was electrodeposited onto Cu alloy using various bath compositions, and according to the multiple findings, increased Ni salt content led to increased deposition rate and CCE due to an increased pH and depleting hydrogen evolution, which impacted grain size, more roughness, less crystallite size and presenting small amount of a Ni in the film. The formed crystal structure was a single-phase FCC with the dominant (111) plane. The hardness increment is due to a decrease in crystallite size. Lesser lattice strain contributed to a higher corrosion resistance. The films have more roughness and impact on the higher water contact angle. The 99.8Cu0.3Ni alloy has the best corrosion resistance and is recommended as an alternative to change Monel-400.

5. ACKNOWLEDGMENT

This project was financially supported by Universitas Trisakti based on the assignment letter number 800/C-4/FTKE/USA KTI/X/2023.

REFERENCES

Ahmad, Z. (2006). *Principles of Corrosion Engineering and Corrosion Control*. 1st edition. Elsevier

Al Kharafi, F., I. Ghayad, and R. Abdullah (2012). Corrosion Inhibition of Copper in Non-Polluted and Polluted Sea Water Using 5-Phenyl-1-H-Tetrazole. *International Journal of Electrochemical Science*, 7(4); 3289-3298

Augustin, A., P. Huilgol, K. R. Udupa, and U. Bhat (2016). Effect of Current Density during Electrodeposition on Microstructure and Hardness of Textured Cu Coating in the Application of Antimicrobial Al Touch Surface. *Journal of the mechanical behavior of Biomedical materials*, 63(October); 352-360

Baskaran, I., T. S. Narayanan, and A. Stephen (2006). Pulsed Electrodeposition of Nanocrystalline Cu-Ni Alloy Films and Evaluation of Their Characteristic Properties. *Materials Letters*, 60(16); 1990-1995

Basori, B., B. Soegijono, S. Yudanto, D. Nanto, and F. Susetyo (2023). Effect of Low Magnetic Field during Nickel Electroplating on Morphology, Structure, and Hardness. In *Journal of Physics: Conference Series*, volume 2596. IOP Publishing, page 012014

Dai, P., C. Zhang, J. Wen, H. Rao, and Q. Wang (2016). Tensile Properties of Electrodeposited Nanocrystalline Ni-Cu Alloys. *Journal of Materials Engineering and Performance*, 25(January); 594-600

Deo, Y., S. Guha, K. Sarkar, P. Mohanta, D. Pradhan, and A. Mondal (2020). Electrodeposited Ni-Cu Alloy Coatings on Mild Steel for Enhanced Corrosion Properties. *Applied Surface Science*, 515(June); 146078

Ganesan, M., C.-C. Liu, S. Pandiyarajan, C.-T. Lee, and H.-C. Chuang (2022). Post-Supercritical CO₂ Electrodeposition Approach for Ni-Cu Alloy Fabrication: An Innovative Eco-Friendly Strategy for High-Performance Corrosion Resistance with Durability. *Applied Surface Science*, 577(1); 151955

Ghosh, S., A. Grover, G. Dey, U. Kulkarni, R. Dusane, A. Suri, and S. Banerjee (2006). Structural Characterization of Electrodeposited Nanophase Ni-Cu Alloys. *Journal of Materials Research*, 21(1); 45-61

Ghosh, S., A. Grover, G. Dey, and M. Totlani (2000). Nanocrystalline Ni-Cu Alloy Plating by Pulse Electrolysis. *Surface and Coatings Technology*, 126(1); 48-63

Gomez, E., S. Pane, and E. Valles (2005). Electrodeposition of Co-Ni and Co-Ni-Cu Systems in Sulphate-Citrate Medium. *Electrochimica Acta*, 51(1); 146-153

Goranova, D., R. Rashkov, G. Avdeev, and V. Tonchev (2016). Electrodeposition of Ni-Cu Alloys at High Current Densities: Details of the Elements Distribution. *Journal of Materials Science*, 51(June); 8663-8673

Güler, E. S., E. Konca, and I. Karakaya (2013). Effect of Electrodeposition Parameters on the Current Density of Hydrogen Evolution Reaction in Ni and Ni-MoS₂ Composite Coatings. *International Journal of Electrochemical Science*, 8(4); 5496-5505

Hacıismailoğlu, M. Ş. and M. Alper (2011). Effect of Electrolyte pH and Cu Concentration on Microstructure of Electrodeposited Ni-Cu Alloy Films. *Surface and Coatings Technology*, 206(6); 1430-1438

Hakim, M. S. and H. Pangestu (2022). Preparation and Application of Nickel Electroplating on Copper (Ni/EC) Electrode for Glucose Detection. *Science and Technology Indonesia*, 7(2);

- 208–212
- Huang, X. and L. Gates (2020). Apparent Contact Angle around the Periphery of a Liquid Drop on Roughened Surfaces. *Scientific Reports*, **10**(1); 8220
- Jariwala, F., R. Gohil, P. Trivedi, J. Parmar, B. Borda, S. Patel, B. Goyal, and V. Rao (2018). Electroplating of Nickel and Chromium on Aluminum 6082-T6 Alloy. *Proceedings of the International Conference on Recent Advances in Metallurgy for Sustainable Development*, pages 1–3
- Kalubowila, K., K. Jayathileka, L. Kumara, K. Ohara, S. Kohara, O. Sakata, M. Guncwardene, J. Jayasundara, D. Dissanayake, and J. Jayanetti (2019). Effect of Bath pH on Electronic and Morphological Properties of Electrodeposited Cu₂O Thin Films. *Journal of The Electrochemical Society*, **166**(4); D113
- Kukliniski, M., A. Bartkowska, D. Przestacki, and G. Kinal (2020). Influence of Microstructure and Chemical Composition on Microhardness and Wear Properties of Laser Borided Monel 400. *Materials*, **13**(24); 5757
- Lajevardi, S., T. Shahrabi, J. Szpumar, A. S. Rouhaghdam, and S. Sanjabi (2013). Characterization of the Microstructure and Texture of Functionally Graded Nickel-Al₂O₃ Nano Composite Coating Produced by Pulse Deposition. *Surface and Coatings Technology*, **232**(October); 851–859
- Lee, J. M., K. M. Bae, K. K. Jung, J. H. Jeong, and J. S. Ko (2014). Creation of Microstructured Surfaces Using Cu–Ni Composite Electrodeposition and Their Application to Superhydrophobic Surfaces. *Applied Surface Science*, **289**(January); 14–20
- Matsuda, T., R. Sacki, M. Hayashida, and T. Ohgai (2022). Microhardness and Heat-Resistance Performance of Ferromagnetic Cobalt-Molybdenum Nanocrystals Electrodeposited from an Aqueous Solution Containing Citric Acid. *Materials Research Express*, **9**(4); 046502
- Nady, H. and M. Negem (2016). Ni-Cu Nano-Crystalline Alloys for Efficient Electrochemical Hydrogen Production in Acid Water. *RSC Advances*, **6**(56); 51111–51119
- Ollivier, A., L. Muhr, S. Delbos, P. Grand, M. Matlosz, and E. Chassaing (2009). Copper–Nickel Codeposition As a Model for Mass-Transfer Characterization in Copper–Indium–Selenium Thin-Film Production. *Journal of Applied Electrochemistry*, **39**(May); 2337–2344
- Park, B. N., Y. S. Solm, and S. Y. Choi (2008). Effects of a Magnetic Field on the Copper Metallization Using the Electroplating Process. *Microelectronic Engineering*, **85**(2); 308–314
- Rosyidan, C., B. Kurniawan, B. Soegijono, V. Vidia Putra, D. R. Munazat, and F. B. Susetyo (2024). Effect of Current Density on Magnetic and Hardness Properties of Ni-Cu Alloy Coated on Al Via Electrodeposition. *International Journal of Engineering*, **37**(2); 213–223
- Sarac, U., R. M. Öksüzoglu, and M. C. Baykul (2012). Deposition Potential Dependence of Composition, Microstructure, and Surface Morphology of Electrodeposited Ni–Cu Alloy Films. *Journal of Materials Science: Materials in Electronics*, **23**(April); 2110–2116
- Seakr, R. (2017). Microstructure and Crystallographic Characteristics of Nanocrystalline Copper Prepared from Acetate Solutions by Electrodeposition Technique. *Transactions of Nonferrous Metals Society of China*, **27**(6); 1423–1430
- Setiamukti, D., A. Khusnani, and M. Toifur (2020). The Effect of Electrolyte Concentration on the Sensitivity of Low-Temperature Sensor Performance of Cu/Ni Film. *Science and Technology Indonesia*, **5**(2); 28–33
- Silaimani, S., G. Vivekanandan, and P. Veeramani (2015). Nano-Nickel-Copper Alloy Deposit for Improved Corrosion Resistance in Marine Environment. *International Journal of Environmental Science and Technology*, **12**(May); 2299–2306
- Soegijono, B. and F. Susetyo (2022). Magnetic Field Exposure on Electroplating Process of Ferromagnetic Nickel Ion on Copper Substrate. In *Journal of Physics: Conference Series*, volume 2377. IOP Publishing, page 012002
- Thurber, C. R., Y. H. Ahmad, S. F. Sanders, A. Al-Shenawa, N. D'Souza, A. M. Mohamed, and T. D. Golden (2016). Electrodeposition of 70–30 Cu–Ni Nanocomposite Coatings for Enhanced Mechanical and Corrosion Properties. *Current Applied Physics*, **16**(3); 387–396
- Wang, S., X. Guo, H. Yang, J. Dai, R. Zhu, J. Gong, L. Peng, and W. Ding (2014). Electrodeposition Mechanism and Characterization of Ni–Cu Alloy Coatings from a Eutectic-Based Ionic Liquid. *Applied Surface Science*, **288**(January); 530–536
- Yu, Q., Z. Zeng, W. Zhao, M. Li, X. Wu, and Q. Xue (2013). Fabrication of Adhesive Superhydrophobic Ni–Cu–P Alloy Coatings with High Mechanical Strength by One Step Electrodeposition. *Colloids and Surfaces A: Physicochemical and Engineering Aspects*, **427**(June); 1–6

Nickel Salt Dependency as Catalyst in the Plating Bath on the Film Properties of Cu/Cu-Ni

ORIGINALITY REPORT

13%
SIMILARITY INDEX

8%
INTERNET SOURCES

9%
PUBLICATIONS

3%
STUDENT PAPERS

PRIMARY SOURCES

1	Submitted to Sriwijaya University Student Paper	1%
2	sciencetechindonesia.com Internet Source	1%
3	journal.unimma.ac.id Internet Source	1%
4	www.mdpi.com Internet Source	1%
5	"Proceedings of the 9th International Conference and Exhibition on Sustainable Energy and Advanced Materials", Springer Science and Business Media LLC, 2024 Publication	1%
6	Submitted to Universitas Indonesia Student Paper	1%
7	www.sciencetechindonesia.com Internet Source	1%

8

P. Q. Dai, C. Zhang, J. C. Wen, H. C. Rao, Q. T. Wang. "Tensile Properties of Electrodeposited Nanocrystalline Ni-Cu Alloys", Journal of Materials Engineering and Performance, 2016

Publication

1 %

9

eprints.utm.my

Internet Source

<1 %

10

link.springer.com

Internet Source

<1 %

11

Yashwardhan Deo, Sounak Guha, Kuntal Sarkar, Puspanjali Mohanta, Debabrata Pradhan, Avik Mondal. "Electrodeposited Ni-Cu alloy coatings on mild steel for enhanced corrosion properties", Applied Surface Science, 2020

Publication

<1 %

12

Submitted to Indian Institute of Technology, Kanpur

Student Paper

<1 %

13

Imam Basori, Irene Angela, David Jendra, Bondan T. Sofyan. "Deformation Characteristics and Texture Development of Biadded Cu-29Zn Alloys", IOP Conference Series: Materials Science and Engineering, 2018

Publication

<1 %

14

Syamsuir Syamsuir, Ferry Budhi Susetyo, Bambang Soegijono, Sigit Dwi Yudanto et al. "Rotating-Magnetic-Field-Assisted Electrodeposition of Copper for Ambulance Medical Equipment", Automotive Experiences, 2023

Publication

<1 %

15

Wego Wang. "Reverse Engineering - Technology of Reinvention", CRC Press, 2019

Publication

<1 %

16

He, Z.r.. "Influencing factors of martensitic transformation behavior of Ni₆₀Al₁₉Mn₁₆Fe₅ high-temperature shape memory alloy", Journal of Alloys and Compounds, 20030825

Publication

<1 %

17

coek.info

Internet Source

<1 %

18

eprints.polsri.ac.id

Internet Source

<1 %

19

Lin, Xiao, Lili Tan, Peng Wan, Xiaoming Yu, Ke Yang, Zhuangqi Hu, Yangde Li, and Weirong Li. "Characterization of micro-arc oxidation coating post-treated by hydrofluoric acid on biodegradable ZK60 magnesium alloy", Surface and Coatings Technology, 2013.

Publication

<1 %

20 Savaş Kaya, Ime Bassey Obot, Demet Özkır, Goncagül Serdaroğlu, Ambrish Singh. "Corrosion Science - Theoretical and Practical Applications", Apple Academic Press, 2023
Publication <1 %

21 Zainul Huda. "Metallurgy for Physicists and Engineers - Fundamentals, Applications, and Calculations", CRC Press, 2020
Publication <1 %

22 ir.uitm.edu.my
Internet Source <1 %

23 www.science.gov
Internet Source <1 %

24 Baosong Li, Tianyong Mei, Dandan Li, Shengsong Du, Weiwei Zhang. "Structural and corrosion behavior of Ni-Cu and Ni-Cu/ZrO₂ composite coating electrodeposited from sulphate-citrate bath at low Cu concentration with additives", Journal of Alloys and Compounds, 2019
Publication <1 %

25 F. L. G. Silva, D. C. B. do Lago, E. D'Elia, L. F. Senna. "Electrodeposition of Cu-Zn alloy coatings from citrate baths containing benzotriazole and cysteine as additives", Journal of Applied Electrochemistry, 2010
Publication <1 %

26

Hongbin Zhang, Fengxia Xu, Jindong Wang, Xiulin Liu. "Impact of SiC particle size upon the microstructure and characteristics of Ni-SiC nanocomposites", Journal of the Indian Chemical Society, 2022

Publication

<1 %

27

Ivana O. Mladenović, Jelena S. Lamovec, Dana Vasiljević-Radović, Nikola Vuković, Vesna Radojević, Nebojša D. Nikolić. "Correlation between morphology and hardness of electrolytically produced copper thin films", Journal of Solid State Electrochemistry, 2024

Publication

<1 %

28

MohammadBagher Sohrabi, Hossein Tavakoli, Hassan Koohestani, Matin Akbari. "Utilization of Ni-Cu/Al₂O₃ co-deposition composite coatings on mild steel surface via electroplating method and evaluation of its tribological, electrochemical properties", Surface and Coatings Technology, 2023

Publication

<1 %

29

Y. Raghupathy, K.A. Natarajan, Chandan Srivastava. "Microstructure, electrochemical behaviour and bio-fouling of electrodeposited nickel matrix-silver nanoparticles composite coatings on copper", Surface and Coatings Technology, 2017

Publication

<1 %

30

open.library.ubc.ca

Internet Source

<1 %

31

www.ije.ir

Internet Source

<1 %

32

www.nature.com

Internet Source

<1 %

33

www.scielo.br

Internet Source

<1 %

34

Casey R. Thurber, Yahia H. Ahmad, Stephen F. Sanders, Amaal Al-Shenawa, Nandika D'Souza, Adel M.A. Mohamed, Teresa D. Golden. "Electrodeposition of 70-30 Cu-Ni nanocomposite coatings for enhanced mechanical and corrosion properties", Current Applied Physics, 2016

Publication

<1 %

35

Yang, Xuchao. "Investigation of Dual-phase Nanocrystalline Ni-Cu Electrodeposits.", University of Toronto (Canada), 2018

Publication

<1 %

Exclude quotes

Off

Exclude matches

Off

Exclude bibliography

On

Nickel Salt Dependency as Catalyst in the Plating Bath on the Film Properties of Cu/Cu-Ni

GRADEMARK REPORT

FINAL GRADE

GENERAL COMMENTS

/100

PAGE 1

PAGE 2

PAGE 3

PAGE 4

PAGE 5

PAGE 6

PAGE 7

PAGE 8

PAGE 9

BUKTI KORESPONDENSI
ARTIKEL JURNAL NASIONAL TERKREDITASI dan INTERNASIONAL
BEREPUTASI

Judul Artikel : Nickel Salt Dependency as Catalyst in the Plating Bath on the Film Properties of Cu/Cu-Ni

Jurnal : Science and Technology Indonesia

Penulis : Cahaya Rosyidan, Budhy Kurniawan, Bambang Soegijono, Mustamina Maulani, Lisa Samura, Frederik Gresia Nababan, Valentinus Galih Vidia Putra, Ferry Budhi Susetyo

No	Perihal	Tanggal
1	Bukti konfirmasi submit artikel dan artikel yang disubmit	5 Febuari 2025
2	Bukti konfirmasi reviewer	28 Maret 2025
3	Bukti menjawab reviewer	3 April 2025
4	Keputusan Editor	4 April 2025
5	Bukti artikel terbit	Juli 2025

1. Bukti konfirmasi submit artikel
dan artikel yang disubmit
(5 Februari 2025)

Bukti pengiriman di OJS

The screenshot displays the 'Publication' tab in the OJS workflow. It features a 'Submission Files' section with a search bar and a table of files. Below this is a 'Pre-Review Discussions' section with an 'Add discussion' button and a table that currently shows 'No Items'.

Submission Files			
6494	Cahaya STI 5 Feb 2024.docx	February 5, 2024	Manuscript
6495	CTA-STI 2020.pdf	February 5, 2024	Statement of Agreement
6932	Double blind_STI 1142.docx	March 28, 2024	Manuscript

[Download All Files](#)

Pre-Review Discussions				
Name	From	Last Reply	Replies	Closed
No Items				

Bukti melalui Email

The email is titled '[STI] Submission Acknowledgement' and is from Prof. Aldes Lesbani, Ph.D. to the user. It acknowledges the submission of a manuscript and provides instructions on how to track its progress through the journal's website.

[STI] Submission Acknowledgement External Inbox x

Prof. Aldes Lesbani, Ph.D. <scitechindones@gmail.com>
to me ▾ Feb 5, 2024, 9:10 PM ☆ ↶ ⋮

Dear cahaya:

Thank you for submitting your manuscript entitled "Nickel Salt Dependency as Catalyst in the Plating Bath on the Film Properties of Cu/Cu-Ni" to Science and Technology Indonesia. Now, your manuscript will be considered by the editor and section editor before further peer-review process. With the online journal management system that we are using, you will be able to track its progress through the editorial process by logging in to the journal website:

Submission URL: <https://scitechindonesia.com/index.php/sti/authorDashboard/submission/1142>
Username: cahayarosyidan

If you have any questions, please contact me. Thank you for considering this journal as a venue for your work.

Science and Technology Indonesia

A Peer-Reviewed Research Journal of Science and Technology
p-ISSN: 2580-4405 | e-ISSN: 2580-4391
E-mail: admin@scitechindonesia.com | scitechindonesia@gmail.com
Homepage: <http://scitechindonesia.com/index.php/sti>

Nickel Salt Dependency as Catalyst in the Plating Bath on the Film Properties of Cu/Cu-Ni

Cahaya Rosyidan^{1,*}, Budhy Kurniawan², Bambang Soegijono³, Mustamina Maulani¹, Lisa Samura¹, Frederik Gresia Nababan¹, Valentinus Galih Vidia Putra⁴, Ferry Budhi Susetyo⁵

¹*Petroleum Engineering, Universitas Trisakti, Jakarta 11440, Indonesia*

²*Departement of Physics, Universitas Indonesia, Depok 16424, Indonesia*

³*Department of Geoscience, Universitas Indonesia, Depok 16424, Indonesia*

⁴*Plasma and Nanomaterial Research Group, Politeknik STTT Bandung, Bandung 40272, Indonesia*

⁵*Department of Mechanical Engineering, Universitas Negeri Jakarta, Jakarta 13220, Indonesia*

*Corresponding Author e-mail: cahayarosyidan@trisakti.ac.id

Abstract

Metal plating frequently employs nickel (Ni) and copper (Cu) as anodes. Cu/ Cu-Ni film formed has many advantages, such as better corrosion resistance and high hardness characteristics. This study aims to assess the properties of Cu/Cu-Ni film, such as phase, surface morphology, crystallographic orientation, hardness, corrosion analysis, and contact angle, which were fabricated using electrodeposition with various Ni salt additions. In addition, the cathode current efficiency (CCE) and deposition rate of the Cu/Cu-Ni electrodeposition were also investigated. An increase in Ni salt in the plating bath could enhance the pH, promoting higher CCE and depleting hydrogen evolution at the cathode, leading to the presenting Ni phase in the alloy. The higher concentration of Ni salt in the solution could also enhance the deposition rate due to a shift to a pH value, which affects the roughening of the surface morphology, promoting a higher contact angle. All crystal structures generated by Cu/Cu-Ni electrodeposition were FCC, with the preferred orientation of the (111) plane. Crystallite size and lattice strain depend on the deposition rate. Less crystallite size and lattice strain affect the film's hardness and corrosion resistance. Moreover, the third bath had the resulting Cu-Ni layer with the best hardness and corrosion rate of around 136 HV and 0.081mmpy.

Keywords: *Electrodeposition, SEM-EDS, XRD, Corrosion, Hardness*

1. Introduction

The electrodeposition procedure is one of the numerous metal coating methods. Metal coating

using electrodeposition technology has created many industries that work on coating vehicle engine parts such as pistons, drums, shafts, and other engine parts (Jariwala et al., 2018; Lajevardi, Shahrabi, Szpunar, Sabour Rouhaghdam, & Sanjabi, 2013). Electrodeposition is done to take advantage of the better properties of the coating element than a substrate. These benefits include heat resistance, a low coefficient of friction, and the prevention of corrosion and erosion properties (Basori, Soegijono, Yudanto, Nanto, & Susetyo, 2023; Ghosh, Grover, Dey, & Totlani, 2000; Matsuda, Saeki, Hayashida, & Ohgai, 2022).

Many factors influence these properties, including solution concentration, temperature, current density, immersion time, pH, and electrical voltage (Kalubowila et al., 2019; Ollivier et al., 2009). Those factors could significantly influence the deposition rate during the electrodeposition process. Moreover, by adjusting the deposition rate, structure, grain size, crystallite size, and surface morphology could be controlled (Augustin, Huilgol, Udupa, & Bhat K, 2016; Gómez, Pané, & Vallés, 2005; Rosyidan et al., 2024).

Metals such as copper (Cu) and nickel (Ni) are commonly employed in metal electrodeposition (Hakim, Pangestu, & Riyanto, 2022; Setiamukti, Toifur, & Khusnani, 2020). Ni is corrosion resistant and has sufficient strength and hardness properties; meanwhile, Cu is a soft and ductile metal that is not too oxidized by air. Cu's reduction potential (+0.34 V) and Ni's reduction potential (-0.25 V) indicate that copper is nobler than Ni. As a result, Cu ions dissolve in solution via diffusion, and Ni ions dissolve via charge transfer (Ghosh et al., 2006; Goranova, Rashkov, Avdeev, & Tonchev, 2016). Therefore, the concentration of Ni and Cu needs special attention (Ganesan, Liu, Pandiyarajan, Lee, & Chuang, 2021). In addition, a complexing agent is needed to reduce the potential gap between Ni and Cu. Several studies reported the use of pyrophosphate, citrate, acetate, sulfamate, and glycine as complexing agents (Silaimani, Vivekanandan, & Veeramani, 2015).

Gosh et al. conducted Ni-Cu plating with PC and DC apparatus using bath composition 0.475 M $\text{NiSO}_4 \cdot 7\text{H}_2\text{O}$, 0.125 M $\text{CuSO}_4 \cdot 5\text{H}_2\text{O}$, and 0.2 M sodium citrate (pH was maintained using ammonia solution) and resulting corrosion current between 0.17- 5.77 A cm^{-2} in 3% NaCl, hardness between 384-482 KHN₅₀ (Ghosh et al., 2000). Dai et al. fabricated Ni-Cu film with an electrodeposition technique using 300 g l^{-1} Ni sulfamic acid, 2.5 to 15 g l^{-1} Cu sulfates, 20 g l^{-1} Ni chloride, and 20 g l^{-1} boric acid, resulting in a reduction grain size by increasing Cu content in the alloy (Dai, Zhang, Wen, Rao, & Wang, 2016). Nady and Negem studied the electrodeposition of

Ni-Cu alloys using various pH and concentration of NiSO_4 and CuSO_4 , with fixed sodium gluconate boric acid and cysteine at 0.025 A cm^{-2} of current density resulting in mostly FCC (111) and FCC (200) crystal planes of the alloys (Nady & Negem, 2016). Garanova et al. fabricated Ni-Cu using electrodeposition in $0.2 \text{ C}_6\text{H}_5\text{Na}_3\text{O}_7 \cdot 2\text{H}_2\text{O}$ with different concentrations of Ni salts (0.2, 0.25, 0.5, and 0.6 M $\text{NiSO}_4 \cdot 7\text{H}_2\text{O}$) and 0.1M $\text{CuSO}_4 \cdot 5\text{H}_2\text{O}$. The pH (≈ 9) was maintained using a 25% NH_4OH solution. The study found that increasing Ni salt (0.6 M NiSO_4) has a levelling effect (Garanova et al., 2016).

Unfortunately, presenting a complexing agent could enhance the cost of production of Cu-Ni alloy. Therefore, presenting a Ni salt as a catalyst (without a complexing agent) in the plating bath needs further investigation. This study aims to create a Cu/Cu-Ni alloy on Cu alloy through electrodeposition and investigate the relationship between physical and hardness-corrosion properties. The layers were made using various solutions at 25°C , and then the CCE and deposition rate were investigated. The Cu/Cu-Ni coating underwent characterization for scanning electron microscope-energy dispersive spectroscopy (SEM-EDS), x-ray diffraction (XRD), hardness, corrosion, and water droplets.

2. Experimental Section

2.1. Materials and Preparation

Electrodeposition solutions were made using $\text{CuSO}_4 \cdot 5\text{H}_2\text{O}$ and $\text{NiSO}_4 \cdot 6\text{H}_2\text{O}$. All chemicals used in the present research are analytical grade from Merck manufacturer. Pure Cu and Ni were used as an anode, while Cu alloy was used as a cathode with chemical compositions of P 0.22 wt.%, Cd 0.684 wt.%, Si 0.137 wt.%, and Cu balance. Before electrodeposition, the cathode was cleaned using ultrasonic cleaner (DELTA D68H) for 5 min. Electrodeposition was performed with a current density of 30 mA/cm^2 for 1 hour at 25°C using a power supply (SANFIX 305 E). The specimens were electrodeposited using various plating baths, as seen in Table 1.

2.2. Characterization

The CCE and deposition rate of the Cu/Cu-Ni electrodeposition were investigated by weighing samples before (initial weight) and after (final weight) electrodeposition and then calculated using equations in the previously reported (Basori, Soegijono, & Susetyo, 2022; Rosyidan et al., 2024).

XRD (PANalytical Aeris with Cu K radiation, $\lambda=0.15418 \text{ nm}$, step size= 0.02°) was used to determine the crystal structure of the Cu-Ni coating. MAUD software was used to refine and find the crystal parameter using XRD data. Moreover, the Debye-Scherrer formula was used to

calculate the crystal size of various samples (SEAKR, 2017).

$$D = \frac{0.9\lambda}{\beta \cos \theta} \quad (1)$$

Where D is the average crystallite size, k is a Scherrer constant of (0.9), λ is radiation wavelength (nm), β is the width of the FWHM diffraction peak (radians), and θ is peak position ($^{\circ}$ or radians).

FE-SEM equipped with EDS (Thermofisher Quanta 650 EDAX EDS Analyzer) was used to analyze the film surface morphology and phase. Afterward, roughness analysis was performed according to SEM picture using ImageJ software.

The hardness of the Cu-Ni film was measured using a MicroMet® 5100 Series micro indentation Vickers hardness tester using 100 g of load for 10 s. Measurement was conducted for five spot indentation.

Corrosion investigation was performed using potentiodynamic polarization methods (Digi-Ivy DY2311) in a 3.5% NaCl solution with a volume of 100 ml, the reference electrode being Ag/AgCl and the counter electrode being platinum (Pt) wire. Potentiodynamic polarization was carried out at a speed of 0.002 Vs^{-1} from -1.35 to -0.05 V. Information on corrosion current (i_{corr}) and corrosion voltage (E_{corr}) was acquired from the measurement data using the Tafel extrapolation method. The corrosion rate was calculated using Equation 5 utilizing the corrosion current information (Ahmad, 2006).

$$Cr = C \frac{Mi_{\text{corr}}}{n\rho} \quad (2)$$

Where Cr is the corrosion rate (mmpy), C is a constant for the corrosion rate calculation and is 3.27 mmpy, M is the atomic weight (g mol^{-1}), i_{corr} is corrosion current density (A cm^{-2}), n is the number of electrons involved, and ρ is the density of Cu and Ni (g cm^{-3}).

The contact angle was observed with a water droplet test on the film surface coated. Some criteria of the angle θ were determined by the value as $\theta < 90^{\circ}$, $90^{\circ} \leq \theta < 150^{\circ}$, and $150^{\circ} \leq \theta < 180^{\circ}$ for being hydrophilic, hydrophobic, and super hydrophobic, respectively (Lee, Bae, Jung, Jeong, & Ko, 2014).

3. Results and Discussion

3.1. CCE and Deposition Rate

The composition of $\text{CuSO}_4 \cdot 5\text{H}_2\text{O}$ and $\text{NiSO}_4 \cdot 6\text{H}_2\text{O}$ was determined at the start of the experiment. Figure 1 shows the CCE and deposition rate results of various experiments. CCE and deposition rate have similar tendencies; an increase in Ni salt would increase both CCE and deposition rate. CCE refers to the fraction of total current used for metal plating (Rosyidan et al.,

2024). At the same time, the deposition rate is the amount of anode material deposited on the cathode at a particular current and time (Park, Sohn, & Choi, 2008). The first, second, and third solutions had a CCE of 35.71, 89.28, and 91.07 %, respectively. The first, second, and third solutions had a deposition rate of 48.66, 72.99, and 92.46, respectively. Hacıismailoglu and Alper have found that increased pH leads to increased transient current (Hacıismailoglu & Alper, 2011). Moreover, Rosyidan et al. have seen that an increase in the current leads to a rise in CCE and deposition rate (Rosyidan et al., 2024). Therefore, increased Ni salt promotes increased CCE and deposition rate due to rise and pH (see Table 1).

Hydrogen evolution could happen at the cathode when electrodeposition is conducted. Hydrogen evolution could disrupt ion's movement to the substrate's surfaces during deposition by blocking the cathode surface. Deo et al. have stated that hydrogen evolution is a competitor at Ni and Cu electrodeposition (Deo et al., 2020). According to the CCE result, higher hydrogen evolution occurred in the samples made using the first solution, and increasing a Ni salt in the solution led to a decrease in hydrogen evolution. Guler et al. have stated that presenting a hydrogen evolution at the cathode during electrodeposition leads to a decrease in CCE (Saraloğlu Güler, Konca, & Karakaya, 2013).

3.2. Phase and Surface Morphology

In this study, film deposition involved diffusion and charge transfer by Cu/Cu-Ni. The various films were obtained using a current density of 30 mA cm^{-2} for an hour for all solution variations. The results of the EDS investigation can be seen in Figure 2.

Based on Figure 2, it can be seen that 100 wt.% Cu phases are seen when electrodeposited using baths 1 and 2. This means presenting a Ni salt 0.3 and 0.5 M doesn't cause an exhibit of Ni in the film. Meanwhile, when Ni salt concentration rises to 0.7 M, Ni is exhibited in the film around 0.2 wt. %. The solution seems to have a salt limitation, resulting in a Cu-Ni Alloy. Decrease a Cu salt by less than 0.1 M or increasing a Ni salt by more than 0.7 M is needed. Baskaran et al. electrodeposited Ni using the composition between Ni and Cu salt, which is 20:1 (Baskaran, Sankara Narayanan, & Stephen, 2006). Sarac et al. electrodeposited Ni using the composition between Ni and Cu salt are 50:1 (Sarac, Öksüzoğlu, & Baykul, 2012).

Moreover, Hacıismailoglu and Alper have stated that hydrogen evolution was occurring at the surface of the substrate during the electrodeposition process, which could prevent the reduction of

Ni in the film (Haciismailoglu & Alper, 2011). This statement is corroborated by the fact that Ni formed in the sample was made using a third solution due to electrodeposition using the first and second solutions, which still caused hydrogen evolution on the substrate surface.

Figures 3 (a)-(c) show the morphology of the deposited non-uniform and compact films, which is affected by the hydrogen evolution. Guler et al. have stated the disruption is due to hydrogen evolution at the cathode, which could be resulting a non-uniform film (Saraloglu Güler et al., 2013). Moreover, pure Cu (Figures (a) and (b)) show morphology with nodules form. In contrast, presenting a Ni in the alloy, which changes nodules to a cauliflower-like form. As mentioned above, exhibiting a Ni salt in the solution could increase the pH of the solution (Table 1). Kalubowila et al. have found that increasing the pH bath could transform surface morphology (Kalubowila et al., 2019). furthermore, raising a pH solution leads to an increased deposition rate and change in surface morphology. Therefore, there is transformation from nodules to a cauliflower-like form.

Statistical analysis using ImageJ combined Origin with the corresponding Gauss fitting function was used to identify the grain size distribution. The result is presented in Figure 3.

Image-J software was used to calculate the average grain size diameter. Table 2 shows the results of calculating the average grain size. The calculation results show that the grain size average has decreased by increasing the Ni salt in the solution. Baskaran et al. stated that grain size decreased due to increased electrodeposition current density (Baskaran et al., 2006). Previous research shows that increasing current density increases deposition rate (Rosyidan et al., 2024). Compared to Figure 1, it is seen that rising Ni salt leads to an increased deposition rate. An increase in the deposition rate leads to an increased speed of the ion species deposited on the cathode surface. Therefore, grain size is decreasing in the present research.

Image processing was done using Image J software to obtain detailed information about the resulting image pattern. Image patterns were investigated from SEM pictures to interpret the results of surface roughness parameters and 3-D images from surface scanning. The result of the Image J software investigation can be seen in Figure 4, which presents the relationship between distance (μm) and gray value varies with increasing distance.

Table 3 shows the average surface roughness of Cu-Ni/Cu coating morphology fabricated from

various baths according to Image J software investigation.

According to Table 3, increasing Ni salt in the solution increases the films' roughness average. Deo et al. reported that increasing a current density led to an increase in surface roughness (Deo et al., 2020). As mentioned above, increasing current density increases deposition rate (Rosyidan et al., 2024). Compared to the deposition rate measurement (Figure 1), it can be seen that rising Ni salt leads to an increased deposition rate due to pH increments. An increase in the deposition rate leads to an increased speed of the ion species deposited on the cathode surface. Therefore, the roughness average is increased in the present research.

3.3. Crystallographic Orientation

According to the XRD data in Figure 5, three planes formed namely the (111), (002), and (022) planes. The (111) plane dominated when the films were made using baths 1, 2, and 3. The dominance of the (111) plane orientation had benefits such as anticorrosion, increased electrical conductivity, and improved mechanical properties (SEAKR, 2017).

All of the collected XRD data were then analyzed using MAUD software, and the crystal parameters are shown in Table 4. All led to the same crystal structure and space group, FCC and Fm-3m, which can be concluded that atoms of the Cu and Ni form a substitutional solid solution (Dai et al., 2016).

Table 4 shows that the lattice constant and cell volume decrease due to the increase in the Ni phase in the alloy, which perfectly agrees with other reports (Baskaran et al., 2006). Moreover, increased Ni salt in the plating bath decreases crystallite size. Augustin et al. have reported an increase in current density promoting reduced crystallite size (Augustin et al., 2016). Increasing the electrodeposition process's current density influences the deposition rate's increase; the amount of ion species deposited on the cathode rose; therefore, crystallite size decreased. Small crystal size indicates that the distance between grains is close, contributing to material qualities with more roughness properties (Dai et al., 2016). This result is in perfect agreement with the average roughness in Table 3. Moreover, a smaller lattice strain is seen in the sample made using bath 3.

3.4. Hardness

Hardness is a material's resistance to plastic deformation. A coating procedure is considered successful if it can enhance the qualities of the coated objects. One of the purposes of

electrodeposition in the present research is to improve material deposited hardness. The results of the hardness of the coating were obtained using a Vickers micro-hardness tester.

The Vickers microhardness method obtained 58 HV in the first solution, 68 HV in the second solution, and 136 HV in the third solution. It seems an increase in Ni salt would increase the hardness. In their study, Augustin et al. found that a decrease in crystallite size promotes an increase in hardness, which is in perfect agreement with the present research (Augustin et al., 2016). Besides crystallite size, the exhibit of Ni in the alloy also influences the hardness of the sample (Rosyidan et al., 2024). As seen in Figure 6, a sample was made using bath 3, resulting in higher hardness, which is affected by the exhibit of Ni in the alloy. According to the EDS result, only one sample was made using bath 3, resulting in Ni in the alloy. Compared to the Monel 400, hardness is between 150 to 200 HV, and present research has lower hardness (Kukliński, Bartkowska, Przestacki, & Kinal, 2020).

3.5. Corrosion

Figure 7 shows the corrosion curves of the electrodeposition of Cu/Cu-Ni on the Cu alloy substrate.

The i_{corr} and E_{corr} were found using the Tafel extrapolation method. Meanwhile, CR was calculated using equation (2). The summary of the calculations for the CR of various samples is shown in Table 5.

The crystal plane could determine the corrosion rate behavior of materials with the FCC crystal system. The (111) crystal plane is more corrosion-resistant in materials with the FCC system than the (002) and (022) crystal planes (Al Kharafi, Ghayad, & Abdullah, 2012). Therefore, all of the samples met good and excellent criteria. Moreover, based on Table 5, it can be seen that the third solution has the best corrosion rate. This behavior is influenced by the lattice strain that was formed. Lattice strain is sample defect concentration measured due to a void core in the lattice (Basori et al., 2022). Therefore, the smallest lattice strain leads to the highest corrosion resistance.

According to Wang et al. and Ghosh et al. studies, Monel-400 i_{corr} is 2.24×10^{-6} and 2.2×10^{-6} (A cm^{-2}) (Ghosh et al., 2000; Wang et al., 2014). Compared with Table 5, it can be seen that the sample made using a third solution has lower i_{corr} than Monel-400.

3.6. Contact Angle

The water droplet test can be used to determine the hydrophilic, hydrophobic, and superhydrophobic properties of a film. Figure 8 shows a snapshot of the drip test findings for various samples. All samples possess hydrophilic properties since they have contact angles between 0° and 90° (Thurber et al., 2016). The contact angles achieved in the first, second, and third solution 1 are 69.2°, 79.4° and 88.6°, respectively. Increment of the water contact angle is probably due to an increased film surface roughness. In their research, Huang et al. found that increasing roughness would increase the water contact angle (Huang & Gates, 2020). Moreover, Yu et al. found that increasing electrolyte pH from 2 to 4 increases the film's water contact angle (Yu et al., 2013), probably due to an increase in the surface roughness of the samples.

4. Conclusion

Cu/Cu-Ni film was electrodeposited onto Cu alloy using various bath compositions, and according to the multiple findings, increased Ni salt content led to increased deposition rate and CCE due to an increased pH and depleting hydrogen evolution, which impacted grain size, more roughness, less crystallite size and presenting small amount of a Ni in the film. The formed crystal structure was a single-phase FCC with the dominant (111) plane. The hardness increment is due to a decrease in crystallite size. Lesser lattice strain contributed to a higher corrosion resistance. The films have more roughness and impact on the higher water contact angle. The 99.8Cu0.3Ni alloy has the best corrosion resistance and is recommended as an alternative to change Monel-400.

Acknowledgement

This project was financially supported by Universitas Trisakti based on the assignment letter number 800/C-4/FTKE/USAKTI/X/2023.

References

- Ahmad, Z. (2006). Principles of Corrosion Engineering and Corrosion Control. In *Principles of Corrosion Engineering and Corrosion Control* (1st ed.). Oxford, United Kingdom: Butterworth-Heinemann. <https://doi.org/10.1016/b978-0-7506-5924-6.x5000-4>
- Al Kharafi, F. M., Ghayad, I. M., & Abdullah, R. M. (2012). Corrosion inhibition of copper in non-polluted and polluted sea water using 5-phenyl-1-H-tetrazole. *International Journal of Electrochemical Science*, 7(4), 3289–3298. [https://doi.org/10.1016/s1452-3981\(23\)13954-x](https://doi.org/10.1016/s1452-3981(23)13954-x)

- Augustin, A., Huilgol, P., Udupa, K. R., & Bhat K, U. (2016). Effect of current density during electrodeposition on microstructure and hardness of textured Cu coating in the application of antimicrobial Al touch surface. *Journal of the Mechanical Behavior of Biomedical Materials*, 63, 352–360. <https://doi.org/10.1016/j.jmbbm.2016.07.013>
- Baskaran, I., Sankara Narayanan, T. S. N., & Stephen, A. (2006). Pulsed electrodeposition of nanocrystalline Cu-Ni alloy films and evaluation of their characteristic properties. *Materials Letters*, 60(16), 1990–1995. <https://doi.org/10.1016/j.matlet.2005.12.065>
- Basori, B., Soegijono, B., Yudanto, S. D., Nanto, D., & Susetyo, F. B. (2023). Effect of low magnetic field during nickel electroplating on morphology, structure, and hardness. *Journal of Physics: Conference Series*, 2596(1). <https://doi.org/10.1088/1742-6596/2596/1/012014>
- Basori, Soegijono, B., & Susetyo, F. B. (2022). Magnetic field exposure on electroplating process of ferromagnetic nickel ion on copper substrate. *Journal of Physics: Conference Series*, 2377, 012002. <https://doi.org/10.1088/1742-6596/2377/1/012002>
- Dai, P. Q., Zhang, C., Wen, J. C., Rao, H. C., & Wang, Q. T. (2016). Tensile Properties of Electrodeposited Nanocrystalline Ni-Cu Alloys. *Journal of Materials Engineering and Performance*, 25(2), 594–600. <https://doi.org/10.1007/s11665-016-1881-2>
- Deo, Y., Guha, S., Sarkar, K., Mohanta, P., Pradhan, D., & Mondal, A. (2020). Electrodeposited Ni-Cu alloy coatings on mild steel for enhanced corrosion properties. *Applied Surface Science*, 515, 146078. <https://doi.org/10.1016/j.apsusc.2020.146078>
- Ganesan, M., Liu, C. C., Pandiyarajan, S., Lee, C. T., & Chuang, H. C. (2021). Post-supercritical CO₂ electrodeposition approach for Ni-Cu alloy fabrication: An innovative eco-friendly strategy for high-performance corrosion resistance with durability. *Applied Surface Science*, (November). <https://doi.org/10.1016/j.apsusc.2021.151955>
- Ghosh, S. K., Grover, A. K., Dey, G. K., Kulkarni, U. D., Dusane, R. O., Suri, A. K., & Banerjee, S. (2006). Structural characterization of electrodeposited nanophase Ni-Cu alloys. *Journal of Materials Research*, 21(1), 45–61. <https://doi.org/10.1557/jmr.2006.0034>
- Ghosh, S. K., Grover, A. K., Dey, G. K., & Totlani, M. K. (2000). Nanocrystalline Ni-Cu alloy plating by pulse electrolysis. *Surface and Coatings Technology*, 126(1), 48–63. [https://doi.org/10.1016/S0257-8972\(00\)00520-X](https://doi.org/10.1016/S0257-8972(00)00520-X)
- Gómez, E., Pané, S., & Vallés, E. (2005). Electrodeposition of Co-Ni and Co-Ni-Cu systems in sulphate-citrate medium. *Electrochimica Acta*, 51(1), 146–153. <https://doi.org/10.1016/j.electacta.2005.04.010>
- Goranova, D., Rashkov, R., Avdeev, G., & Tonchev, V. (2016). Electrodeposition of Ni–Cu alloys at high current densities: details of the elements distribution. *Journal of Materials Science*, 51(18), 8663–8673. <https://doi.org/10.1007/s10853-016-0126-y>
- Haciismailoglu, M., & Alper, M. (2011). Effect of electrolyte pH and Cu concentration on microstructure of electrodeposited Ni-Cu alloy films. *Surface and Coatings Technology*,

206(6), 1430–1438. <https://doi.org/10.1016/j.surfcoat.2011.09.010>

- Hakim, M. S., Pangestu, H., & Riyanto. (2022). Preparation and Application of Nickel Electroplating on Copper (Ni/EC) Electrode for Glucose Detection. *Science and Technology Indonesia*, 7(2), 208–212. <https://doi.org/10.26554/sti.2022.7.2.208-212>
- Huang, X., & Gates, I. (2020). Apparent Contact Angle around the Periphery of a Liquid Drop on Roughened Surfaces. *Scientific Reports*, 10(1), 1–11. <https://doi.org/10.1038/s41598-020-65122-w>
- Jariwala, F., Gohil, R., Trivedi, P., Parmar, J., Borda, B., Patel, S., ... Rao, V. (2018). Electroplating of Nickel and Chromium on Aluminum 6082-T6 alloy. *Proceedings of the International Conference on Recent Advances in Metallurgy for Sustainable Development*, 1–3.
- Kalubowila, K. D. R. N., Jayathileka, K. M. D. C., Kumara, L. S. R., Ohara, K., Kohara, S., Sakata, O., ... Jayanetti, J. K. D. S. (2019). Effect of Bath pH on Electronic and Morphological Properties of Electrodeposited Cu₂O Thin Films. *Journal of The Electrochemical Society*, 166(4), D113–D119. <https://doi.org/10.1149/2.0551904jes>
- Kukliński, M., Bartkowska, A., Przestacki, D., & Kinal, G. (2020). Influence of microstructure and chemical composition on microhardness and wear properties of laser borided monel 400. *Materials*, 13(24), 1–15. <https://doi.org/10.3390/ma13245757>
- Lajevardi, S. A., Shahrabi, T., Szpunar, J. A., Sabour Rouhaghdam, A., & Sanjabi, S. (2013). Characterization of the microstructure and texture of functionally graded nickel-Al₂O₃ nano composite coating produced by pulse deposition. *Surface and Coatings Technology*, 232, 851–859. <https://doi.org/10.1016/j.surfcoat.2013.06.111>
- Lee, J. M., Bae, K. M., Jung, K. K., Jeong, J. H., & Ko, J. S. (2014). Creation of microstructured surfaces using Cu-Ni composite electrodeposition and their application to superhydrophobic surfaces. *Applied Surface Science*, 289, 14–20. <https://doi.org/10.1016/j.apsusc.2013.10.066>
- Matsuda, T., Saeki, R., Hayashida, M., & Ohgai, T. (2022). Microhardness and heat-resistance performance of ferromagnetic cobalt-molybdenum nanocrystals electrodeposited from an aqueous solution containing citric acid. *Materials Research Express*, 9(4). <https://doi.org/10.1088/2053-1591/ac60e3>
- Nady, H., & Negem, M. (2016). Ni-Cu nano-crystalline alloys for efficient electrochemical hydrogen production in acid water. *RSC Advances*, 6(56), 51111–51119. <https://doi.org/10.1039/c6ra08348j>
- Ollivier, A., Muhr, L., Delbos, S., Grand, P. P., Matlosz, M., & Chassaing, E. (2009). Copper-nickel codeposition as a model for mass-transfer characterization in copper-indium-selenium thin-film production. *Journal of Applied Electrochemistry*, 39(12), 2337–2344. <https://doi.org/10.1007/s10800-009-9918-y>
- Park, B. N., Sohn, Y. S., & Choi, S. Y. (2008). Effects of a magnetic field on the copper

- metallization using the electroplating process. *Microelectronic Engineering*, 85(2), 308–314. <https://doi.org/10.1016/j.mee.2007.06.018>
- Rosyidan, C., Kurniawan, B., Soegijono, B., Putra, V. G. V., Munazat, D. R., & Susetyo, F. B. (2024). Effect of Current Density on Magnetic and Hardness Properties of Ni-Cu Alloy Coated on Al via Electrodeposition. *International Journal of Engineering, Transaction B: Applications*, 37(02), 213–223. <https://doi.org/10.5829/IJE.2024.37.02B.01>
- Sarac, U., Öksüzöğlü, R. M., & Baykul, M. C. (2012). Deposition potential dependence of composition, microstructure, and surface morphology of electrodeposited Ni-Cu alloy films. *Journal of Materials Science: Materials in Electronics*, 23(12), 2110–2116. <https://doi.org/10.1007/s10854-012-0709-6>
- Saraloğlu Güler, E., Konca, E., & Karakaya, I. (2013). Effect of electrodeposition parameters on the current density of hydrogen evolution reaction in Ni and Ni-MoS₂ composite coatings. *International Journal of Electrochemical Science*, 8(4), 5496–5505. [https://doi.org/10.1016/s1452-3981\(23\)14699-2](https://doi.org/10.1016/s1452-3981(23)14699-2)
- SEAKR, R. (2017). Microstructure and crystallographic characteristics of nanocrystalline copper prepared from acetate solutions by electrodeposition technique. *Transactions of Nonferrous Metals Society of China (English Edition)*, 27(6), 1423–1430. [https://doi.org/10.1016/S1003-6326\(17\)60164-X](https://doi.org/10.1016/S1003-6326(17)60164-X)
- Setiamukti, D., Toifur, M., & Khusnani, A. (2020). The effect of electrolyte concentration on the sensitivity of low-temperature sensor performance of Cu/Ni film. *Science and Technology Indonesia*, 5(2), 28–33. <https://doi.org/10.26554/sti.2020.5.2.28-33>
- Silaimani, S. M., Vivekanandan, G., & Veeramani, P. (2015). Nano-nickel–copper alloy deposit for improved corrosion resistance in marine environment. *International Journal of Environmental Science and Technology*, 12(7), 2299–2306. <https://doi.org/10.1007/s13762-014-0591-2>
- Thurber, C. R., Ahmad, Y. H., Sanders, S. F., Al-Shenawa, A., D’Souza, N., Mohamed, A. M. A., & Golden, T. D. (2016). Electrodeposition of 70-30 Cu-Ni nanocomposite coatings for enhanced mechanical and corrosion properties. *Current Applied Physics*, 16(3), 387–396. <https://doi.org/10.1016/j.cap.2015.12.022>
- Wang, S., Guo, X., Yang, H., Dai, J., Zhu, R., Gong, J., ... Ding, W. (2014). Electrodeposition mechanism and characterization of Ni-Cu alloy coatings from a eutectic-based ionic liquid. *Applied Surface Science*, 288, 530–536. <https://doi.org/10.1016/j.apsusc.2013.10.065>
- Yu, Q., Zeng, Z., Zhao, W., Li, M., Wu, X., & Xue, Q. (2013). Fabrication of adhesive superhydrophobic Ni-Cu-P alloy coatings with high mechanical strength by one step electrodeposition. *Colloids and Surfaces A: Physicochemical and Engineering Aspects*, 427, 1–6. <https://doi.org/10.1016/j.colsurfa.2013.02.067>

Figures

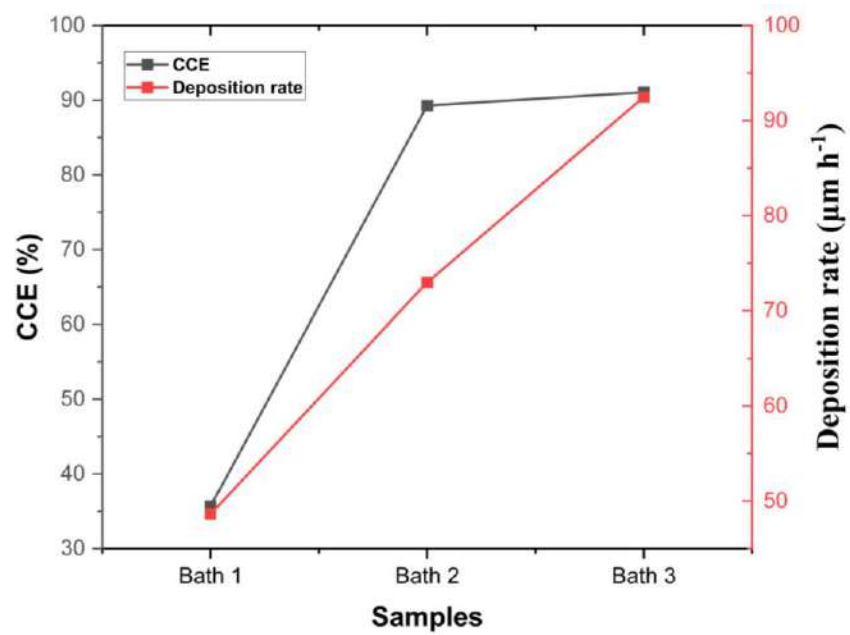
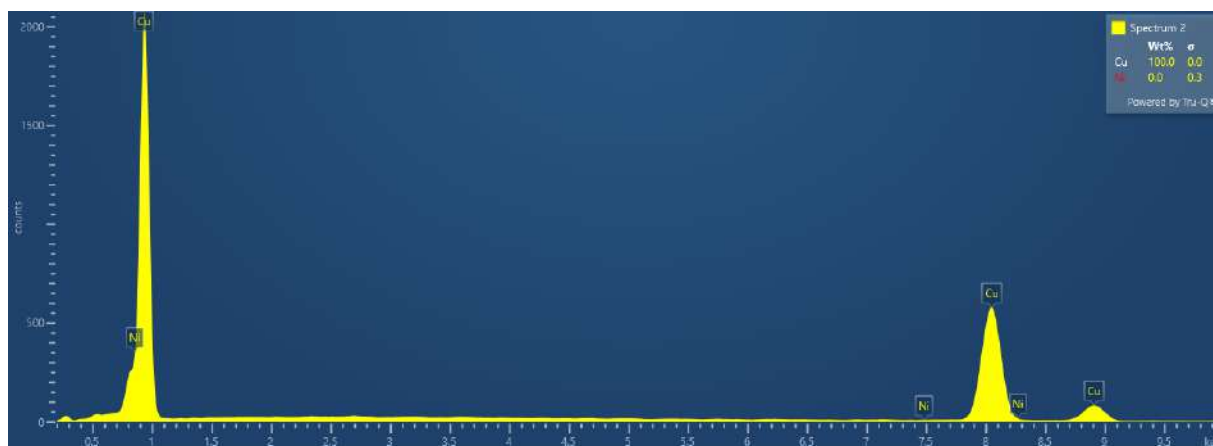


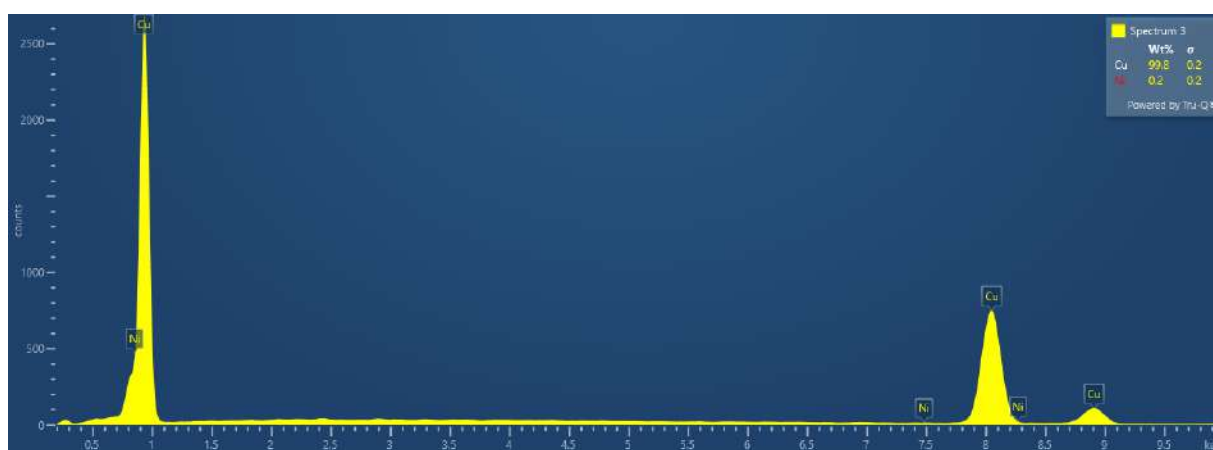
Figure 1. CCE and deposition rate for Cu/Cu-Ni electrodeposited from bath 1, 2, and 3



(a)

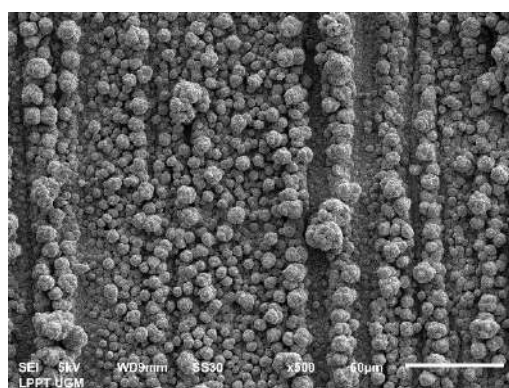


(b)

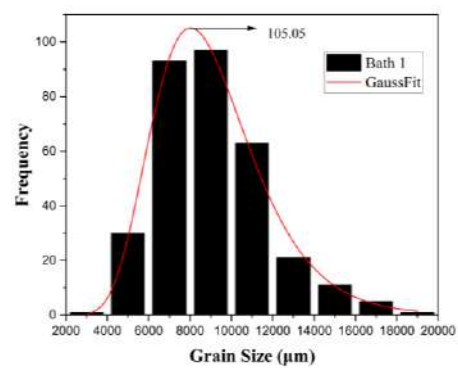


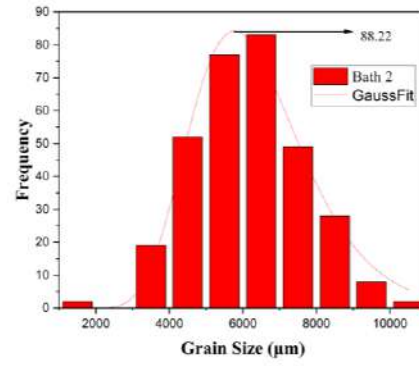
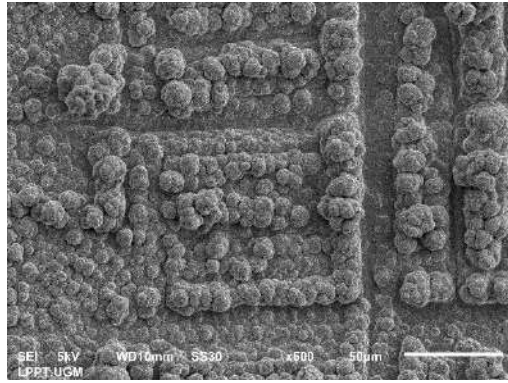
(c)

Figure 2. EDS test results of various samples

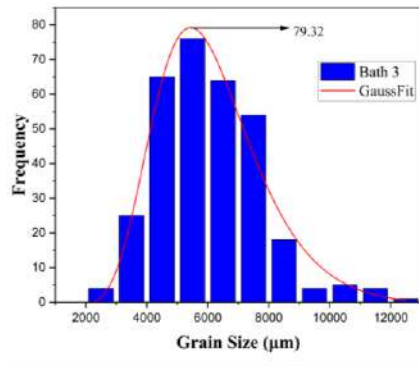
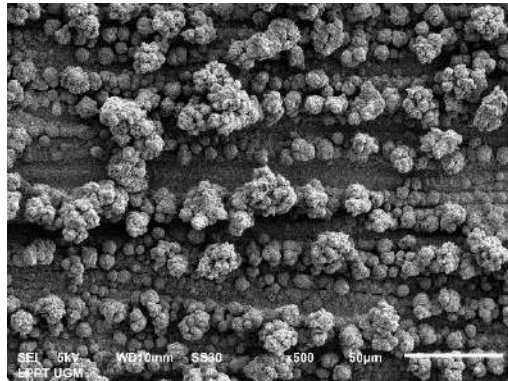


(a)



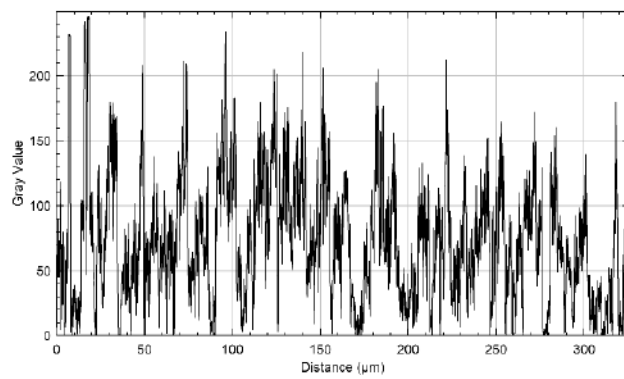
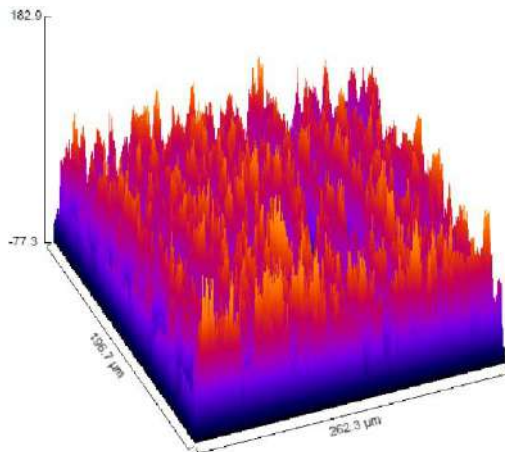


(b)

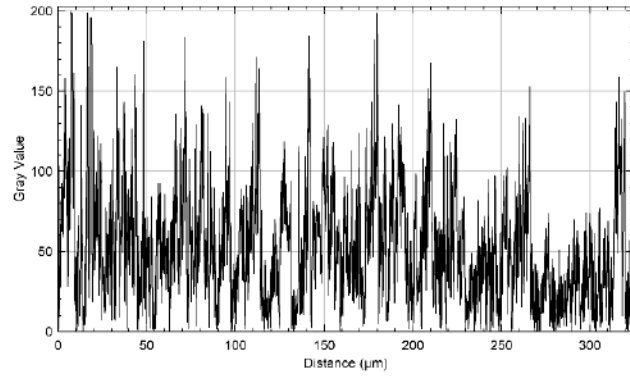
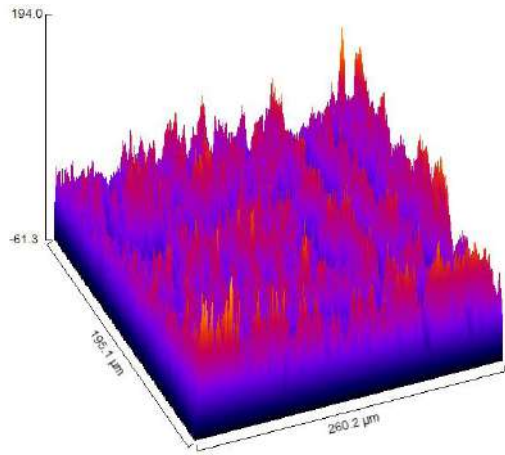


(c)

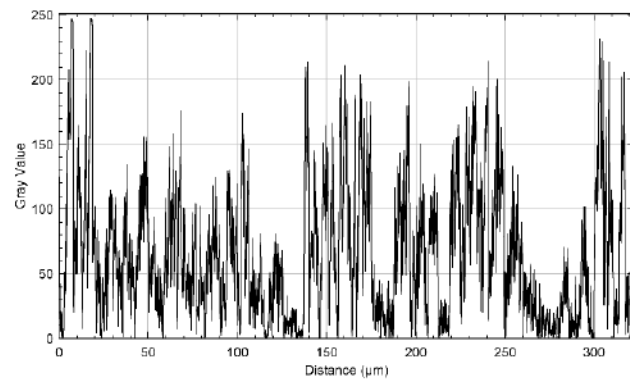
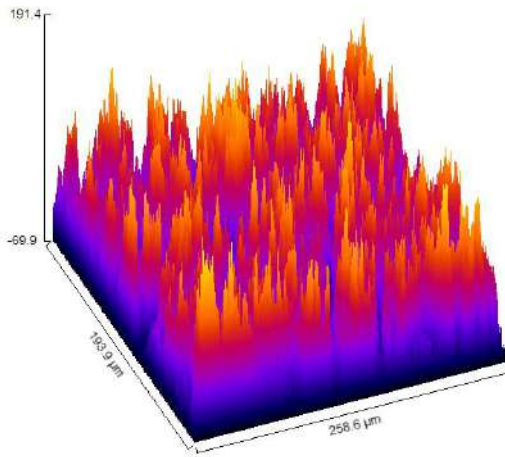
Figure 3. SEM micrographs and grain distribution for different samples (a) Bath 1, (b) Bath 2, and (c) Bath 3



(a)



(b)



(c)

Figure 4. Analysis of sample surfaces roughness in 3D SEM image and graph of grey value against distance (left-right) (a) Bath 1, (b) Bath 2, and (c) Bath 3

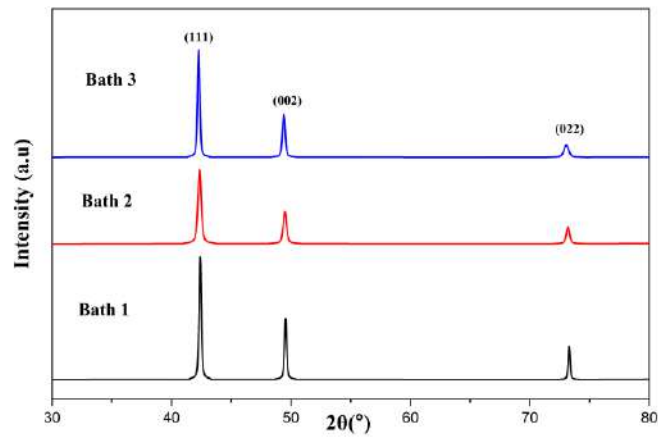


Figure 5. XRD pattern of various samples

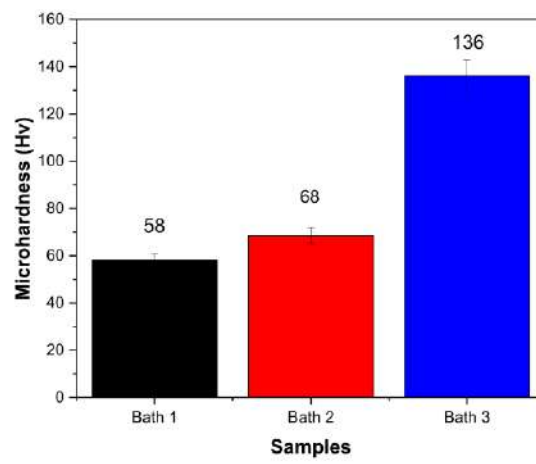


Figure 6. Hardness test results of various samples

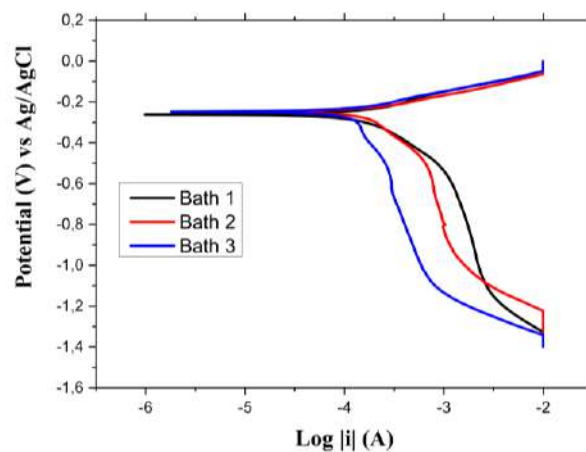


Figure 7. Corrosion curve for various samples

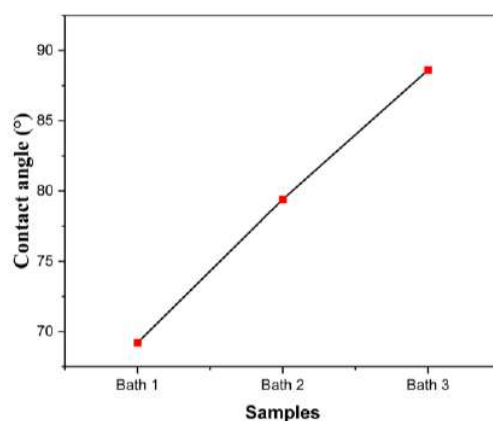


Figure 8. Water contact angle of various samples

Tables

Table 1. Plating baths composition for Cu/Cu-Ni electrodeposition

Plating bath	Composition (M)		Measured pH
	CuSO ₄ .5H ₂ O	NiSO ₄ .7H ₂ O	
Bath 1	0.1	0.3	2.35
Bath 2	0.1	0.5	2.51
Bath 3	0.1	0.7	2.53

Table 2. Average grain size calculation results of various samples

Sample	Grain Size (μm)
Bath 1	105.05
Bath 2	88.22
Bath 3	79.32

Table 3. Average roughness value of various samples

Sample	Roughness Average (Ra) μm
Bath 1	30.63
Bath 2	37.49
Bath 3	37.82

Table 4. Crystal parameters of various samples

Parameter	Sample		
	Bath 1	Bath 2	Bath 3
Crystal structure	FCC		
Space Group	Fm-3m		
Lattice constant (\AA) $a = b = c$	3.631	3.618	3.612
Cell volume (\AA^3)	47.89	47.37	47.14
d-spacing (\AA)	1.7530	1.7549	1.7578
Crystallite Size (nm)	43.39	27.54	25.70
Lattice strain	0.27	0.41	0.25

Table 5. Corrosion measurements of various samples

Sample	i_{corr} (Acm^{-2})	E_{corr} (V)	Cr (mmpy)	Criteria
Bath 1	4.40×10^{-6}	-0.261	0.196	Good
Bath 2	5.01×10^{-6}	-0.244	0.223	Good
Bath 3	1.82×10^{-6}	-0.248	0.081	Excellent

2. Bukti konfirmasi Review (28 Maret 2025)

1142 / Rosyidan et al. / Nickel Salt Dependency as Catalyst in the Plating Bath on the Film Properties of Cu/Cu-Ni

Library

Workflow

Publication

Submission

Review

Copyediting

Production

Submission Files

Q Search

	6494	Cahaya STI 5 Feb 2024.docx	February 5, 2024	Manuscript
	6495	CTA-STI 2020.pdf	February 5, 2024	Statement of Agreement
	6932	Double blind_STI 1142.docx	March 28, 2024	Manuscript

Download All Files

Bukti dari email

[STI] Editor Decision External



Prof. Aldes Lesbani <scitechindones@gmail.com>

Thu, Mar 28, 2024, 12:06 PM



to me, Budhy, Bambang, Mustamina, Lisa, Frederik, Valentinus, Ferry ▾

Dear Cahaya Rosyidan, Budhy Kurniawan, Bambang Soegijono, Mustamina Maulani, Lisa Samura, Frederik Gresia Nababan, Valentinus Galih Vidia Putra, Ferry Budhi Susetyo:

Reviewers have now commented on your paper (attached below this email). You will see that they are advising that you must revise your manuscript. If you are prepared to undertake the work required, I would be pleased to reconsider my decision.

For your guidance, reviewers' comments can be read in your Author online interface. If you decide to revise the work, please submit a list of changes or a rebuttal against each point which is being raised when you submit the revised manuscript.

****>>>Please be noted that you have up to **3 (three) weeks from now** to revise your manuscript, unless your manuscript will be considered as a new submitted manuscript. If you need additional time to complete your revision, please let us know by replying to this email and informing us of the date you expect to submit it. <<<<****

To submit a revision, please upload your revised manuscript documents to SCIENCE AND TECHNOLOGY INDONESIA online submission interface at (<https://scitechindonesia.com>) after you log in as Author. Important: Please indicate the revision as RED-highlighting the revision sentences or words within your revised manuscript.

The revised document files (three files) MUST include:

- One (1) file of Revision Note file in a table form with respect to Reviewers comments including the location of the revision on the revised manuscript.
- One (1) file of Revised Manuscript file according to Template-based format (MS Word file) (please RED-color highlighted texts in the revised sentences).
- One (1) file of Graphical Abstract file according to Guideline of Graphical Abstract

GUIDELINE TO UPLOAD REVISION: To upload your revised manuscript, please login to Science and Technology Indonesia journal submission interface (<https://scitechindonesia.com>) login using your user and password as usual. **Therefore, click on "Review" and upload to "revision box"**.

For second and continuing order of revision of manuscript, please just add your latest version file(s), do not delete the previous round of file(s) of manuscript.

IMPORTANT NOTE: A GRAPHICAL ABSTRACT of each article is mandatory for this journal. This graphic should capture the reader's attention and, in conjunction with the manuscript title, should give the reader a quick visual impression of the essence of the manuscript without providing specific results. Choosing/Creating a Graphical Abstract: The graphic should be simple, but informative; The use of color is encouraged; The graphic should uphold the standards of a scholarly, professional publication; The graphic must be entirely original, unpublished artwork created by one of the coauthors; The graphic should not include a photograph, drawing, or caricature of any person, living or deceased; Do not include postage stamps or currency from any country, or trademarked items (company logos, images, and products); Avoid choosing a graphic that already appears within the text of the manuscript. Image size: please provide an image with a size of 500 × 800 pixels (height × width). Preferred file types: TIFF, JPG, PNG, PDF, or MS Office files.

The Graphical Abstracts should be submitted as a separate file during the revised manuscript submission system or otherwise, it can be submitted by email to: scitechindonesia@gmail.com

Thank you for submitting to this journal.

Science and Technology Indonesia

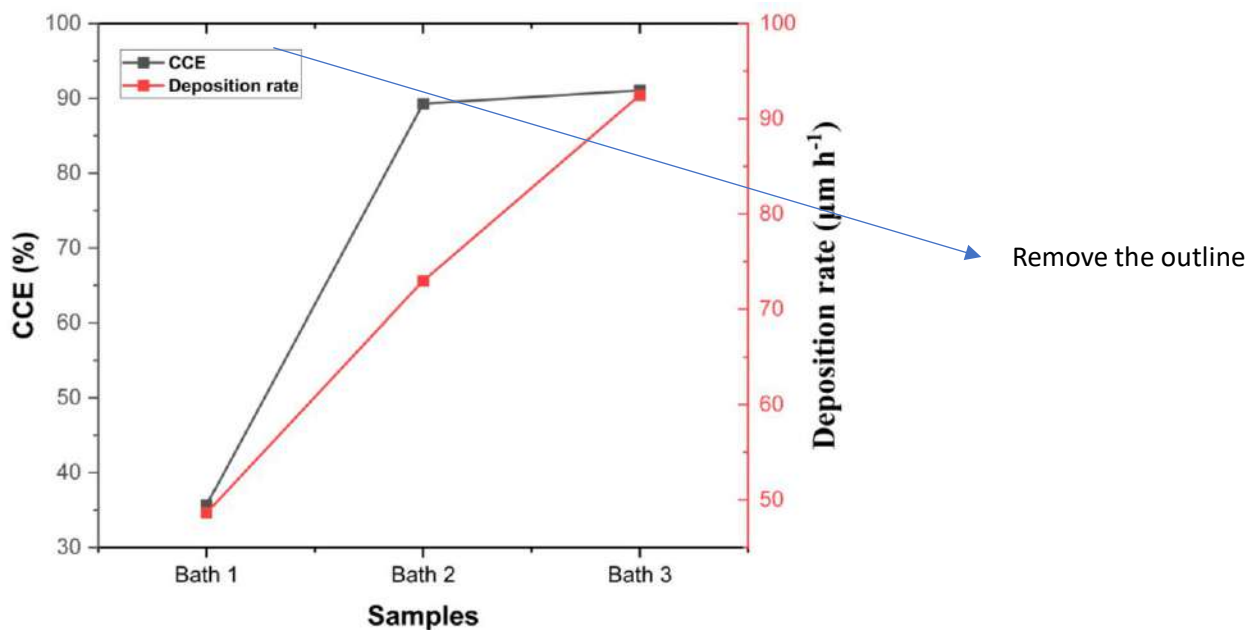
A Peer-Reviewed Research Journal of Science and Technology

p-ISSN: 2580-4405 | e-ISSN: 2580-4391

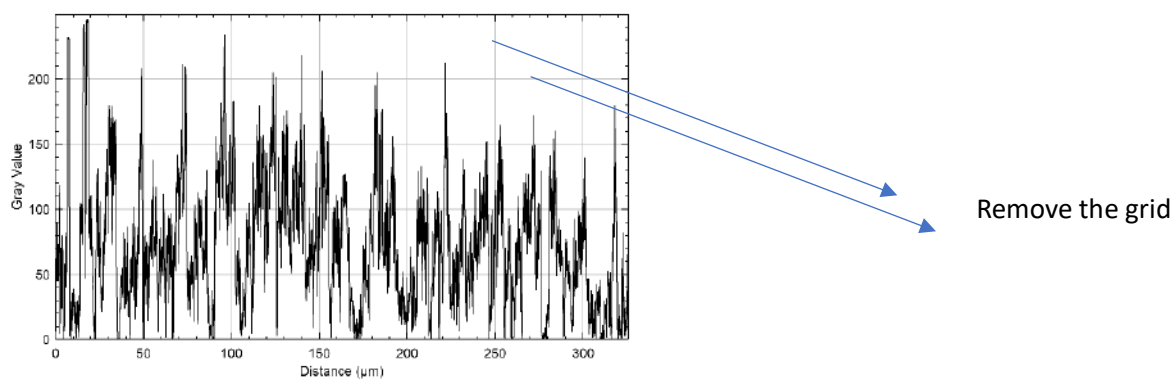
E-mail: admin@scitechindonesia.com | scitechindonesia@gmail.com

Homepage: <http://scitechindonesia.com/index.php/sti>

1. Keyword should be specific related with the experiment not instrument analysis
2. Abstract should contain: what you do, method, and results. Please consider with this item
3. Make sure each paragraph contain at least several sentences. Too many paragraph in your manuscript
- 4.



- 5.
6. The outline on Figure 3 and 7 in the line caption was also removed



- 7.
8. Please check the use of periods and commas in figures, tables, and text.
9. Figure, Table, and Equation must be mentioned in the text

3. Bukti menjawab reviewer (3 April 2025)

Nickel Salt Dependency as Catalyst in the Plating Bath on the Film Properties of Cu/Cu-Ni

Cahaya Rosyidan^{1,*}, Budhy Kurniawan², Bambang Soegijono³, Mustamina Maulani¹, Lisa Samura¹, Frederik Gresia Nababan¹, Valentinus Galih Vidia Putra⁴, Ferry Budhi Susetyo⁵

¹*Petroleum Engineering, Universitas Trisakti, Jakarta 11440, Indonesia*

²*Departement of Physics, Universitas Indonesia, Depok 16424, Indonesia*

³*Department of Geoscience, Universitas Indonesia, Depok 16424, Indonesia*

⁴*Plasma and Nanomaterial Research Group, Politeknik STTT Bandung, Bandung 40272, Indonesia*

⁵*Department of Mechanical Engineering, Universitas Negeri Jakarta, Jakarta 13220, Indonesia*

*Corresponding Author e-mail: cahayarosyidan@trisakti.ac.id

Abstract

Metal plating frequently employs nickel (Ni) and copper (Cu) as anodes. Cu/ Cu-Ni film formed has many advantages, such as better corrosion resistance and high hardness characteristics. This study aims to assess the properties of Cu/Cu-Ni film, such as phase, surface morphology, crystallographic orientation, hardness, corrosion analysis, and contact angle, which were fabricated using electrodeposition with various Ni salt additions (0.3, 0.5 and 0.7 M). In addition, the cathode current efficiency (CCE) and deposition rate of the Cu/Cu-Ni electrodeposition were also investigated. An increase in Ni salt in the plating bath could enhance the pH, promoting higher CCE and depleting hydrogen evolution at the cathode, leading to the presenting Ni phase in the alloy. The higher concentration of Ni salt in the solution could also enhance the deposition rate due to a shift to a pH value, which affects the roughening of the surface morphology, promoting a higher contact angle. All crystal structures generated by Cu/Cu-Ni electrodeposition were FCC, with the preferred orientation of the (111) plane. Crystallite size and lattice strain depend on the deposition rate. Less crystallite size and lattice strain affect the film's hardness and corrosion resistance. Moreover, the third bath had the resulting Cu-Ni layer with the best hardness and corrosion rate of around 136 HV and 0.081mmpy.

Keywords: *Cathode current efficiency, Deposition rate, Electrodeposition, Corrosion, Hardness*

5. Introduction

The electrodeposition procedure is one of the numerous metal coating methods. Metal coating

using electrodeposition technology has created many industries that work on coating vehicle engine parts such as pistons, drums, shafts, and other engine parts (Jariwala et al., 2018; Lajevardi, Shahrabi, Szpunar, Sabour Rouhaghdam, & Sanjabi, 2013). Electrodeposition is done to take advantage of the better properties of the coating element than a substrate. These benefits include heat resistance, a low coefficient of friction, and the prevention of corrosion and erosion properties (Basori, Soegijono, Yudanto, Nanto, & Susetyo, 2023; Ghosh, Grover, Dey, & Totlani, 2000; Matsuda, Saeki, Hayashida, & Ohgai, 2022). Many factors influence these properties, including solution concentration, temperature, current density, immersion time, pH, and electrical voltage (Kalubowila et al., 2019; Ollivier et al., 2009). Those factors could significantly influence the deposition rate during the electrodeposition process. Moreover, by adjusting the deposition rate, structure, grain size, crystallite size, and surface morphology could be controlled (Augustin, Huilgol, Udupa, & Bhat K, 2016; Gómez, Pané, & Vallés, 2005; Rosyidan et al., 2024).

Metals such as copper (Cu) and nickel (Ni) are commonly employed in metal electrodeposition (Hakim, Pangestu, & Riyanto, 2022; Setiamukti, Toifur, & Khusnani, 2020). Ni is corrosion resistant and has sufficient strength and hardness properties; meanwhile, Cu is a soft and ductile metal that is not too oxidized by air. Cu's reduction potential (+0.34 V) and Ni's reduction potential (-0.25 V) indicate that copper is nobler than Ni. As a result, Cu ions dissolve in solution via diffusion, and Ni ions dissolve via charge transfer (Ghosh et al., 2006; Goranova, Rashkov, Avdeev, & Tonchev, 2016). Therefore, the concentration of Ni and Cu needs special attention (Ganesan, Liu, Pandiyarajan, Lee, & Chuang, 2021). In addition, a complexing agent is needed to reduce the potential gap between Ni and Cu. Several studies reported the use of pyrophosphate, citrate, acetate, sulfamate, and glycine as complexing agents (Silaimani, Vivekanandan, & Veeramani, 2015). Gosh et al. conducted Ni-Cu plating with PC and DC apparatus using bath composition 0.475 M $\text{NiSO}_4 \cdot 7\text{H}_2\text{O}$, 0.125 M $\text{CuSO}_4 \cdot 5\text{H}_2\text{O}$, and 0.2 M sodium citrate (pH was maintained using ammonia solution) and resulting corrosion current between 0.17- 5.77 A cm^{-2} in 3% NaCl, hardness between 384-482 KHN₅₀ (Ghosh et al., 2000). Dai et al. fabricated Ni-Cu film with an electrodeposition technique using 300 g l^{-1} Ni sulfamic acid, 2.5 to 15 g l^{-1} Cu sulfates, 20 g l^{-1} Ni chloride, and 20 g l^{-1} boric acid, resulting in a reduction grain size by increasing Cu content in the alloy (Dai, Zhang, Wen, Rao, & Wang, 2016). Nady and Negem studied the electrodeposition of Ni-Cu alloys using various pH and concentration of NiSO_4 and CuSO_4 , with fixed sodium gluconate boric acid and cysteine at 0.025 A cm^{-2} of current density resulting in

mostly FCC (111) and FCC (200) crystal planes of the alloys (Nady & Negem, 2016). Garanova et al. fabricated Ni-Cu using electrodeposition in 0.2 $\text{C}_6\text{H}_5\text{Na}_3\text{O}_7 \cdot 2\text{H}_2\text{O}$ with different concentrations of Ni salts (0.2, 0.25, 0.5, and 0.6 M $\text{NiSO}_4 \cdot 7\text{H}_2\text{O}$) and 0.1M $\text{CuSO}_4 \cdot 5\text{H}_2\text{O}$. The pH (≈ 9) was maintained using a 25% NH_4OH solution. The study found that increasing Ni salt (0.6 M NiSO_4) has a levelling effect (Garanova et al., 2016).

Unfortunately, presenting a complexing agent could enhance the cost of production of Cu-Ni alloy. Therefore, presenting a Ni salt as a catalyst (without a complexing agent) in the plating bath needs further investigation. This study aims to create a Cu/Cu-Ni alloy on Cu alloy through electrodeposition and investigate the relationship between physical and hardness-corrosion properties. The layers were made using various solutions at 25 °C, and then the CCE and deposition rate were investigated. The Cu/Cu-Ni coating underwent characterization for scanning electron microscope-energy dispersive spectroscopy (SEM-EDS), x-ray diffraction (XRD), hardness, corrosion, and water droplets.

6. Experimental Section

6.1. Materials and Preparation

Electrodeposition solutions were made using $\text{CuSO}_4 \cdot 5\text{H}_2\text{O}$ and $\text{NiSO}_4 \cdot 6\text{H}_2\text{O}$. All chemicals used in the present research are analytical grade from Merck manufacturer. Pure Cu and Ni were used as an anode, while Cu alloy was used as a cathode with chemical compositions of P 0.22 wt.%, Cd 0.684 wt.%, Si 0.137 wt.%, and Cu balance. Before electrodeposition, the cathode was cleaned using ultrasonic cleaner (DELTA D68H) for 5 min. Electrodeposition was performed with a current density of 30 mA/cm^2 for 1 hour at 25 °C using a power supply (SANFIX 305 E). The specimens were electrodeposited using various plating baths, as seen in [Table 1](#).

6.2. Characterization

The CCE and deposition rate of the Cu/Cu-Ni electrodeposition were investigated by weighing samples before (initial weight) and after (final weight) electrodeposition and then calculated using equations in the previously reported (Basori, Soegijono, & Susetyo, 2022; Rosyidan et al., 2024). Afterward, XRD (PANalytical Aeris with Cu K radiation, $\lambda=0.15418$ nm, step size=0.02°) was used to determine the crystal structure of the Cu-Ni coating. MAUD software was used to refine and find the crystal parameter using XRD data. Moreover, the Debye-Scherrer formula ([Equation 1](#)) was used to calculate the crystal size of various samples (SEAKR, 2017).

$$D = \frac{0.9\lambda}{\beta \cos \theta} \quad (1)$$

Where D is the average crystallite size, k is a Scherrer constant of (0.9), λ is radiation wavelength (nm), β is the width of the FWHM diffraction peak (radians), and θ is peak position ($^\circ$ or radians).

FE-SEM equipped with EDS (Thermofisher Quanta 650 EDAX EDS Analyzer) was used to analyze the film surface morphology and phase. Afterward, roughness analysis was performed according to SEM picture using ImageJ software. Moreover, the hardness of the Cu-Ni film was measured using a MicroMet® 5100 Series micro indentation Vickers hardness tester using 100 g of load for 10 s. Measurement was conducted for five spot indentation.

Corrosion investigation was performed using potentiodynamic polarization methods (Digi-Ivy DY2311) in a 3.5% NaCl solution with a volume of 100 ml, the reference electrode being Ag/AgCl and the counter electrode being platinum (Pt) wire. Potentiodynamic polarization was carried out at a speed of 0.002 Vs^{-1} from -1.35 to -0.05 V. Information on corrosion current (i_{corr}) and corrosion voltage (E_{corr}) was acquired from the measurement data using the Tafel extrapolation method. The corrosion rate was calculated using Equation 2 utilizing the corrosion current information (Ahmad, 2006).

$$Cr = C \frac{Mi_{\text{corr}}}{n\rho} \quad (2)$$

Where Cr is the corrosion rate (mmpy), C is a constant for the corrosion rate calculation and is 3.27 mmpy, M is the atomic weight (g mol^{-1}), i_{corr} is corrosion current density (A cm^{-2}), n is the number of electrons involved, and ρ is the density of Cu and Ni (g cm^{-3}). Last step of the samples characterization is measured water contact angle. The contact angle was observed with a water droplet test on the film surface coated. Some criteria of the angle θ were determined by the value as $\theta < 90^\circ$, $90^\circ \leq \theta < 150^\circ$, and $150^\circ \leq \theta < 180^\circ$ for being hydrophilic, hydrophobic, and super hydrophobic, respectively (Lee, Bae, Jung, Jeong, & Ko, 2014).

7. Results and Discussion

7.1. CCE and Deposition Rate

The composition of $\text{CuSO}_4 \cdot 5\text{H}_2\text{O}$ and $\text{NiSO}_4 \cdot 6\text{H}_2\text{O}$ was determined at the start of the experiment. Figure 1 shows the CCE and deposition rate results of various experiments. CCE and deposition rate have similar tendencies; an increase in Ni salt would increase both CCE and deposition rate. CCE refers to the fraction of total current used for metal plating (Rosyidan et al., 2024). At the same time, the deposition rate is the amount of anode material deposited on the cathode at a particular current and time (Park, Sohn, & Choi, 2008). The first, second, and third solutions had a CCE of 35.71, 89.28, and 91.07 %, respectively. The first, second, and third solutions had a deposition rate of 48.66, 72.99, and 92.46, respectively. Hacıismailoglu and Alper

have found that increased pH leads to increased transient current (Haciismailoglu & Alper, 2011). Moreover, Rosyidan et al. have seen that an increase in the current leads to a rise in CCE and deposition rate (Rosyidan et al., 2024). Therefore, increased Ni salt promotes increased CCE and deposition rate due to rise and pH (see [Table 1](#)).

Hydrogen evolution could happen at the cathode when electrodeposition is conducted. Hydrogen evolution could disrupt ion's movement to the substrate's surfaces during deposition by blocking the cathode surface. Deo et al. have stated that hydrogen evolution is a competitor at Ni and Cu electrodeposition (Deo et al., 2020). According to the CCE result, higher hydrogen evolution occurred in the samples made using the first solution, and increasing a Ni salt in the solution led to a decrease in hydrogen evolution. Guler et al. have stated that presenting a hydrogen evolution at the cathode during electrodeposition leads to a decrease in CCE (Saraloğlu Güler, Konca, & Karakaya, 2013).

7.2. Phase and Surface Morphology

In this study, film deposition involved diffusion and charge transfer by Cu/Cu-Ni. The various films were obtained using a current density of 30 mA cm^{-2} for an hour for all solution variations. The results of the EDS investigation can be seen in [Figure 2](#). Based on [Figure 2](#), it can be seen that 100 wt.% Cu phases are seen when electrodeposited using baths 1 and 2. This means presenting a Ni salt 0.3 and 0.5 M doesn't cause an exhibit of Ni in the film. Meanwhile, when Ni salt concentration rises to 0.7 M, Ni is exhibited in the film around 0.2 wt. %. The solution seems to have a salt limitation, resulting in a Cu-Ni Alloy. Decrease a Cu salt by less than 0.1 M or increasing a Ni salt by more than 0.7 M is needed. Baskaran et al. electrodeposited Ni using the composition between Ni and Cu salt, which is 20:1 (Baskaran, Sankara Narayanan, & Stephen, 2006). Sarac et al. electrodeposited Ni using the composition between Ni and Cu salt are 50:1 (Sarac, Öksüzoğlu, & Baykul, 2012). Moreover, Haciismailoglu and Alper have stated that hydrogen evolution was occurring at the surface of the substrate during the electrodeposition process, which could prevent the reduction of Ni in the film (Haciismailoglu & Alper, 2011). This statement is corroborated by the fact that Ni formed in the sample was made using a third solution due to electrodeposition using the first and second solutions, which still caused hydrogen evolution on the substrate surface.

[Figures 3 \(a\)-\(c\)](#) show the morphology of the deposited non-uniform and compact films, which

is affected by the hydrogen evolution. Guler et al. have stated the disruption is due to hydrogen evolution at the cathode, which could be resulting a non-uniform film (Saraloğlu Güler et al., 2013). Moreover, pure Cu (Figures 3 (a) and (b)) show morphology with nodules form. In contrast, presenting a Ni in the alloy, which changes nodules to a cauliflower-like form (Figure 3 (c)). As mentioned above, exhibiting a Ni salt in the solution could increase the pH of the solution (Table 1). Kalubowila et al. have found that increasing the pH bath could transform surface morphology (Kalubowila et al., 2019). furthermore, raising a pH solution leads to an increased deposition rate and change in surface morphology. Therefore, there is transformation from nodules to a cauliflower-like form. Statistical analysis using ImageJ combined Origin with the corresponding Gauss fitting function was used to identify the grain size distribution. The result is presented in Figure 3.

Image-J software was used to calculate the average grain size diameter. Table 2 shows the results of calculating the average grain size. The calculation results show that the grain size average has decreased by increasing the Ni salt in the solution. Baskaran et al. stated that grain size decreased due to increased electrodeposition current density (Baskaran et al., 2006). Previous research shows that increasing current density increases deposition rate (Rosyidan et al., 2024). Compared to Figure 1, it is seen that rising Ni salt leads to an increased deposition rate. An increase in the deposition rate leads to an increased speed of the ion species deposited on the cathode surface. Therefore, grain size is decreasing in the present research.

Image processing was done using Image J software to obtain detailed information about the resulting image pattern. Image patterns were investigated from SEM pictures to interpret the results of surface roughness parameters and 3-D images from surface scanning. The result of the Image J software investigation can be seen in Figure 4, which presents the relationship between distance (μm) and gray value varies with increasing distance.

Table 3 shows the average surface roughness of Cu-Ni/Cu coating morphology fabricated from various baths according to Image J software investigation. According to Table 3, increasing Ni salt in the solution increases the films' roughness average. Deo et al. reported that increasing a current density led to an increase in surface roughness (Deo et al., 2020). As mentioned above, increasing current density increases deposition rate (Rosyidan et al., 2024). Compared to the deposition rate

measurement (Figure 1), it can be seen that rising Ni salt leads to an increased deposition rate due to pH increments. An increase in the deposition rate leads to an increased speed of the ion species deposited on the cathode surface. Therefore, the roughness average is increased in the present research.

7.3. Crystallographic Orientation

According to the XRD data in Figure 5, three planes formed namely the (111), (002), and (022) planes. The (111) plane dominated when the films were made using baths 1, 2, and 3. The dominance of the (111) plane orientation had benefits such as anticorrosion, increased electrical conductivity, and improved mechanical properties (SEAKR, 2017). Moreover, all of the collected XRD data were then analyzed using MAUD software, and the crystal parameters are shown in Table 4. All led to the same crystal structure and space group, FCC and Fm-3m, which can be concluded that atoms of the Cu and Ni form a substitutional solid solution (Dai et al., 2016).

Table 4 shows that the lattice constant and cell volume decrease due to the increase in the Ni phase in the alloy, which perfectly agrees with other reports (Baskaran et al., 2006). Moreover, increased Ni salt in the plating bath decreases crystallite size. Augustin et al. have reported an increase in current density promoting reduced crystallite size (Augustin et al., 2016). Increasing the electrodeposition process's current density influences the deposition rate's increase; the amount of ion species deposited on the cathode rose; therefore, crystallite size decreased. Small crystal size indicates that the distance between grains is close, contributing to material qualities with more roughness properties (Dai et al., 2016). This result is in perfect agreement with the average roughness in Table 3. Moreover, a smaller lattice strain is seen in the sample made using bath 3.

7.4. Hardness

Hardness is a material's resistance to plastic deformation. A coating procedure is considered successful if it can enhance the qualities of the coated objects. One of the purposes of electrodeposition in the present research is to improve material deposited hardness. The results of the hardness of the coating were obtained using a Vickers micro-hardness tester. The Vickers microhardness method obtained 58 HV in the first solution, 68 HV in the second solution, and 136 HV in the third solution. It seems an increase in Ni salt would increase the hardness. In their study, Augustin et al. found that a decrease in crystallite size promotes an increase in hardness, which is

in perfect agreement with the present research (Augustin et al., 2016). Besides crystallite size, the exhibit of Ni in the alloy also influences the hardness of the sample (Rosyidan et al., 2024). As seen in **Figure 6**, a sample was made using bath 3, resulting in higher hardness, which is affected by the exhibit of Ni in the alloy. According to the EDS result, only one sample was made using bath 3, resulting in Ni in the alloy. Compared to the Monel 400, hardness is between 150 to 200 HV, and present research has lower hardness (Kukliński, Bartkowska, Przestacki, & Kinal, 2020).

7.5. Corrosion

Figure 7 shows the corrosion curves of the electrodeposition of Cu/Cu-Ni on the Cu alloy substrate. The i_{corr} and E_{corr} were found using the Tafel extrapolation method. Meanwhile, CR was calculated using equation (2). The summary of the calculations for the CR of various samples is shown in **Table 5**. The crystal plane could determine the corrosion rate behavior of materials with the FCC crystal system. The (111) crystal plane is more corrosion-resistant in materials with the FCC system than the (002) and (022) crystal planes (Al Kharafi, Ghayad, & Abdullah, 2012). Therefore, all of the samples met good and excellent criteria. Moreover, based on **Table 5**, it can be seen that the third solution has the best corrosion rate. This behavior is influenced by the lattice strain that was formed. Lattice strain is sample defect concentration measured due to a void core in the lattice (Basori et al., 2022). Therefore, the smallest lattice strain leads to the highest corrosion resistance. According to Wang et al. and Ghosh et al. studies, Monel-400 i_{corr} is 2.24×10^{-6} and 2.2×10^{-6} (A cm^{-2}) (Ghosh et al., 2000; Wang et al., 2014). Compared with **Table 5**, it can be seen that the sample made using a third solution has lower i_{corr} than Monel-400.

7.6. Contact Angle

The water droplet test can be used to determine the hydrophilic, hydrophobic, and superhydrophobic properties of a film. **Figure 8** shows a snapshot of the drip test findings for various samples. All samples possess hydrophilic properties since they have contact angles between 0° and 90° (Thurber et al., 2016). The contact angles achieved in the first, second, and third solution 1 are 69.2° , 79.4° and 88.6° , respectively. Increment of the water contact angle is probably due to an increased film surface roughness. In their research, Huang et al. found that increasing roughness would increase the water contact angle (Huang & Gates, 2020). Moreover, Yu et al. found that increasing electrolyte pH from 2 to 4 increases the film's water contact angle

(Yu et al., 2013), probably due to an increase in the surface roughness of the samples.

8. Conclusion

Cu/Cu-Ni film was electrodeposited onto Cu alloy using various bath compositions, and according to the multiple findings, increased Ni salt content led to increased deposition rate and CCE due to an increased pH and depleting hydrogen evolution, which impacted grain size, more roughness, less crystallite size and presenting small amount of a Ni in the film. The formed crystal structure was a single-phase FCC with the dominant (111) plane. The hardness increment is due to a decrease in crystallite size. Lesser lattice strain contributed to a higher corrosion resistance. The films have more roughness and impact on the higher water contact angle. The 99.8Cu0.3Ni alloy has the best corrosion resistance and is recommended as an alternative to change Monel-400.

Acknowledgement

This project was financially supported by Universitas Trisakti based on the assignment letter number 800/C-4/FTKE/USAKTI/X/2023.

References

- Ahmad, Z. (2006). Principles of Corrosion Engineering and Corrosion Control. In *Principles of Corrosion Engineering and Corrosion Control* (1st ed.). Oxford, United Kingdom: Butterworth-Heinemann. <https://doi.org/10.1016/b978-0-7506-5924-6.x5000-4>
- Al Kharafi, F. M., Ghayad, I. M., & Abdullah, R. M. (2012). Corrosion inhibition of copper in non-polluted and polluted sea water using 5-phenyl-1-H-tetrazole. *International Journal of Electrochemical Science*, 7(4), 3289–3298. [https://doi.org/10.1016/s1452-3981\(23\)13954-x](https://doi.org/10.1016/s1452-3981(23)13954-x)
- Augustin, A., Huilgol, P., Udupa, K. R., & Bhat K, U. (2016). Effect of current density during electrodeposition on microstructure and hardness of textured Cu coating in the application of antimicrobial Al touch surface. *Journal of the Mechanical Behavior of Biomedical Materials*, 63, 352–360. <https://doi.org/10.1016/j.jmbbm.2016.07.013>
- Baskaran, I., Sankara Narayanan, T. S. N., & Stephen, A. (2006). Pulsed electrodeposition of nanocrystalline Cu-Ni alloy films and evaluation of their characteristic properties. *Materials Letters*, 60(16), 1990–1995. <https://doi.org/10.1016/j.matlet.2005.12.065>
- Basori, B., Soegijono, B., Yudanto, S. D., Nanto, D., & Susetyo, F. B. (2023). Effect of low magnetic field during nickel electroplating on morphology, structure, and hardness. *Journal of Physics: Conference Series*, 2596(1). <https://doi.org/10.1088/1742-6596/2596/1/012014>

- Basori, Soegijono, B., & Susetyo, F. B. (2022). Magnetic field exposure on electroplating process of ferromagnetic nickel ion on copper substrate. *Journal of Physics: Conference Series*, 2377, 012002. <https://doi.org/10.1088/1742-6596/2377/1/012002>
- Dai, P. Q., Zhang, C., Wen, J. C., Rao, H. C., & Wang, Q. T. (2016). Tensile Properties of Electrodeposited Nanocrystalline Ni-Cu Alloys. *Journal of Materials Engineering and Performance*, 25(2), 594–600. <https://doi.org/10.1007/s11665-016-1881-2>
- Deo, Y., Guha, S., Sarkar, K., Mohanta, P., Pradhan, D., & Mondal, A. (2020). Electrodeposited Ni-Cu alloy coatings on mild steel for enhanced corrosion properties. *Applied Surface Science*, 515, 146078. <https://doi.org/10.1016/j.apsusc.2020.146078>
- Ganesan, M., Liu, C. C., Pandiyarajan, S., Lee, C. T., & Chuang, H. C. (2021). Post-supercritical CO₂ electrodeposition approach for Ni-Cu alloy fabrication: An innovative eco-friendly strategy for high-performance corrosion resistance with durability. *Applied Surface Science*, (November). <https://doi.org/10.1016/j.apsusc.2021.151955>
- Ghosh, S. K., Grover, A. K., Dey, G. K., Kulkarni, U. D., Dusane, R. O., Suri, A. K., & Banerjee, S. (2006). Structural characterization of electrodeposited nanophase Ni-Cu alloys. *Journal of Materials Research*, 21(1), 45–61. <https://doi.org/10.1557/jmr.2006.0034>
- Ghosh, S. K., Grover, A. K., Dey, G. K., & Totlani, M. K. (2000). Nanocrystalline Ni-Cu alloy plating by pulse electrolysis. *Surface and Coatings Technology*, 126(1), 48–63. [https://doi.org/10.1016/S0257-8972\(00\)00520-X](https://doi.org/10.1016/S0257-8972(00)00520-X)
- Gómez, E., Pané, S., & Vallés, E. (2005). Electrodeposition of Co-Ni and Co-Ni-Cu systems in sulphate-citrate medium. *Electrochimica Acta*, 51(1), 146–153. <https://doi.org/10.1016/j.electacta.2005.04.010>
- Goranova, D., Rashkov, R., Avdeev, G., & Tonchev, V. (2016). Electrodeposition of Ni–Cu alloys at high current densities: details of the elements distribution. *Journal of Materials Science*, 51(18), 8663–8673. <https://doi.org/10.1007/s10853-016-0126-y>
- Haciismailoglu, M., & Alper, M. (2011). Effect of electrolyte pH and Cu concentration on microstructure of electrodeposited Ni-Cu alloy films. *Surface and Coatings Technology*, 206(6), 1430–1438. <https://doi.org/10.1016/j.surfcoat.2011.09.010>
- Hakim, M. S., Pangestu, H., & Riyanto. (2022). Preparation and Application of Nickel Electroplating on Copper (Ni/EC) Electrode for Glucose Detection. *Science and Technology Indonesia*, 7(2), 208–212. <https://doi.org/10.26554/sti.2022.7.2.208-212>
- Huang, X., & Gates, I. (2020). Apparent Contact Angle around the Periphery of a Liquid Drop on Roughened Surfaces. *Scientific Reports*, 10(1), 1–11. <https://doi.org/10.1038/s41598-020-65122-w>
- Jariwala, F., Gohil, R., Trivedi, P., Parmar, J., Borda, B., Patel, S., ... Rao, V. (2018). Electroplating of Nickel and Chromium on Aluminum 6082-T6 alloy. *Proceedings of the International Conference on Recent Advances in Metallurgy for Sustainable Development*,

1–3.

- Kalubowila, K. D. R. N., Jayathileka, K. M. D. C., Kumara, L. S. R., Ohara, K., Kohara, S., Sakata, O., ... Jayanetti, J. K. D. S. (2019). Effect of Bath pH on Electronic and Morphological Properties of Electrodeposited Cu₂O Thin Films. *Journal of The Electrochemical Society*, 166(4), D113–D119. <https://doi.org/10.1149/2.0551904jes>
- Kukliński, M., Bartkowska, A., Przestacki, D., & Kinal, G. (2020). Influence of microstructure and chemical composition on microhardness and wear properties of laser borided monel 400. *Materials*, 13(24), 1–15. <https://doi.org/10.3390/ma13245757>
- Lajevardi, S. A., Shahrabi, T., Szpunar, J. A., Sabour Rouhaghdam, A., & Sanjabi, S. (2013). Characterization of the microstructure and texture of functionally graded nickel-Al₂O₃ nano composite coating produced by pulse deposition. *Surface and Coatings Technology*, 232, 851–859. <https://doi.org/10.1016/j.surfcoat.2013.06.111>
- Lee, J. M., Bae, K. M., Jung, K. K., Jeong, J. H., & Ko, J. S. (2014). Creation of microstructured surfaces using Cu-Ni composite electrodeposition and their application to superhydrophobic surfaces. *Applied Surface Science*, 289, 14–20. <https://doi.org/10.1016/j.apsusc.2013.10.066>
- Matsuda, T., Saeki, R., Hayashida, M., & Ohgai, T. (2022). Microhardness and heat-resistance performance of ferromagnetic cobalt-molybdenum nanocrystals electrodeposited from an aqueous solution containing citric acid. *Materials Research Express*, 9(4). <https://doi.org/10.1088/2053-1591/ac60e3>
- Nady, H., & Negem, M. (2016). Ni-Cu nano-crystalline alloys for efficient electrochemical hydrogen production in acid water. *RSC Advances*, 6(56), 51111–51119. <https://doi.org/10.1039/c6ra08348j>
- Ollivier, A., Muhr, L., Delbos, S., Grand, P. P., Matlosz, M., & Chassaing, E. (2009). Copper-nickel codeposition as a model for mass-transfer characterization in copper-indium-selenium thin-film production. *Journal of Applied Electrochemistry*, 39(12), 2337–2344. <https://doi.org/10.1007/s10800-009-9918-y>
- Park, B. N., Sohn, Y. S., & Choi, S. Y. (2008). Effects of a magnetic field on the copper metallization using the electroplating process. *Microelectronic Engineering*, 85(2), 308–314. <https://doi.org/10.1016/j.mee.2007.06.018>
- Rosyidan, C., Kurniawan, B., Soegijono, B., Putra, V. G. V., Munazat, D. R., & Susetyo, F. B. (2024). Effect of Current Density on Magnetic and Hardness Properties of Ni-Cu Alloy Coated on Al via Electrodeposition. *International Journal of Engineering, Transaction B: Applications*, 37(02), 213–223. <https://doi.org/10.5829/IJE.2024.37.02B.01>
- Sarac, U., Öksüzöğlü, R. M., & Baykul, M. C. (2012). Deposition potential dependence of composition, microstructure, and surface morphology of electrodeposited Ni-Cu alloy films. *Journal of Materials Science: Materials in Electronics*, 23(12), 2110–2116. <https://doi.org/10.1007/s10854-012-0709-6>

- Saraloğlu Güler, E., Konca, E., & Karakaya, I. (2013). Effect of electrodeposition parameters on the current density of hydrogen evolution reaction in Ni and Ni-MoS₂ composite coatings. *International Journal of Electrochemical Science*, 8(4), 5496–5505. [https://doi.org/10.1016/s1452-3981\(23\)14699-2](https://doi.org/10.1016/s1452-3981(23)14699-2)
- SEAKR, R. (2017). Microstructure and crystallographic characteristics of nanocrystalline copper prepared from acetate solutions by electrodeposition technique. *Transactions of Nonferrous Metals Society of China (English Edition)*, 27(6), 1423–1430. [https://doi.org/10.1016/S1003-6326\(17\)60164-X](https://doi.org/10.1016/S1003-6326(17)60164-X)
- Setiamukti, D., Toifur, M., & Khusnani, A. (2020). The effect of electrolyte concentration on the sensitivity of low-temperature sensor performance of Cu/Ni film. *Science and Technology Indonesia*, 5(2), 28–33. <https://doi.org/10.26554/sti.2020.5.2.28-33>
- Silaimani, S. M., Vivekanandan, G., & Veeramani, P. (2015). Nano-nickel–copper alloy deposit for improved corrosion resistance in marine environment. *International Journal of Environmental Science and Technology*, 12(7), 2299–2306. <https://doi.org/10.1007/s13762-014-0591-2>
- Thurber, C. R., Ahmad, Y. H., Sanders, S. F., Al-Shenawa, A., D’Souza, N., Mohamed, A. M. A., & Golden, T. D. (2016). Electrodeposition of 70-30 Cu-Ni nanocomposite coatings for enhanced mechanical and corrosion properties. *Current Applied Physics*, 16(3), 387–396. <https://doi.org/10.1016/j.cap.2015.12.022>
- Wang, S., Guo, X., Yang, H., Dai, J., Zhu, R., Gong, J., ... Ding, W. (2014). Electrodeposition mechanism and characterization of Ni-Cu alloy coatings from a eutectic-based ionic liquid. *Applied Surface Science*, 288, 530–536. <https://doi.org/10.1016/j.apsusc.2013.10.065>
- Yu, Q., Zeng, Z., Zhao, W., Li, M., Wu, X., & Xue, Q. (2013). Fabrication of adhesive superhydrophobic Ni-Cu-P alloy coatings with high mechanical strength by one step electrodeposition. *Colloids and Surfaces A: Physicochemical and Engineering Aspects*, 427, 1–6. <https://doi.org/10.1016/j.colsurfa.2013.02.067>

Figures

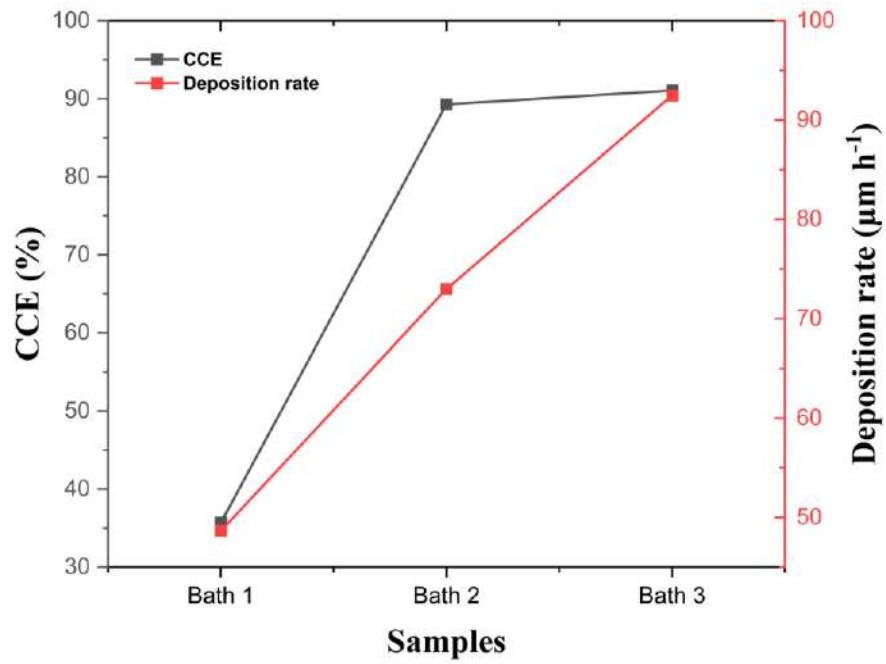


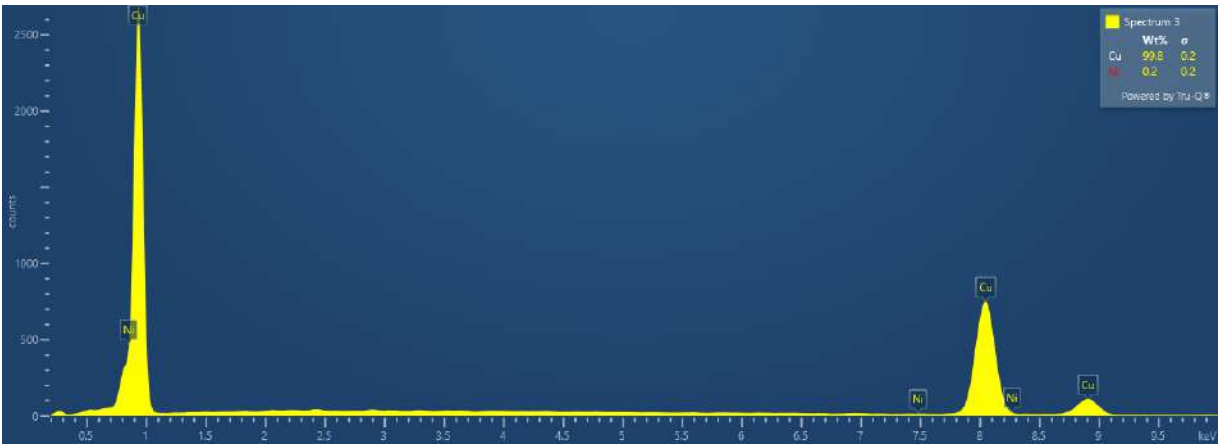
Figure 1. CCE and deposition rate for Cu/Cu-Ni electrodeposited from bath 1, 2, and 3



(a)

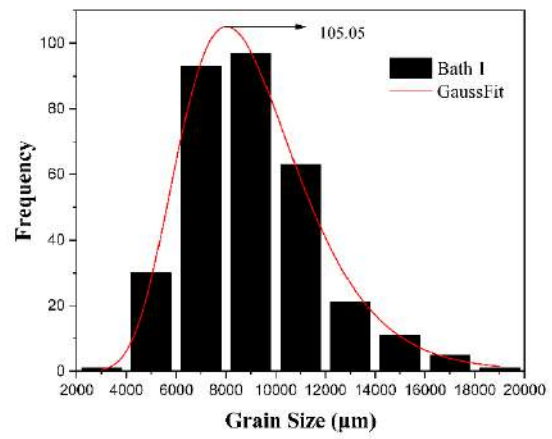
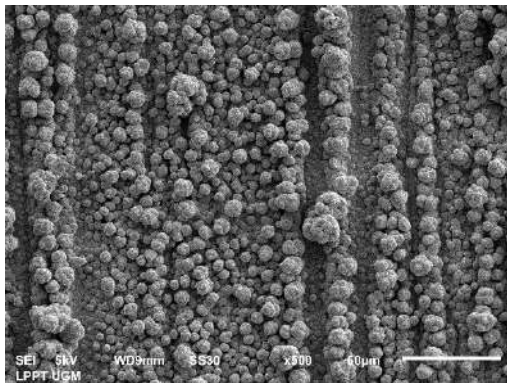


(b)

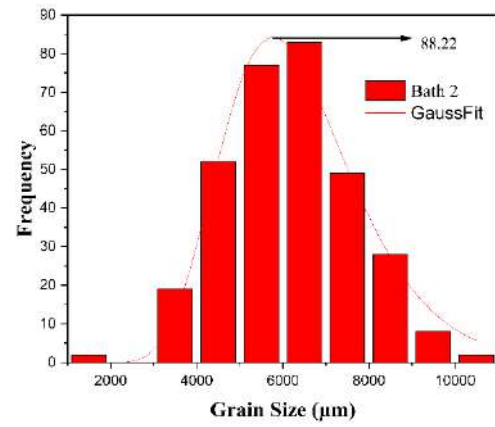
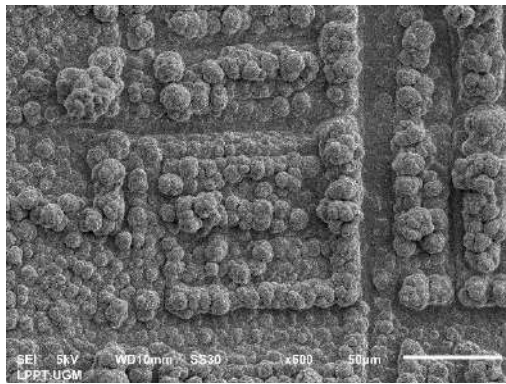


(c)

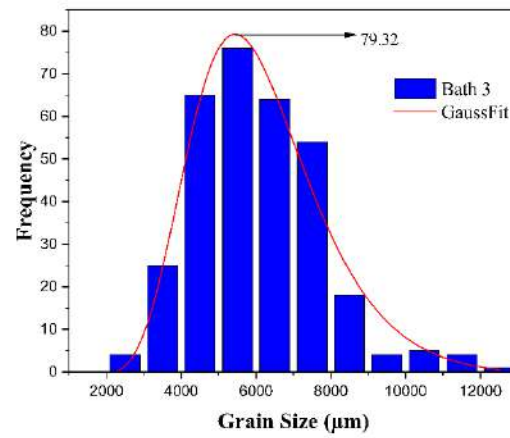
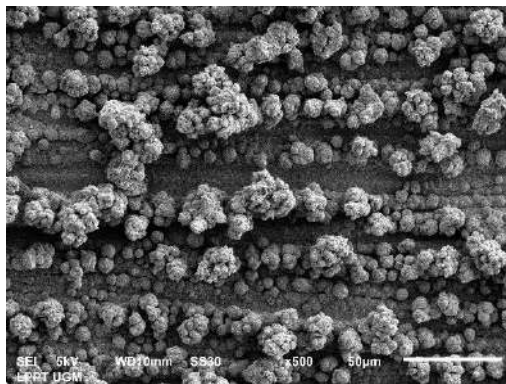
Figure 2. EDS test results of various samples



(a)

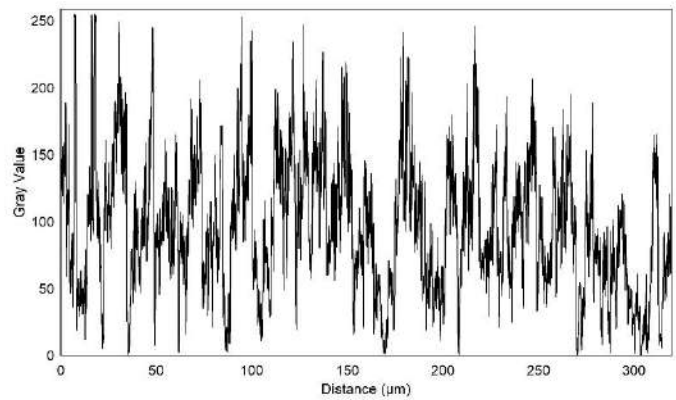
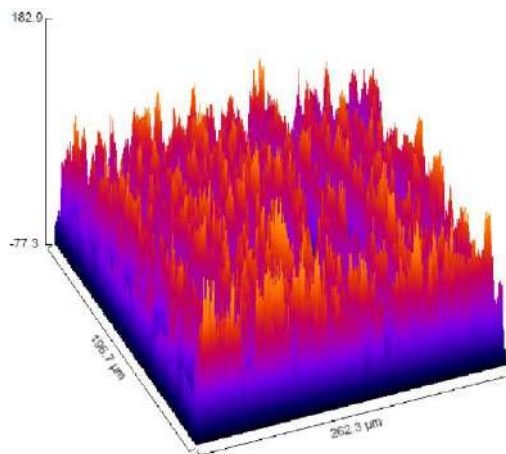


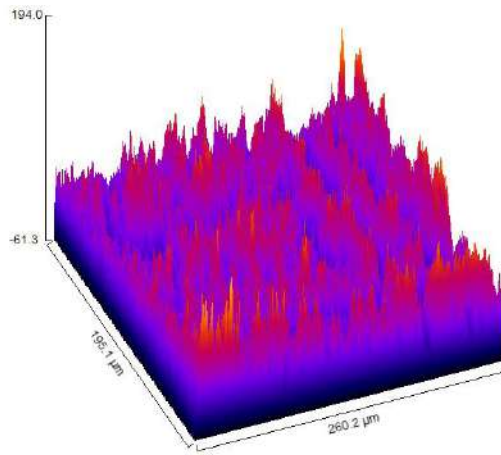
(b)



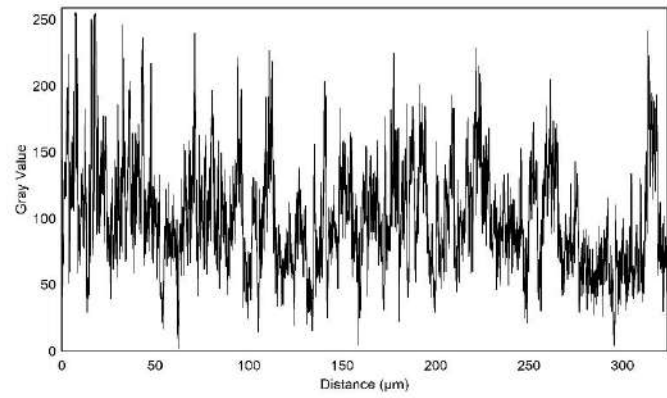
(c)

Figure 3. SEM micrographs and grain distribution for different samples (a) Bath 1, (b) Bath 2, and (c) Bath 3

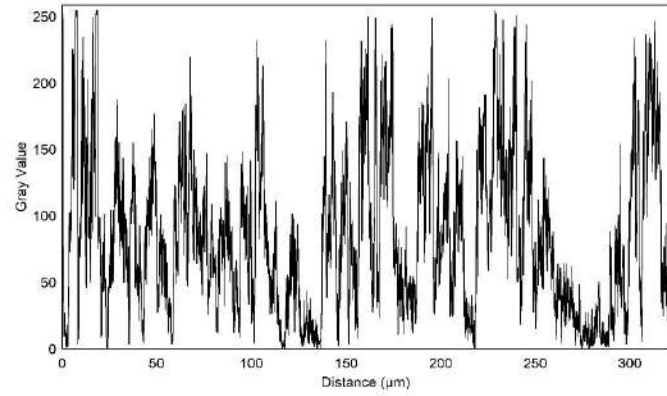
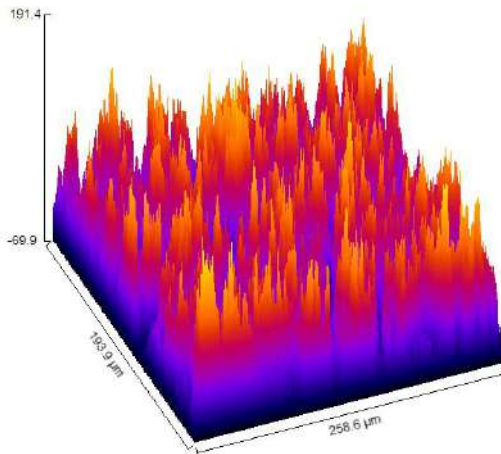




(a)



(b)



(c)

Figure 4. Analysis of sample surfaces roughness in 3D SEM image and graph of grey value against distance (left-right) (a) Bath 1, (b) Bath 2, and (c) Bath 3

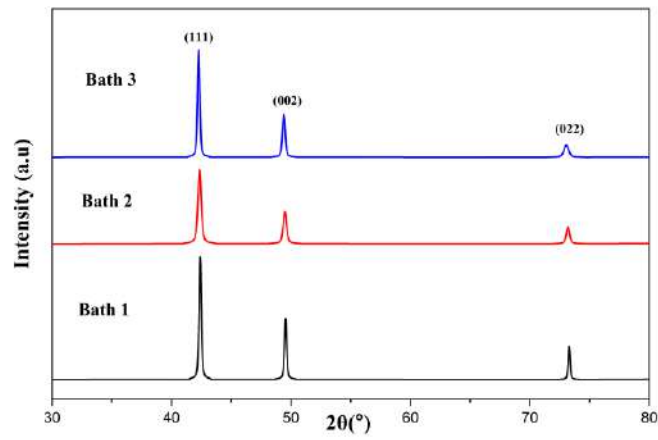


Figure 5. XRD pattern of various samples

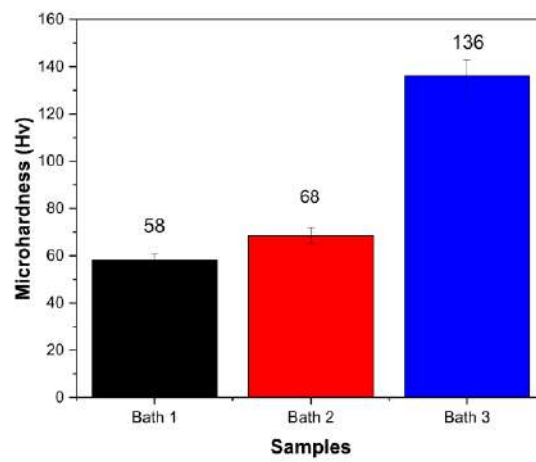


Figure 6. Hardness test results of various samples

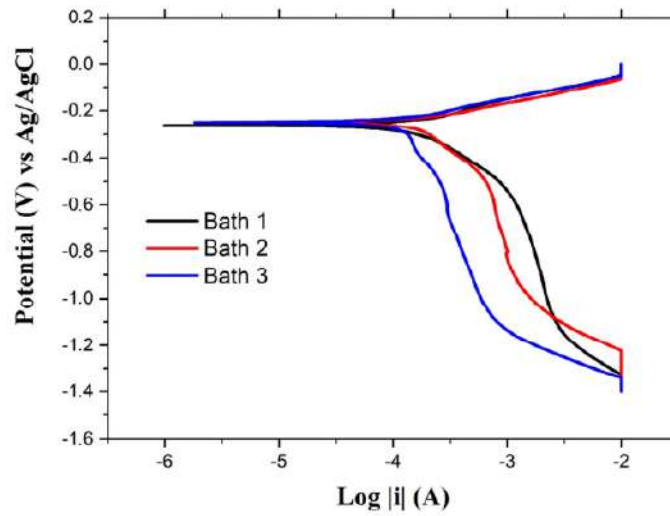


Figure 7. Corrosion curve for various samples

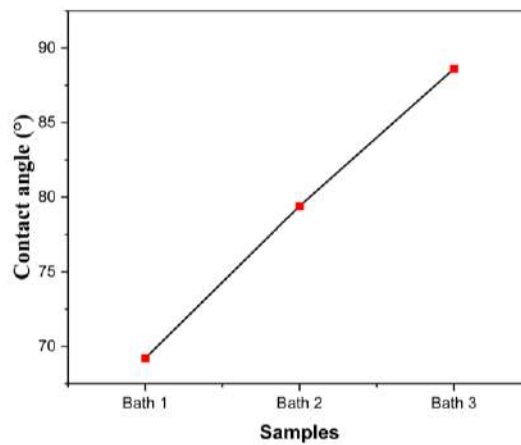


Figure 8. Water contact angle of various samples

Tables

Table 1. Plating baths composition for Cu/Cu-Ni electrodeposition

Plating bath	Composition (M)		Measured pH
	CuSO ₄ .5H ₂ O	NiSO ₄ .7H ₂ O	
Bath 1	0.1	0.3	2.35
Bath 2	0.1	0.5	2.51
Bath 3	0.1	0.7	2.53

Table 2. Average grain size calculation results of various samples

Sample	Grain Size (μm)
Bath 1	105.05
Bath 2	88.22
Bath 3	79.32

Table 3. Average roughness value of various samples

Sample	Roughness Average (Ra) μm
Bath 1	30.63
Bath 2	37.49
Bath 3	37.82

Table 4. Crystal parameters of various samples

Parameter	Sample		
	Bath 1	Bath 2	Bath 3
Crystal structure	FCC		
Space Group	Fm-3m		
Lattice constant (\AA) $a = b = c$	3.631	3.618	3.612
Cell volume (\AA^3)	47.89	47.37	47.14
d-spacing (\AA)	1.7530	1.7549	1.7578
Crystallite Size (nm)	43.39	27.54	25.70
Lattice strain	0.27	0.41	0.25

Table 5. Corrosion measurements of various samples

Sample	i_{corr} (Acm^{-2})	E_{corr} (V)	Cr (mmpy)	Criteria
Bath 1	4.40×10^{-6}	-0.261	0.196	Good
Bath 2	5.01×10^{-6}	-0.244	0.223	Good
Bath 3	1.82×10^{-6}	-0.248	0.081	Excellent

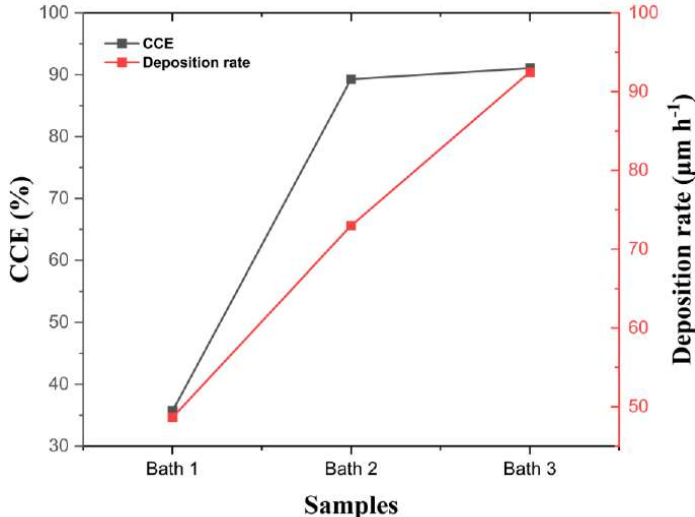
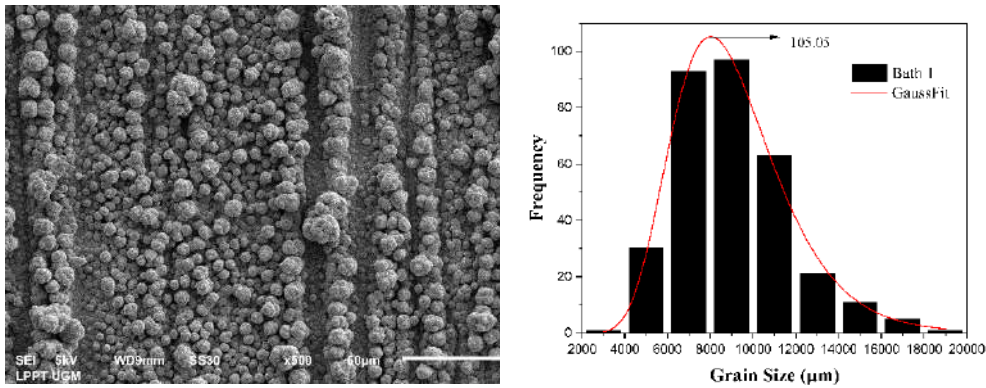
Title : Nickel Salt Dependency as Catalyst in the Plating Bath on the Film Properties of Cu/Cu-Ni

Authors : Cahaya Rosyidan, Budhy Kurniawan, Bambang Soegijono, Mustamina Maulani, Lisa Samura, Frederik Gresia Nababan,Valentinus Galih Vidia Putra, Ferry Budhi Susetyo

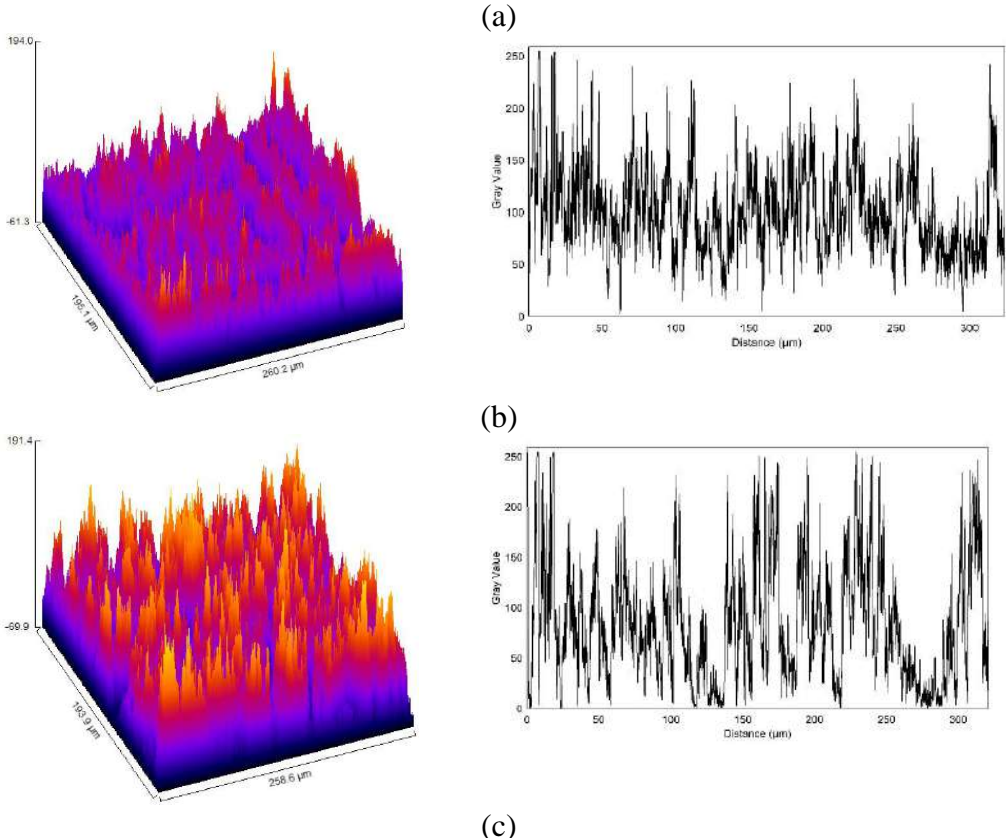
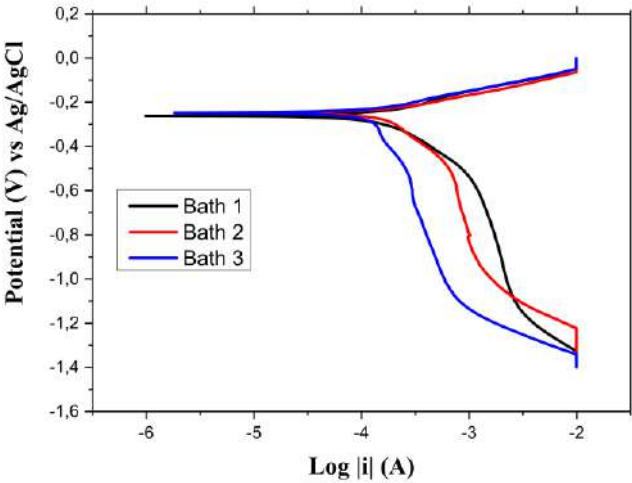
Corresponding author : Cahaya Rosyidan

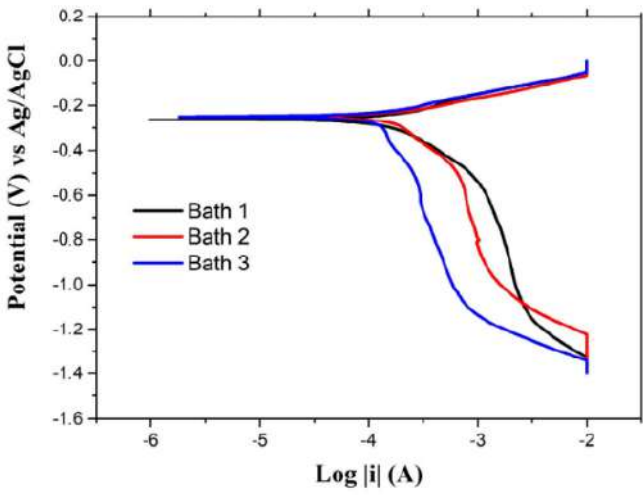
Review STI 1142

No.	Comment from Reviewer	Revision
1	Keyword should be specific related with the experiment not instrument analysis	keywords have been replaced with appropriate experiment instead of instrument. Thank you Example: Keywords: <i>Cathode current efficiency, Deposition rate, Electrodeposition, Corrosion, Hardness</i>
2	Abstract should contain: what you do, method, and results. Please consider with this item	What you do and method: This study aims to assess the properties of Cu/Cu-Ni film, such as phase, surface morphology, crystallographic orientation, hardness, corrosion analysis, and contact angle, which were fabricated using electrodeposition with various Ni salt additions (0.3, 0.5 and 0.7 M). In addition, the cathode current efficiency (CCE) and deposition rate of the Cu/Cu-Ni electrodeposition were also investigated. Result: An increase in Ni salt in the plating bath could enhance the pH, promoting higher CCE and depleting hydrogen evolution at the cathode, leading to the presenting Ni phase in the alloy. The higher concentration of Ni salt in the solution could also enhance the deposition rate due to a shift to a pH value, which affects the roughening of the surface morphology, promoting a higher contact angle. All crystal structures generated by Cu/Cu-Ni electrodeposition were FCC, with the preferred orientation of the (111) plane. Crystallite size and lattice strain depend on the deposition rate. Less crystallite size and lattice strain affect the film's hardness and corrosion resistance. Moreover, the third bath had the resulting Cu-Ni layer with the best hardness and corrosion rate of around 136 HV and 0.081mmpy.
3	Make sure each paragraph	Several paragraph has been merge. Thank you.

	contain at least several sentences. Too many paragraph in your manuscript													
4	Remove the outline	<p>Yes, we have removed the lines in the legend.</p>  <table border="1"><thead><tr><th>Samples</th><th>CCE (%)</th><th>Deposition rate ($\mu\text{m h}^{-1}$)</th></tr></thead><tbody><tr><td>Bath 1</td><td>35</td><td>50</td></tr><tr><td>Bath 2</td><td>89</td><td>72</td></tr><tr><td>Bath 3</td><td>91</td><td>90</td></tr></tbody></table> <p>Figure 1. CCE and deposition rate for Cu/Cu-Ni electrodeposited from bath 1, 2, and 3</p>	Samples	CCE (%)	Deposition rate ($\mu\text{m h}^{-1}$)	Bath 1	35	50	Bath 2	89	72	Bath 3	91	90
Samples	CCE (%)	Deposition rate ($\mu\text{m h}^{-1}$)												
Bath 1	35	50												
Bath 2	89	72												
Bath 3	91	90												
5	The outline on Figure 3 and 7 in the line caption was also removed	<p>Yes, we have removed the lines in the legends in figures 3 and 7.</p>  <p>(a)</p>												

		<div data-bbox="520 190 1476 1064" data-label="Figure"> <p>(a)</p> <p>(b)</p> <p>(c)</p> </div> <div data-bbox="566 1064 1532 1131" data-label="Caption"> <p>Figure 3. SEM micrographs and grain distribution for different samples (a) Bath 1, (b) Bath 2, and (c) Bath 3</p> </div> <div data-bbox="774 1131 1316 1534" data-label="Figure"> </div> <div data-bbox="750 1545 1348 1585" data-label="Caption"> <p>Figure 7. Corrosion curve for various samples</p> </div>
6	Remove the grid	<p>yes, we have removed the grid</p> <div data-bbox="502 1691 1508 2027" data-label="Figure"> </div>

		<div data-bbox="507 197 1517 1032">  <p>(a)</p> <p>(b)</p> <p>(c)</p> </div> <p>Figure 4. Analysis of sample surfaces roughness in 3D SEM image and graph of grey value against distance (left-right) (a) Bath 1, (b) Bath 2, and (c) Bath 3</p>
7	<p>Please check the use of periods and commas in figures, tables, and text.</p>	<p>Yes, we have corrected the use of periods and commas in the image, such as the example below:</p> <p>Before:</p> <div data-bbox="539 1346 1174 1827">  </div>

		<p>After:</p> 
8	Figure, Table, and Equation must be mentioned in the text	<p>Yes, both tables and figures have been mentioned in the body text and we give a red color mark.</p>

4. Keputusan Editor

(4 April 2025)

Bukti dari Email

[STI] Editor Decision

External

Inbox x



Prof. Aldes Lesbani <scitechindones@gmail.com>

Apr 4, 2024, 11:08 AM



to me, Budhy, Bambang, Mustamina, Lisa, Frederik, Valentinus, Ferry ▾

Dear Cahaya Rosyidan, Budhy Kurniawan, Bambang Soegijono, Mustamina Maulani, Lisa Samura, Frederik Gresia Nababan, Valentinus Galih Vidia Putra, Ferry Budhi Susetyo:

We have reached a decision regarding your submission to Science and Technology Indonesia, "Nickel Salt Dependency as Catalyst in the Plating Bath on the Film Properties of Cu/Cu-Ni".

Our decision is to accept your submitted manuscript for publication in

Thank you for publishing with us and please do not hesitate to contact us if you have any inquiry.

Science and Technology Indonesia

A Peer-Reviewed Research Journal of Science and Technology

p-ISSN: 2580-4405 | e-ISSN: 2580-4391

E-mail: admin@scitechindonesia.com | scitechindonesia@gmail.com

Homepage: <http://scitechindonesia.com/index.php/sti>

5. Bukti Artikel Terbit (Juli 2024)

Nickel Salt Dependency as Catalyst in the Plating Bath on the Film Properties of Cu/Cu-Ni

Cahaya Rosyidan^{1*}, Budhy Kurniawan², Bambang Soegijono³, Mustamina Maulani¹, Lisa Samura¹, Frederik Gresia Nababan¹, Valentinus Galih Vidia Putra⁴ Ferry Budhi Susetyo⁵

¹Department of Petroleum Engineering, Universitas Trisakti, Jakarta, 11440, Indonesia

²Department of Physics, Universitas Indonesia, Depok, 16424, Indonesia

³Department of Geoscience, Universitas Indonesia, Depok, 16424, Indonesia

⁴Plasma and Nanomaterial Research Group, Politeknik STTT Bandung, Bandung, 40272, Indonesia

⁵Department of Mechanical Engineering, Universitas Negeri Jakarta, Jakarta, 13220, Indonesia

*Corresponding author: cahayarosyidan@trisakti.ac.id

Abstract

Metal plating frequently employs nickel (Ni) and copper (Cu) as anodes. Cu/ Cu-Ni film formed has many advantages, such as better corrosion resistance and high hardness characteristics. This study aims to assess the properties of Cu/Cu-Ni film, such as phase, surface morphology, crystallographic orientation, hardness, corrosion analysis, and contact angle, which were fabricated using electrodeposition with various Ni salt additions (0.3, 0.5 and 0.7 M). In addition, the cathode current efficiency (CCE) and deposition rate of the Cu/Cu-Ni electrodeposition were also investigated. An increase in Ni salt in the plating bath could enhance the pH, promoting higher CCE and depleting hydrogen evolution at the cathode, leading to the presenting Ni phase in the alloy. The higher concentration of Ni salt in the solution could also enhance the deposition rate due to a shift to a pH value, which affects the roughening of the surface morphology, promoting a higher contact angle. All crystal structures generated by Cu/Cu-Ni electrodeposition were FCC, with the preferred orientation of the (111) plane. Crystallite size and lattice strain depend on the deposition rate. Less crystallite size and lattice strain affect the film's hardness and corrosion resistance. Moreover, the third bath had the resulting Cu-Ni layer with the best hardness and corrosion rate of around 136 HV and 0.081 mmpy.

Keywords

Cathode Current Efficiency, Deposition Rate, Electrodeposition, Corrosion, Hardness

Received: , Accepted:

<https://doi.org/10.26554/sti.2024.9.3.->

1. INTRODUCTION

The electrodeposition procedure is one of the numerous metal coating methods. Metal coating using electrodeposition technology has created many industries that work on coating vehicle engine parts such as pistons, drums, shafts, and other engine parts (Jariwala et al., 2018; Lajevardi et al., 2013). Electrodeposition is done to take advantage of the better properties of the coating element than a substrate. These benefits include heat resistance, a low coefficient of friction, and the prevention of corrosion and erosion properties (Soegijono and Susetyo, 2022; Ghosh et al., 2000; Matsuda et al., 2022). Many factors influence these properties, including solution concentration, temperature, current density, immersion time, pH, and electrical voltage (Kalubowila et al., 2019; Ollivier et al., 2009). Those factors could significantly influence the deposition rate during the electrodeposition process. Moreover, by adjusting

the deposition rate, structure, grain size, crystallite size, and surface morphology could be controlled (Augustin et al., 2016; Gomez et al., 2005; Rosyidan et al., 2024).

Metals such as copper (Cu) and nickel (Ni) are commonly employed in metal electrodeposition (Hakim and Pangestu, 2022; Setiamukti et al., 2020). Ni is corrosion resistant and has sufficient strength and hardness properties; meanwhile, Cu is a soft and ductile metal that is not too oxidized by air. Cu's reduction potential (+0.34 V) and Ni's reduction potential (-0.25 V) indicate that copper is nobler than Ni. As a result, Cu ions dissolve in solution via diffusion, and Ni ions dissolve via charge transfer (Ghosh et al., 2006; Goranova et al., 2016). Therefore, the concentration of Ni and Cu needs special attention (Ganesan et al., 2022). In addition, a complexing agent is needed to reduce the potential gap between Ni and Cu. Several studies reported the use of pyrophosphate, citrate, acetate, sulfamate, and glycine as complexing agents (Silaimani et al., 2015).

Ghosh et al. (2000) conducted Ni-Cu plating with PC and DC apparatus using bath composition 0.475 M $\text{NiSO}_4 \cdot 7\text{H}_2\text{O}$, 0.125 M $\text{CuSO}_4 \cdot 5\text{H}_2\text{O}$, and 0.2 M sodium citrate (pH was maintained using ammonia solution) and resulting corrosion current between 0.17- 5.77 A cm^{-2} in 3% NaCl, hardness between 384-482 KHN₅₀. Dai et al. (2016) fabricated Ni-Cu film with an electrodeposition technique using 300 g L^{-1} Ni sulfamic acid, 2.5 to 15 g L^{-1} Cu sulfates, 20 g L^{-1} Ni chloride, and 20 g L^{-1} boric acid, resulting in a reduction grain size by increasing Cu content in the alloy. Nady and Negem (2016) studied the electrodeposition of Ni-Cu alloys using various pH and concentration of NiSO_4 and CuSO_4 , with fixed sodium gluconate boric acid and cysteine at 0.025 A cm^{-2} of current density resulting in mostly FCC (111) and FCC (200) crystal planes of the alloys. Goranova et al. (2016) fabricated Ni-Cu using electrodeposition in 0.2 $\text{C}_6\text{H}_5\text{Na}_3\text{O}_7 \cdot 2\text{H}_2\text{O}$ with different concentrations of Ni salts (0.2, 0.25, 0.5, and 0.6 M $\text{NiSO}_4 \cdot 7\text{H}_2\text{O}$) and 0.1M $\text{CuSO}_4 \cdot 5\text{H}_2\text{O}$. The pH (~ 9) was maintained using a 25% NH_4OH solution. The study found that increasing Ni salt (0.6 M NiSO_4) has a levelling effect.

Unfortunately, presenting a complexing agent could enhance the cost of production of Cu-Ni alloy. Therefore, presenting a Ni salt as a catalyst (without a complexing agent) in the plating bath needs further investigation. This study aims to create a Cu/Cu-Ni alloy on Cu alloy through electrodeposition and investigate the relationship between physical and hardness-corrosion properties. The layers were made using various solutions at 25°C, and then the CCE and deposition rate were investigated. The Cu/Cu-Ni coating underwent characterization for scanning electron microscope-energy dispersive spectroscopy (SEM-EDS), x-ray diffraction (XRD), hardness, corrosion, and water droplets.

2. EXPERIMENTAL SECTION

2.1 Materials and Preparation

Electrodeposition solutions were made using $\text{CuSO}_4 \cdot 5\text{H}_2\text{O}$ and $\text{NiSO}_4 \cdot 6\text{H}_2\text{O}$. All chemicals used in the present research are analytical grade from Merck manufacturer. Pure Cu and Ni were used as an anode, while Cu alloy was used as a cathode with chemical compositions of P 0.22 wt.%, Cd 0.684 wt.%, Si 0.137 wt.%, and Cu balance. Before electrodeposition, the cathode was cleaned using ultrasonic cleaner (DELTA D68H) for 5 min. Electrodeposition was performed with a current density of 30 mA/cm^2 for 1 hour at 25°C using a power supply (SANFIX 305 E). The specimens were electrodeposited using various plating baths, as seen in Table 1.

2.2 Characterization

The CCE and deposition rate of the Cu/Cu-Ni electrodeposition were investigated by weighing samples before (initial weight) and after (final weight) electrodeposition and then calculated using equations in the previously reported (Soegijono and Susetyo, 2022; Rosyidan et al., 2024). Afterward, XRD (PANalytical Aeris with Cu K radiation, $\lambda=0.15418$ nm, step size=0.02°) was used to determine the crystal structure of the

Table 1. Plating Baths Composition for Cu/Cu-Ni Electrodeposition

Plating Bath	Composition (M)		Measured pH
	$\text{CuSO}_4 \cdot 5\text{H}_2\text{O}$	$\text{NiSO}_4 \cdot 7\text{H}_2\text{O}$	
Bath 1	0.1	0.3	2.35
Bath 2	0.1	0.5	2.51
Bath 3	0.1	0.7	2.53

Cu-Ni coating. MAUD software was used to refine and find the crystal parameter using XRD data. Moreover, the Debye-Scherrer formula (Equation 1) was used to calculate the crystal size of various samples (Seakr, 2017).

$$D = \frac{0.9\lambda}{\beta \cos \theta} \quad (1)$$

Where D is the average crystallite size, k is a Scherrer constant of (0.9), λ is radiation wavelength (nm), β is the width of the FWHM diffraction peak (radians), and θ is peak position (° or radians).

FE-SEM equipped with EDS (Thermofisher Quanta 650 EDAX EDS Analyzer) was used to analyze the film surface morphology and phase. Afterward, roughness analysis was performed according to SEM picture using Image J software. Moreover, the hardness of the Cu-Ni film was measured using a MicroMet®5100 Series micro indentation Vickers hardness tester using 100 g of load for 10 s. Measurement was conducted for five spot indentation.

Corrosion investigation was performed using potentiodynamic polarization methods (Digi-Ivy DY2311) in a 3.5% NaCl solution with a volume of 100 ml, the reference electrode being Ag/AgCl and the counter electrode being platinum (Pt) wire. Potentiodynamic polarization was carried out at a speed of 0.002 Vs^{-1} from -1.35 to -0.05 V. Information on corrosion current (i_{corr}) and corrosion voltage (E_{corr}) was acquired from the measurement data using the Tafel extrapolation method. The corrosion rate was calculated using Equation 2 utilizing the corrosion current information (Ahmad, 2006).

$$\text{Cr} = C \frac{M_{\text{corr}}}{n_r} \quad (2)$$

Where Cr is the corrosion rate (mmpy), C is a constant for the corrosion rate calculation and is 3.27 mmpy, M is the atomic weight (g mol^{-1}), i_{corr} is corrosion current density (A cm^{-2}), n is the number of electrons involved, and p is the density of Cu and Ni (g cm^{-3}). Last step of the samples characterization is measured water contact angle. The contact angle was observed with a water droplet test on the film surface coated. Some criteria of the angle θ were determined by the value as $\theta < 90^\circ$, $90^\circ \leq \theta < 150^\circ$, and $150^\circ \leq \theta < 180^\circ$ for being hydrophilic, hydrophobic, and super hydrophobic, respectively (Lee et al., 2014).

3. RESULTS AND DISCUSSION

3.1 CCE and Deposition Rate

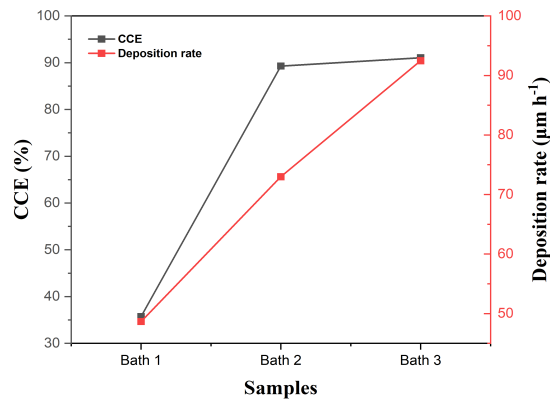


Figure 1. CCE and Deposition Rate for Cu/Cu-Ni Electrodeposited from Bath 1, 2, and 3

Table 2. Average Grain Size Calculation Results of Various Samples

Sample	Grain Size (μm)
Bath 1	105.05
Bath 2	88.22
Bath 3	79.32

Table 3. Average Roughness Value of Various Samples

Sample	Roughness Average (Ra) μm
Bath 1	30.63
Bath 2	37.49
Bath 3	37.82

Table 4. Crystal Parameters of Various Samples

Parameter	Bath 1	Sample Bath 2	Bath 3
Crystal structure		FCC	
Space Group		Fm-3m	
Lattice constant (Å) a = b = c	3.631	3.618	3.612
Cell volume (Å³)	47.89	47.37	47.14
d-spacing (Å)	1.7530	1.7549	1.7578
Crystallite Size (nm)	43.39	27.54	25.70
Lattice strain	0.27	0.41	0.25

The composition of CuSO₄.5H₂O and NiSO₄.6H₂O was determined at the start of the experiment. Figure 1 shows

Table 5. Corrosion Measurements of Various Samples

Sample	i _{corr} (A cm ⁻²)	E _{corr} (V)	Cr (mmpy)	Criteria
Bath 1	4.40×10 ⁻⁶	-0.261	0.196	Good
Bath 2	5.01×10 ⁻⁶	-0.244	0.223	Good
Bath 3	1.82×10 ⁻⁶	-0.248	0.081	Excellent

the CCE and deposition rate results of various experiments. CCE and deposition rate have similar tendencies; an increase in Ni salt would increase both CCE and deposition rate. CCE refers to the fraction of total current used for metal plating (Rosyidan et al., 2024). At the same time, the deposition rate is the amount of anode material deposited on the cathode at a particular current and time (Park et al., 2008). The first, second, and third solutions had a CCE of 35.71, 89.28, and 91.07%, respectively. The first, second, and third solutions had a deposition rate of 48.66, 72.99, and 92.46, respectively. Hacısmailoğlu and Alper (2011) have found that increased pH leads to increased transient current. Moreover, Rosyidan et al. (2024) have seen that an increase in the current leads to a rise in CCE and deposition rate. Therefore, increased Ni salt promotes increased CCE and deposition rate due to rise and pH (see Table 1).

Hydrogen evolution could happen at the cathode when electrodeposition is conducted. Hydrogen evolution could disrupt ion’s movement to the substrate’s surfaces during deposition by blocking the cathode surface. Deo et al. have stated that hydrogen evolution is a competitor at Ni and Cu electrodeposition (Deo et al., 2020). According to the CCE result, higher hydrogen evolution occurred in the samples made using the first solution, and increasing a Ni salt in the solution led to a decrease in hydrogen evolution. Güler et al. (2013) have stated that presenting a hydrogen evolution at the cathode during electrodeposition leads to a decrease in CCE.

3.2 Phase and Surface Morphology

In this study, film deposition involved diffusion and charge transfer by Cu/Cu-Ni. The various films were obtained using a current density of 30 mA cm⁻² for an hour for all solution variations. The results of the EDS investigation can be seen in Figure 2. Based on Figure 2, it can be seen that 100 wt.% Cu phases are seen when electrodeposited using baths 1 and 2. This means presenting a Ni salt 0.3 and 0.5 M doesn’t cause an exhibit of Ni in the film. Meanwhile, when Ni salt concentration rises to 0.7 M, Ni is exhibited in the film around 0.2 wt. %. The solution seems to have a salt limitation, resulting in a Cu-Ni Alloy. Decrease a Cu salt by less than 0.1 M or increasing a Ni salt by more than 0.7 M is needed. Baskaran et al. (2006) electrodeposited Ni using the composition between Ni and Cu salt, which is 20:1.. Sarac et al. (2012) electrodeposited Ni using the composition between Ni and Cu salt are 50:1. Moreover, Hacısmailoğlu and Alper (2011) have stated that hydrogen evolution was occurring at the surface of the substrate during the electrodeposition process, which could prevent the

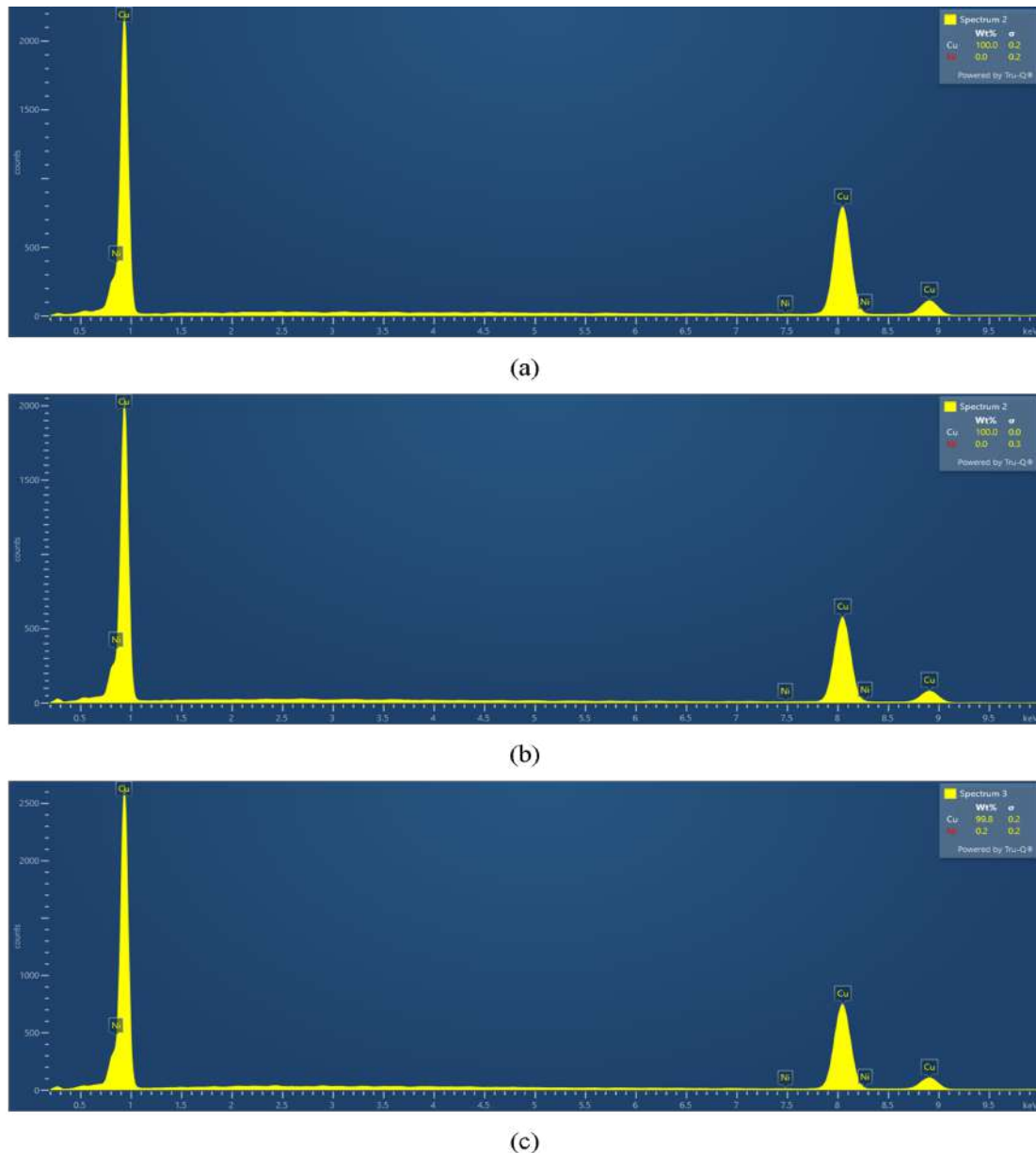


Figure 2. EDS Test Results of Various Samples

reduction of Ni in the film. This statement is corroborated by the fact that Ni formed in the sample was made using a third solution due to electrodeposition using the first and second solutions, which still caused hydrogen evolution on the substrate surface.

Figures 3 (a)-(c) show the morphology of the deposited non-uniform and compact films, which is affected by the hydrogen evolution. Güler et al. (2013) have stated the disruption is due to hydrogen evolution at the cathode, which could be resulting a non-uniform film. Moreover, pure Cu (Figures 3 (a) and (b)) show morphology with nodules form. In contrast, presenting a Ni in the alloy, which changes nodules to a cauliflower-like form (Figure 3 (c)). As mentioned above, exhibiting a Ni salt

in the solution could increase the pH of the solution (Table 1). Kalubowila et al. (2019) have found that increasing the pH bath could transform surface morphology. Furthermore, raising a pH solution leads to an increased deposition rate and change in surface morphology. Therefore, there is transformation from nodules to a cauliflower-like form. Statistical analysis using Image J combined Origin with the corresponding Gauss fitting function was used to identify the grain size distribution. The result is presented in Figure 3.

Image J software was used to calculate the average grain size diameter. Table 2 shows the results of calculating the average grain size. The calculation results show that the grain size average has decreased by increasing the Ni salt in the solution.

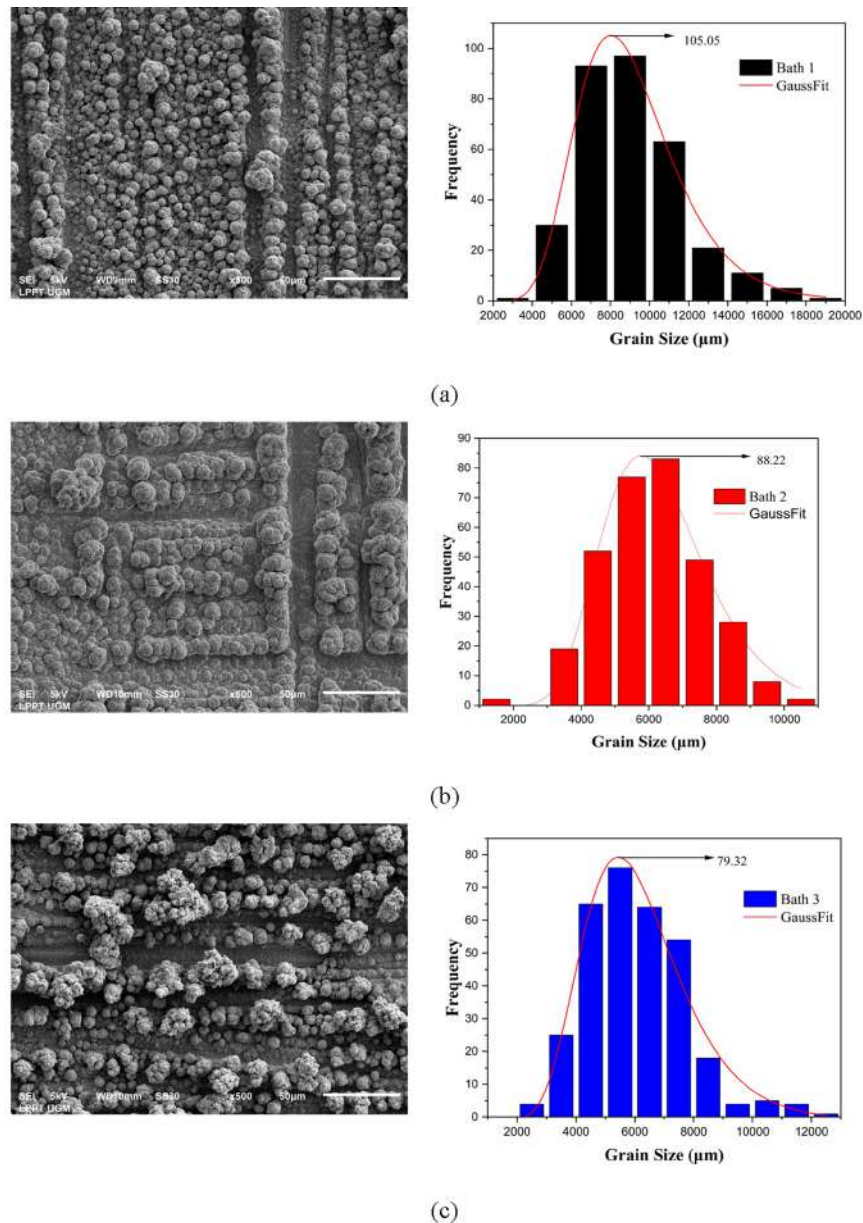


Figure 3. SEM Micrographs and Grain Distribution for Different Samples (a) Bath 1, (b) Bath 2, and (c) Bath 3

Baskaran et al. (2006) stated that grain size decreased due to increased electrodeposition current density. Previous research shows that increasing current density increases deposition rate (Rosyidan et al., 2024). Compared to Figure 1, it is seen that rising Ni salt leads to an increased deposition rate. An increase in the deposition rate leads to an increased speed of the ion species deposited on the cathode surface. Therefore, grain size is decreasing in the present research.

Image processing was done using Image J software to obtain detailed information about the resulting image pattern. Image patterns were investigated from SEM pictures to interpret the results of surface roughness parameters and 3-D images from surface scanning. The result of the Image J software investiga-

tion can be seen in Figure 4, which presents the relationship between distance (μm) and gray value varies with increasing distance.

Table 3 shows the average surface roughness of Cu-Ni/Cu coating morphology fabricated from various baths according to Image J software investigation. According to Table 3, increasing Ni salt in the solution increases the films' roughness average. Deo et al. (2020) reported that increasing a current density led to an increase in surface roughness. As mentioned above, increasing current density increases deposition rate (Rosyidan et al., 2024). Compared to the deposition rate measurement (Figure 1), it can be seen that rising Ni salt leads to an increased deposition rate due to pH increments. An increase in the

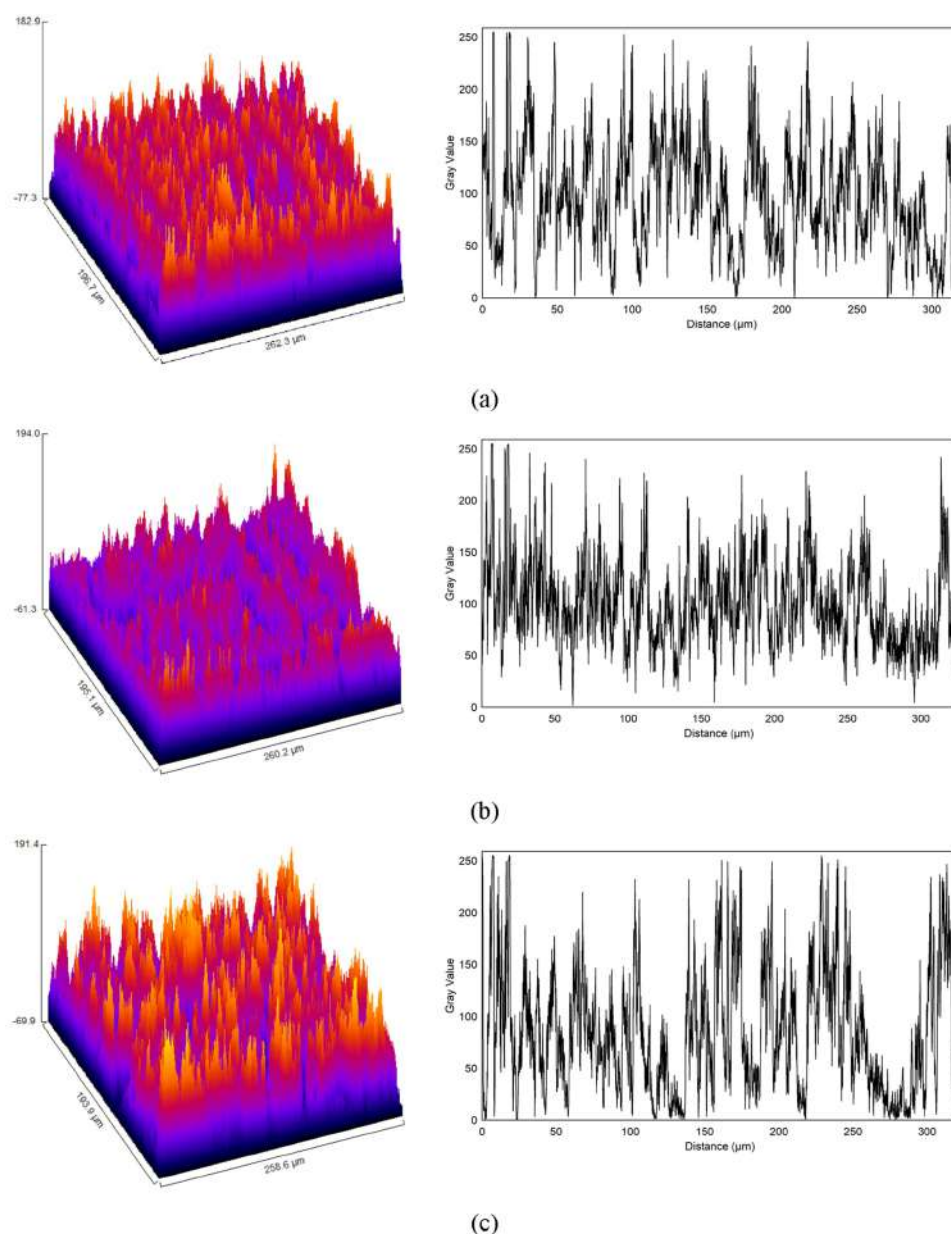


Figure 4. Analysis of Sample Surfaces Roughness in 3D SEM Image and Graph of Grey Value Against Distance (Left-Right) (a) Bath 1, (b) Bath 2, and (c) Bath 3

deposition rate leads to an increased speed of the ion species deposited on the cathode surface. Therefore, the roughness average is increased in the present research.

3.3 Crystallographic Orientation

According to the XRD data in Figure 5, three planes formed namely the (111), (002), and (022) planes. The (111) plane dominated when the films were made using baths 1, 2, and 3. The dominance of the (111) plane orientation had benefits such as anticorrosion, increased electrical conductivity, and improved mechanical properties (Seakr, 2017). Moreover, all of the collected XRD data were then analyzed using MAUD

software, and the crystal parameters are shown in Table 4. All led to the same crystal structure and space group, FCC and Fm-3m, which can be concluded that atoms of the Cu and Ni form a substitutional solid solution (Dai et al., 2016).

Table 4 shows that the lattice constant and cell volume decrease due to the increase in the Ni phase in the alloy, which perfectly agrees with other reports (Baskaran et al., 2006). Moreover, increased Ni salt in the plating bath decreases crystallite size. Augustin et al. (2016) have reported an increase in current density promoting reduced crystallite size. Increasing the electrodeposition process's current density influences the deposition rate's increase; the amount of ion species deposited

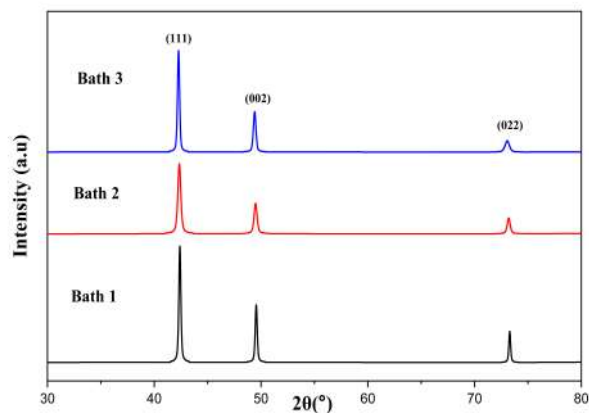


Figure 5. XRD Pattern of Various Samples

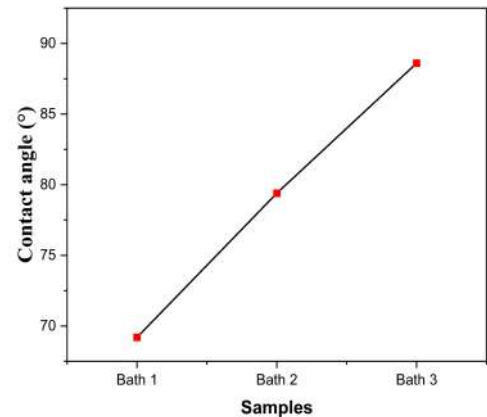


Figure 8. Water contact angle of various samples

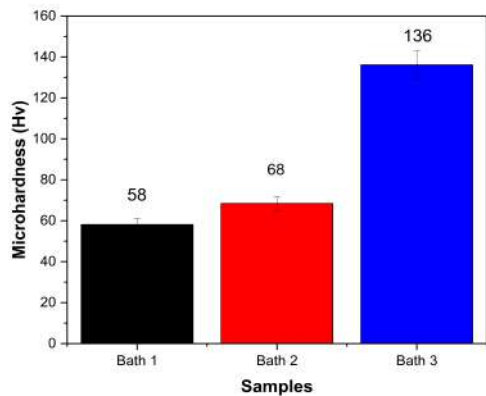


Figure 6. Hardness Test Results of Various Samples

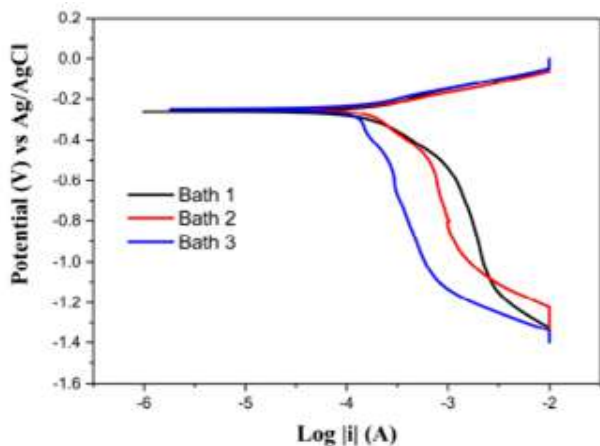


Figure 7. Corrosion Curve for Various Samples

on the cathode rose; therefore, crystallite size decreased. Small crystal size indicates that the distance between grains is close, contributing to material qualities with more roughness proper-

ties (Dai et al., 2016). This result is in perfect agreement with the average roughness in Table 3. Moreover, a smaller lattice strain is seen in the sample made using bath 3.

3.4 Hardness

Hardness is a material’s resistance to plastic deformation. A coating procedure is considered successful if it can enhance the qualities of the coated objects. One of the purposes of electrodeposition in the present research is to improve material deposited hardness. The results of the hardness of the coating were obtained using a Vickers micro-hardness tester. The Vickers microhardness method obtained 58 HV in the first solution, 68 HV in the second solution, and 136 HV in the third solution. It seems an increase in Ni salt would increase the hardness. In their study, Augustin et al. found that a decrease in crystallite size promotes an increase in hardness, which is in perfect agreement with the present research (Augustin et al., 2016). Besides crystallite size, the exhibit of Ni in the alloy also influences the hardness of the sample (Rosyidan et al., 2024). As seen in Figure 6, a sample was made using bath 3, resulting in higher hardness, which is affected by the exhibit of Ni in the alloy. According to the EDS result, only one sample was made using bath 3, resulting in Ni in the alloy. Compared to the Monel 400, hardness is between 150 to 200 HV, and present research has lower hardness (Kukliński et al., 2020).

3.5 Corrosion

Figure 7 shows the corrosion curves of the electrodeposition of Cu/Cu-Ni on the Cu alloy substrate. The i_{corr} and E_{corr} were found using the Tafel extrapolation method. Meanwhile, CR was calculated using Equation (2). The summary of the calculations for the CR of various samples is shown in Table 5. The crystal plane could determine the corrosion rate behavior of materials with the FCC crystal system. The (111) crystal plane is more corrosion-resistant in materials with the FCC system than the (002) and (022) crystal planes (Al Kharafi et al., 2012). Therefore, all of the samples met good and excellent

criteria. Moreover, based on Table 5, it can be seen that the third solution has the best corrosion rate. This behavior is influenced by the lattice strain that was formed. Lattice strain is sample defect concentration measured due to a void core in the lattice (Basori et al., 2023). Therefore, the smallest lattice strain leads to the highest corrosion resistance. According to Wang et al. and Ghosh et al. studies, Monel-400 i_{corr} is 2.24×10^{-6} and 2.2×10^{-6} (A cm^{-2}) (Ghosh et al., 2000; Wang et al., 2014). Compared with Table 5, it can be seen that the sample made using a third solution has lower i_{corr} than Monel-400.

3.6 Contact Angle

The water droplet test can be used to determine the hydrophilic, hydrophobic, and superhydrophobic properties of a film. Figure 8 shows a snapshot of the drip test findings for various samples. All samples possess hydrophilic properties since they have contact angles between 0° and 90° (Thurber et al., 2016). The contact angles achieved in the first, second, and third solution 1 are 69.2° , 79.4° and 88.6° , respectively. Increment of the water contact angle is probably due to an increased film surface roughness. In their research, Huang et al. found that increasing roughness would increase the water contact angle (Huang and Gates, 2020). Moreover, Yu et al. found that increasing electrolyte pH from 2 to 4 increases the film's water contact angle (Yu et al., 2013), probably due to an increase in the surface roughness of the samples.

4. CONCLUSION

Cu/Cu-Ni film was electrodeposited onto Cu alloy using various bath compositions, and according to the multiple findings, increased Ni salt content led to increased deposition rate and CCE due to an increased pH and depleting hydrogen evolution, which impacted grain size, more roughness, less crystallite size and presenting small amount of a Ni in the film. The formed crystal structure was a single-phase FCC with the dominant (111) plane. The hardness increment is due to a decrease in crystallite size. Lesser lattice strain contributed to a higher corrosion resistance. The films have more roughness and impact on the higher water contact angle. The 99.8Cu0.3Ni alloy has the best corrosion resistance and is recommended as an alternative to change Monel-400.

5. ACKNOWLEDGMENT

This project was financially supported by Universitas Trisakti based on the assignment letter number 800/C-4/FTKE/USA KTI/X/2023.

REFERENCES

- Ahmad, Z. (2006). *Principles of Corrosion Engineering and Corrosion Control*. 1th edition. Elsevier
- Al Kharafi, F., I. Ghayad, and R. Abdullah (2012). Corrosion Inhibition of Copper in Non-Polluted and Polluted Sea Water Using 5-Phenyl-1-H-Tetrazole. *International Journal of Electrochemical Science*, 7(4); 3289–3298
- Augustin, A., P. Huilgol, K. R. Udupa, and U. Bhat (2016). Effect of Current Density during Electrodeposition on Microstructure and Hardness of Textured Cu Coating in the Application of Antimicrobial Al Touch Surface. *Journal of the mechanical behavior of Biomedical materials*, 63(October); 352–360
- Baskaran, I., T. S. Narayanan, and A. Stephen (2006). Pulsed Electrodeposition of Nanocrystalline Cu–Ni Alloy Films and Evaluation of Their Characteristic Properties. *Materials Letters*, 60(16); 1990–1995
- Basori, B., B. Soegijono, S. Yudanto, D. Nanto, and F. Susetyo (2023). Effect of Low Magnetic Field during Nickel Electroplating on Morphology, Structure, and Hardness. In *Journal of Physics: Conference Series*, volume 2596. IOP Publishing, page 012014
- Dai, P., C. Zhang, J. Wen, H. Rao, and Q. Wang (2016). Tensile Properties of Electrodeposited Nanocrystalline Ni–Cu Alloys. *Journal of Materials Engineering and Performance*, 25(January); 594–600
- Deo, Y., S. Guha, K. Sarkar, P. Mohanta, D. Pradhan, and A. Mondal (2020). Electrodeposited Ni–Cu Alloy Coatings on Mild Steel for Enhanced Corrosion Properties. *Applied Surface Science*, 515(June); 146078
- Ganesan, M., C.-C. Liu, S. Pandiyarajan, C.-T. Lee, and H.-C. Chuang (2022). Post-Supercritical CO₂ Electrodeposition Approach for Ni–Cu Alloy Fabrication: An Innovative Eco-Friendly Strategy for High-Performance Corrosion Resistance with Durability. *Applied Surface Science*, 577(1); 151955
- Ghosh, S., A. Grover, G. Dey, U. Kulkarni, R. Dusane, A. Suri, and S. Banerjee (2006). Structural Characterization of Electrodeposited Nanophase Ni–Cu Alloys. *Journal of Materials Research*, 21(1); 45–61
- Ghosh, S., A. Grover, G. Dey, and M. Totlani (2000). Nanocrystalline Ni–Cu Alloy Plating by Pulse Electrolysis. *Surface and Coatings Technology*, 126(1); 48–63
- Gomez, E., S. Pane, and E. Valles (2005). Electrodeposition of Co–Ni and Co–Ni–Cu Systems in Sulphate–Citrate Medium. *Electrochimica Acta*, 51(1); 146–153
- Goranova, D., R. Rashkov, G. Avdeev, and V. Tonchev (2016). Electrodeposition of Ni–Cu Alloys at High Current Densities: Details of the Elements Distribution. *Journal of Materials Science*, 51(June); 8663–8673
- Güler, E. S., E. Konca, and İ. Karakaya (2013). Effect of Electrodeposition Parameters on the Current Density of Hydrogen Evolution Reaction in Ni and Ni–MoS₂ Composite Coatings. *International Journal of Electrochemical Science*, 8(4); 5496–5505
- Hacıismailoğlu, M. Ş. and M. Alper (2011). Effect of Electrolyte pH and Cu Concentration on Microstructure of Electrodeposited Ni–Cu Alloy Films. *Surface and Coatings Technology*, 206(6); 1430–1438
- Hakim, M. S. and H. Pangestu (2022). Preparation and Application of Nickel Electroplating on Copper (Ni/EC) Electrode for Glucose Detection. *Science and Technology Indonesia*, 7(2);

- 208–212
- Huang, X. and I. Gates (2020). Apparent Contact Angle around the Periphery of a Liquid Drop on Roughened Surfaces. *Scientific Reports*, **10**(1); 8220
- Jariwala, F., R. Gohil, P. Trivedi, J. Parmar, B. Borda, S. Patel, B. Goyal, and V. Rao (2018). Electroplating of Nickel and Chromium on Aluminum 6082-T6 Alloy. *Proceedings of the International Conference on Recent Advances in Metallurgy for Sustainable Development*, pages 1–3
- Kalubowila, K., K. Jayathileka, L. Kumara, K. Ohara, S. Kohara, O. Sakata, M. Gunewardene, J. Jayasundara, D. Dissanayake, and J. Jayanetti (2019). Effect of Bath pH on Electronic and Morphological Properties of Electrodeposited Cu₂O Thin Films. *Journal of The Electrochemical Society*, **166**(4); D113
- Kukliński, M., A. Bartkowska, D. Przystacki, and G. Kinal (2020). Influence of Microstructure and Chemical Composition on Microhardness and Wear Properties of Laser Borided Monel 400. *Materials*, **13**(24); 5757
- Lajevardi, S., T. Shahrabi, J. Szpunar, A. S. Rouhaghdam, and S. Sanjabi (2013). Characterization of the Microstructure and Texture of Functionally Graded Nickel-Al₂O₃ Nano Composite Coating Produced by Pulse Deposition. *Surface and Coatings Technology*, **232**(October); 851–859
- Lee, J. M., K. M. Bae, K. K. Jung, J. H. Jeong, and J. S. Ko (2014). Creation of Microstructured Surfaces Using Cu–Ni Composite Electrodeposition and Their Application to Superhydrophobic Surfaces. *Applied Surface Science*, **289**(January); 14–20
- Matsuda, T., R. Saeki, M. Hayashida, and T. Ohgai (2022). Microhardness and Heat-Resistance Performance of Ferromagnetic Cobalt-Molybdenum Nanocrystals Electrodeposited from an Aqueous Solution Containing Citric Acid. *Materials Research Express*, **9**(4); 046502
- Nady, H. and M. Negem (2016). Ni-Cu Nano-Crystalline Alloys for Efficient Electrochemical Hydrogen Production in Acid Water. *RSC Advances*, **6**(56); 51111–51119
- Ollivier, A., L. Muhr, S. Delbos, P. Grand, M. Matlosz, and E. Chassaing (2009). Copper–Nickel Codeposition As a Model for Mass-Transfer Characterization in Copper–Indium–Selenium Thin-Film Production. *Journal of Applied Electrochemistry*, **39**(May); 2337–2344
- Park, B. N., Y. S. Sohn, and S. Y. Choi (2008). Effects of a Magnetic Field on the Copper Metallization Using the Electroplating Process. *Microelectronic Engineering*, **85**(2); 308–314
- Rosyidan, C., B. Kurniawan, B. Soegijono, V. Vidia Putra, D. R. Munazat, and F. B. Susetyo (2024). Effect of Current Density on Magnetic and Hardness Properties of Ni-Cu Alloy Coated on Al Via Electrodeposition. *International Journal of Engineering*, **37**(2); 213–223
- Sarac, U., R. M. Öksüzöglü, and M. C. Baykul (2012). Deposition Potential Dependence of Composition, Microstructure, and Surface Morphology of Electrodeposited Ni–Cu Alloy Films. *Journal of Materials Science: Materials in Electronics*, **23**(April); 2110–2116
- Seakr, R. (2017). Microstructure and Crystallographic Characteristics of Nanocrystalline Copper Prepared from Acetate Solutions by Electrodeposition Technique. *Transactions of Nonferrous Metals Society of China*, **27**(6); 1423–1430
- Setiamukti, D., A. Khusnani, and M. Toifur (2020). The Effect of Electrolyte Concentration on the Sensitivity of Low-Temperature Sensor Performance of Cu/nl Film. *Science and Technology Indonesia*, **5**(2); 28–33
- Silaimani, S., G. Vivekanandan, and P. Veeramani (2015). Nano-Nickel-Copper Alloy Deposit for Improved Corrosion Resistance in Marine Environment. *International Journal of Environmental Science and Technology*, **12**(May); 2299–2306
- Soegijono, B. and F. Susetyo (2022). Magnetic Field Exposure on Electroplating Process of Ferromagnetic Nickel Ion on Copper Substrate. In *Journal of Physics: Conference Series*, volume 2377. IOP Publishing, page 012002
- Thurber, C. R., Y. H. Ahmad, S. F. Sanders, A. Al-Shenawa, N. D'Souza, A. M. Mohamed, and T. D. Golden (2016). Electrodeposition of 70-80 Cu-Ni Nanocomposite Coatings for Enhanced Mechanical and Corrosion Properties. *Current Applied Physics*, **16**(3); 387–396
- Wang, S., X. Guo, H. Yang, J. Dai, R. Zhu, J. Gong, L. Peng, and W. Ding (2014). Electrodeposition Mechanism and Characterization of Ni-Cu Alloy Coatings from a Eutectic-Based Ionic Liquid. *Applied Surface Science*, **288**(January); 530–536
- Yu, Q., Z. Zeng, W. Zhao, M. Li, X. Wu, and Q. Xue (2013). Fabrication of Adhesive Superhydrophobic Ni-Cu-P Alloy Coatings with High Mechanical Strength by One Step Electrodeposition. *Colloids and Surfaces A: Physicochemical and Engineering Aspects*, **427**(June); 1–6